Network Risk and Key Players: A Structural Analysis of Interbank Liquidity*

Edward Denbee[a], Christian Julliard[b], Ye Li[c], Kathy Yuan[b]

[a] *Bank of England*
[b] *London School of Economics, Systemic Risk Centre, and Center for Economic and Policy Research*
[c] *The Ohio State University, Fisher College of Business*

Abstract

Using a structural model, we estimate the liquidity multiplier of an interbank network and banks' contributions to systemic risk. To provide payment services, banks hold reserves. Their equilibrium holdings can be strategic complements or substitutes. The former arises when payment velocity and multiplier are high. The latter prevails when the opportunity cost of liquidity is large, incentivising banks to borrow neighbors' reserves instead of holding their own. Consequently, the network can amplify or dampen shocks to individual banks. Empirically, network topology explains cross-sectional heterogeneity in banks' systemic-risk contributions while changes in the equilibrium type drive time-series variation.

*We are grateful to Toni Whited, the editor at the Journal of Financial Economics, and two anonymous referees for helpful comments. We also thank the late Sudipto Bhattacharya, Yan Bodnya, Ben Craig, Douglas Gale, Michael Grady, Charles Khan, Yiming Ma, Seymon Malamud, Antoine Martin, Farzad Saidi, René Stulz, Laura Veldkamp, Mark Watson, David Webb, Anne Wetherilt, Erhao Xie, Kamil Yilmaz, Peter Zimmerman, and conference and seminar participants at the Bank of Canada/Payments Canada Workshop on Payment Systems, the Bank of England, Cass Business School, Cleveland Fed/OFR Financial Stability – Markets and Spillovers, Duisenberg School of Finance, Koc University, the LSE, Macro Finance Society annual meeting, NBER Summer Institute, the Ohio State University, Short-Term Funding Markets Conference, the Stockholm School of Economics, and the WFA for helpful comments and discussions. This research was started when Yuan was a senior Houblon-Norman Fellow at the Bank of England. The views expressed in this paper are those of the authors and not necessarily those of the Bank of England. The support of the Fondation Banque de France, of ERC, the European Research Council and of the Economic and Social Research Council in funding the Systemic Risk Centre is gratefully acknowledged [grant number ES/K002309/1]. Ye Li acknowledges the generous financial support from Don Shackelford Fellowship and Charles A. Dice Center of Financial Economics at the Ohio State University.

Email addresses: `edward.denbee@bankofengland.co.uk` (Edward Denbee), `c.julliard@lse.ac.uk` (Christian Julliard), `li.8935@osu.edu` (Ye Li), `K.Yuan@lse.ac.uk` (Kathy Yuan)

JEL classification: G21, G28, C31, C51, C57, D85, L14.

Keywords: financial networks, liquidity, interbank market, payment systems, payment velocity, payment multiplier, key players, systemic risk, spatial models.

1. Introduction

At the core of the financial infrastructure is the payment system operated by banks. The colossal volume of payment inflows and outflows can result in intraday imbalances of enormous magnitude. Banks hold reserves as buffers, and to overcome individual banks' liquidity shocks, they may borrow reserves from and lend reserves to each other through the interbank network. The aggregate amount of liquidity is crucial in supporting the functioning of the payment system. In this paper, we study the role of the interbank network in transmitting individual banks' liquidity shocks and its implications for the efficiency of aggregate liquidity provision in the payment system.

An interbank network amplifies shocks when banks' decisions to hold reserves are strategic complements. In this case, a shock that depletes one bank's reserves negatively affects other banks, resulting in a large reduction in the aggregate liquidity. When banks' reserve holding decisions are strategic substitutes, the interbank network dampens shocks, so the decline of one bank's reserves triggers the accumulation of reserves at neighboring banks, stabilizing aggregate liquidity. We build a model where the type of strategic interaction on the interbank network depends on the payment system velocity, bank customers' demand for payment services, and the (opportunity) costs of holding reserves. We identify the network effects via structural estimation using data from the U.K. payment system between January 2006 and September 2010.

We find that the network multiplier is procyclical. Before the financial crisis, the interbank network amplified shocks. A £1 shock equally spread across banks would result in a £5.37 shock to the aggregate liquidity. It declined to £1.43 during the crisis. After the introduction of quantitative easing (QE) in the U.K., the network became a buffer, generating a shock of £0.85 to the aggregate liquidity. Such a shift from strategic complementarity to substitution coincided with a decline of payment velocity in the sample period, as predicted by our theory.

Our model decomposes the network-generated systemic risk into contributions of individual banks, and thereby identifies the key players. We find that while the network topology determines banks' relative importance in the transmission and aggregation of shocks, the type of equilibrium strategic interactions on the interbank network (i.e., strategic complementarity or substitution) determines whether banks serve as shock amplifiers or absorbers. We also characterize the wedge between decentralized equilibrium and social optimum. The cyclicality of network externality suggests the need for macroprudential regulation of banks' liquidity choices.

Next we summarize our model, the estimation strategy, and the main findings. In our theoretical model, banks choose the size of reserve holdings based on a cost-benefit analysis. Two opposing forces drive the strategic interactions among banks on the network. First, holding reserves incurs the opportunity costs of forgoing other investments. When the opportunity cost of liquidity increases, banks hold less reserves and rely on neighbors' liquidity via interbank borrowings. The strength of such *strategic substitution* is captured by the parameter ψ.

The second force at play is about the benefits of holding reserves, and it leads to strategic complementarity. Banks use reserves to provide payment services to depositors, e.g., to cover payment flow imbalances.[1] In reality, banks' revenues from payment services take the form of reductions of deposit rates (money premium), depending on two parameters.[2] The first one is the velocity of the payment system, i.e., the volume of payments that can be supported by one unit of reserves. The second parameter, which we call the "payment multi-

[1]Our empirical setting is the U.K. sterling large payment system, the Clearing House Automated Payments System (CHAPS), which features real-time gross settlement (RTGS). RTGS requires reserves to settle payments in real time without netting the inflows and outflows. Major economies have adopted RTGS, such as Fedwire in the U.S. and TARGET2 in the Eurozone. When a bank's depositors instruct payments, the bank has to disperse reserves to the payees' other banks, incurring reserve outflows; when a bank's depositors receive payments from other banks' customers, the bank receives reserve inflows. Banks have to hold reserves to buffer reserve flow imbalances.

[2]Our setup is inspired by the recent literature on bank debts as means of payment enjoying a money premium, i.e., a spread between the prevailing safe return and the lower deposit rate (Bianchi and Bigio, 2014; Hart and Zingales, 2014; Li, 2017; Piazzesi and Schneider, 2017) and the literature on deposit market power (Drechsler et al., 2017; Wang et al., 2019).

plier," captures the fact that payments beget payments – when depositors make more payments, they trigger more economic activities and the new activities require more payments.[3]

The payment velocity and payment multiplier generate *strategic complementarity* in banks' reserve holdings. When neighbors hold more liquidity, a bank can borrow to support more payments, especially so when the *payment velocity* is high. More payments in turn trigger more economic activities and payment needs, especially so when the *payment multiplier* is high. The stronger needs for payment services imply a higher marginal revenue from using the bank's *own* reserves to support payments. Therefore, being able to borrow from neighbors incentivizes a bank to hold more reserves if the payment velocity and/or the payment multiplier are high. Once we solve the model, we obtain a single parameter (δ) that summarizes the impacts of both payment multiplier and payment velocity.

We show that at the (unique interior) Nash equilibrium, the overall impact of the interbank network on banks' reserves depends on a key parameter, the network attenuation factor, ϕ. This single parameter captures the net effect of the two opposing economic forces. It is negative if strategic substitution dominates ($\delta < \psi$), and positive if strategic complementarity dominates ($\delta > \psi$).

In our model, each bank receives shocks to the marginal cost of holding reserves. A crisis shock increases the cost and depletes banks' reserves, as it becomes more difficult to raise funds.[4] The depletion of reserves compromises banks' ability to support payments and posits a significant threat to the financial infrastructure of the economy. Our framework allows us to examine how the interbank network propagates such shocks.

The network shock propagation mechanism depends crucially on its attenu-

[3] One motivation of the payment-begetting-payment mechanism is the input-output linkages in the production sector (Carvalho and Tahbaz-Salehi, 2019). For example, when downstream customers pay upstream suppliers for their products, upstream suppliers may in turn pay their own suppliers along the logistic chains.

[4] Reserves may also be depleted when used to repay short-term debts that cannot be rolled over in crises.

ation factor ϕ. In equilibrium, a bank's reserves depend upon its own shocks, the shocks of its neighbors, of the neighbors of its neighbors, etc., with distant shocks becoming increasingly less important as they are weighted by ϕ^k where k measures the distance. While the network topology determines the routes of shock propagation, whether shocks are amplified ($\phi > 0$) or dampened ($\phi < 0$) depends on the type of strategic interaction on the interbank network. The parameter ϕ and the size of shocks to individual banks are the key structural parameters in our empirical analysis.

Our estimation uses data from the sterling large payment system (CHAPS) in the period from 2006 to 2010. Member banks of this network conduct transactions for their own purposes and on behalf of their clients and hundreds of other nonmember banks. Their reserve holdings ensure the functioning of the payment system, which is crucial for supporting real economic activities. For example, in March 2020, CHAPS processed 4.1 million payments daily worth £8.7 trillion (almost four times the 2019 GDP of the U.K.). CHAPS banks regularly face intraday payment imbalances in excess of £1 billion, and use reserves to cover such exposures.[5]

In our model, the strength of interbank connections determines the amount of accessible credit. Therefore, we measure interbank connections using overnight borrowing and lending data. Specifically, a link between two banks is quantified by the fraction of borrowing by one bank from another in the recent past, so the network is directional and its adjacency matrix is weighted (and right stochastic). These interbank links can be interpreted as (frequentist) probabilities of receiving credit.

In the estimation, we utilize the fact that the equilibrium conditions of our model map exactly to a spatial error model (SEM), which allows us to incorporate the *entire* network structure, banks' characteristics, and macroeconomic

[5]The U.K. monetary framework leaves reserves management largely at individual banks' discretion (both before and after quantitative easing). In the Online Appendix, we provide background information on the policy framework (reserve regimes), including details on the payment system and the interbank markets.

variables into the joint likelihood of banks' reserve holdings.[6] The structural parameters are estimated via quasi-maximum likelihood. Specifically, the key parameter ϕ and the sizes of individual banks' shocks are identified from the covariance of spatial errors. Our approach stands in contrast with the regression models that project variables of interest onto particular network statistics. The structural estimation allows us to identify the type of strategic interaction on the network, to characterize shock propagation, and to conduct counterfactual analysis.

We conduct four empirical exercises. First, we show that ϕ is procyclical. In the period before the global financial crisis, the network equilibrium exhibits strategic complementarity. With a positive and large value of ϕ, the interbank network strongly amplifies shocks. To quantify the network effect, we compute the ratio of aggregate liquidity volatility to counterfactual volatility when there is no network externality (i.e., the attenuation factor ϕ is zero) and obtain 5.59. As the crisis unfolded, strategic complementarity weakens and strategic substitution strengthens, resulting in a smaller volatility ratio of 1.25. After the introduction of quantitative easing in early 2009, the network equilibrium demonstrates the effect of strategic substitution. The interbank network becomes a shock buffer that stabilizes the aggregate liquidity provision in the payment system, and the volatility ratio falls to 0.89 (i.e., an 11% reduction of aggregate reserve volatility due to network connections).

In our theoretical model, strategic complementarity becomes stronger when the payment system velocity is higher. To further investigate the dynamics of network effects, we calculate the velocity in the data, i.e., the ratio of payment volume to reserves in the system. We find that it has an 89% correlation with our rolling estimate of ϕ. This finding lends support to our model and reveals

[6]SEM is a conservative approach, leaving only the residual variation in reserve holdings (orthogonal to bank characteristics and macroeconomic variables) to be driven by the network. We also estimate a spatial Durbin model (SDM), where the network plays a larger role since banks' reserves in this case depend not only on shocks to other banks but also on other banks' characteristics (e.g., balance sheet conditions). Since SEM and SDM are nested models, the SDM estimation also provides a specification test for our framework.

an important driver of the type of strategic interaction on the network.

Second, we empirically characterize the shock propagation mechanism and quantify individual banks' contributions to aggregate liquidity risk in the payment system. Using the model's equilibrium conditions, we define and estimate banks' network impulse response functions (NIRFs) that naturally decompose the *volatility* of aggregate reserves into each bank's risk contribution. We find that in any given period, two or three banks are the risk key players (with relatively large NIRFs), and each bank's risk contribution varies substantially over time. Moreover, the risk key player is typically *not* the largest net borrower – even net lenders can generate substantial risk in the system. These findings are relevant for monitoring and regulating the banking system, as well as policy interventions during crisis.

Third, we conduct two counterfactual analyses. The first one focuses on the role of network topology in generating the cross-sectional variation in banks' contributions to systemic risk. We consider a hypothetical network where all banks are connected to each other and the strength of connection is the same for each pair. We find that, on such a network, banks' risk contributions are largely the same. Therefore, the cross-sectional difference between banks' risk contributions depends crucially on the heterogeneity of network connections. Our second counterfactual exercise examines the time variation of banks' NIRFs. We decompose the variations into the changes due to variation in ϕ (the type of strategic interaction on the network) and the changes due to variation of network topology. We find that the former is clearly the main driver. Therefore, while network topology drives the cross-sectional variation in banks' contributions to systemic risk, it is the type of equilibrium strategic interaction (i.e., complementarity or substitution) that drives the time-series variation.[7]

Finally, we compare the decentralized equilibrium with the planner's optimum using our model and estimates of the structural parameters. The dis-

[7] A corollary of our finding is that in our setting, the endogenous formation and evolution of the network over time plays a limited role in determining the time-variation in the network effects.

crepancies across the boom and crisis periods offer guidance on potential policy interventions. For example, we find that during the boom period the amount of aggregate liquidity held by banks is not too far from the planner's optimum, but the network generates too much volatility through the systemic propagation of shock through the network. During the crisis period, the decentralized equilibrium generates an amount of reserve buffer in the payment system that is below the planner's optimum, and the systemic risk is still too high. After the introduction of quantitative easing, the systemic risk generated by the network subdued.

The remainder of this paper is organized as follows. In Section 2, we review the related literature. In Section 3, we present and solve the network game. Section 4 casts the model equilibrium into the spatial econometric framework, outlines the estimation methodology and identification conditions, and defines risk key players. In Section 5, we describe and summarize the data. In Section 6, we present and discuss the estimation results. Section 7 concludes. In the Appendix, we explain the U.K. monetary policy framework, discuss details of the data construction and estimation method, and provide additional results.

2. Related literature

This paper contributes to the literature on bank liquidity management. Banks in payment systems are at the most fundamental layer of economic transactions. Every transaction ultimately goes through these payment system members. Member banks' decisions have profound influence on the whole economy (Piazzesi and Schneider, 2017). We provide the first evidence on how the liquidity choices of payment system banks depend on the interbank network. Our findings can be embedded in the broad discussion of banks' portfolio choices over an economic cycle (e.g. Cornett et al., 2011). Importantly, our finding that the equilibrium type on the network flips with the start of QE contributes to the literature on bank liquidity management and monetary policy (e.g., Bernanke and Blinder, 1988; Kashyap and Stein, 2000; Bianchi and Bigio, 2014; Drechsler et al., 2014).

We contribute to the literature on bank liquidity regulation by providing an empirical framework to attribute systemic risk to individual banks and by characterizing the wedge between decentralized outcome and the planner's solution. Liquidity regulation has attracted considerable attention since the financial crisis. Stein (2012) argues that reserve requirements may serve as a tool for financial stability regulation. Diamond and Kashyap (2016) study bank liquidity regulation in the setting of Diamond and Dybvig (1983). Allen and Gale (2017) review earlier theories that may provide foundations (i.e., sources of market failures) for bank liquidity regulations, such as liquidity coverage ratio and net stable funding ratio in Basel III. Our findings of procyclical network externality, and banks' time-varying contributions to systemic risk, lend support to a macroprudential perspective on liquidity regulation.

Our work also advances the literature on interbank market, payment system, and banks' liquidity demand. In our model, banks hold liquidity to support depositors' payments (Bech and Garratt, 2003). Ashcraft et al. (2010) find that banks hold excess reserves in response to heightened payment uncertainty. Relatedly, Acharya and Merrouche (2010) document evidence of precautionary liquidity demands of U.K. banks during the subprime crisis. Banks' profits from offering payment services often take the form of deposit rate reductions in reality, which in turn depend on banks' deposit market power (e.g., Drechsler et al., 2017; Wang et al., 2019). Depositors' demand for payment services increases in the level of local economic activities in our model. Such positive spillover effects are motivated by input-output linkages (Carvalho and Tahbaz-Salehi, 2019) and agents' liquidity risk management (Shin, 2019), and echo the spillover effects in the models of economic growth (e.g., Frankel, 1962; Lucas, 1988; Romer, 1986). Finally, we also incorporate banks' free-riding incentives in liquidity choices, motivated by the pioneer work of Bhattacharya and Gale (1987) on interbank markets.

Recent theoretical works on interbank markets highlight the various forms of externalities and inefficiencies (e.g., Freixas et al., 2000; Allen et al., 2008;

Freixas et al., 2011; Moore, 2012; Castiglionesi et al., 2017). Fecht et al. (2010) find that the prices of liquidity depend on counterparties' liquidity levels. Our paper differs by modeling banks' liquidity holdings as an outcome of a network game and estimating time-varying network externality. We are not the first to emphasize that shock propagation depends on complementarity versus substitution (e.g., Jovanovic, 1987). However, to the best of our knowledge, we are the first to estimate such interdependence of players using a network structure and to provide evidence of time-varying network externalities.

Networks have proven to be a useful analytical tool for studying financial contagion and systemic risk from both theoretical and empirical perspectives. Starting from Allen and Gale (2000), recent theories feature increasingly sophisticated networks and shock transmission mechanisms. See Babus and Allen (2009) for a comprehensive review. Recent works include, but are not limited to, Afonso and Shin (2011), Zawadowski (2012), Acemoglu et al. (2012), Herskovic, and Eisfeldt et al. (2020). Recent empirical works also cover a wide range of economic networks (see Diebold and Yılmaz, 2009, 2014; Billio et al., 2012; Kelly et al., 2013; Duarte and Eisenbach, 2013; Greenwood et al., 2015, and Gofman, 2017). We differ from these papers by using the linear-quadratic approach of Ballester et al. (2006) to analyze how economic agents' liquidity holding decisions in a network game generate systemic risk and by structurally estimating network externalities. Herskovic et al. (2017) embed a similar spatial autoregressive structure in firms' growth rates to study the comovement of firm volatilities.

Our result that the interbank network contributes significantly to systemic risk might explain the puzzling finding in the literature where interbank networks, when calibrated to the data, have only limited impact on systemic risk. For example, simulation studies based on reasonably realistic networks show little impact of linkage variation (summarized in Upper, 2011). Using a unique dataset of all Austrian banks, Elsinger et al. (2006) find that contagion happens rarely and that the funds required to prevent contagion are surprisingly small. By applying an Eisenberg and Noe (2001) style model to German banks, Chen et al. (2016) find that the lack of bank capital, rather than the network contagion, is the key contributor to bank failure. We find that instead of variation of the network topology, the change in the type of equilibrium on the network is the main driver of systemic risk. Therefore, it is important to model and estimate time-varying network externalities in order to understand the role of a network in systemic risk formation. Finally, studies on broker-dealer networks often show that trading volume concentrates on a few players (Afonso and Lagos, 2015; Hugonnier et al., 2014; Chang and Zhang, 2019; Farboodi, 2019). Instead of volume distribution, this paper studies risk distribution and finds a similar core-periphery structure – two or three banks contribute most to the systemic liquidity risk.

3. The network model

In this section, we construct a model of banks' liquidity holding decisions that directly guides our empirical analysis of systemic risk in the interbank network. In this setting, given the network structure, a set of banks simultaneously choose the level of liquidity holdings needed to support their payment services. In equilibrium, we show that each i bank's optimal liquidity holding, $z_{i,t}$, not only depends on its own characteristics, but also responds to all other banks' liquidity holding decisions through the network as follows:

$$z^*_{i,t} = \phi \sum_{j \neq i} g_{ij,t} z_{j,t} + \mu_{i,t}, \tag{1}$$

where the subscript t is the time index. Our goal is to empirically estimate this equation. This equilibrium condition, as discussed later in this section, is robust in that it could be in principle derived using microfoundations other than the ones that we postulate. To guide the interpretation of the empirical results, we model the strategic interactions of banks in a payment system, detailing the role of this economic channel while recognising that other forces may also be at play.

Payment services. Consider the t-th period in a dynamic economy where there are N banks. At the beginning of period t, banks decide how much reserves to hold. Banks hold reserves for two reasons: for their own internal liquidity needs independent from the network (denoted by $q_{i,t}$), and to support customers' payment activities ($z_{i,t}$).[8] The first component, $q_{i,t}$, is determined by banks' characteristics ($x_{i,t}^m$) and macroeconomic conditions (x_t^p):

$$q_{i,t} = \alpha_i + \sum_{m=1}^{M} \beta_m x_{i,t}^m + \sum_{p=1}^{P} \beta_p x_t^p, \tag{2}$$

where α_i is a bank fixed effect. The second component, and main focus of our analysis, $z_{i,t}$, is the choice of reserves that support payment activities of the customers (depositors).

Bank i allocates an amount of reserves $z_{i,t}$ at the *beginning* of period t to the payment system. Reserves buffer the intraday payment outflows. When a depositor makes payments, her bank often experiences reserve outflows, because the payees may hold accounts at different banks and, thus, settlement requires her bank to send reserves to the payees' banks while debiting her deposit account.[9] If the depositor pays cash to her payee, she has to withdraw deposits, which also reduces her bank's reserves.

During the period, a bank's reserves are also made available to other banks via interbank loans, so when one bank exhausts its own reserves, it may borrow from other banks to cover the payment outflows. Therefore, a bank's ability to provide payment services depends on the total accessible liquidity that consists of its own reserves, $z_{i,t}$, and interbank borrowing.

Specifically, bank i may expect to borrow up to $\eta \sum_{j \neq i} g_{ij,t} z_{j,t}$, which is a weighted average of other banks' reserves multiplied by η, a scaling parame-

[8] Egan et al. (2017) document that the profit from deposit-taking is a key determinant of bank value because the payment service allows banks to borrow at low deposit rates.

[9] Our empirical setting, the Clearing House Automated Payment System (CHAPS) transaction system in the U.K., features settlement in real time and on gross terms to eliminate counterparty credit risks. For more details, please refer to the Online Appendix.

ter. The strength of interbank connection is measured by $g_{ij,t}$ ($\in (0,1)$) with $\sum_{j\neq i} g_{ij,t} = 1$. The parameter η captures the overall accessibility of interbank credit and the network linkages, $g_{ij,t}$, capture the cross-sectional heterogeneity. Therefore, the total accessible liquidity at the beginning of the period is $z_{i,t} + \eta \sum_{j\neq i} g_{ij,t} z_{j,t}$, depending on the interbank linkages and neighboring banks' reserves committed to the payment system.

The time-t network is predetermined and characterized by an N-square adjacency matrix $\mathbf{G}_t$. If its element $g_{ij,t} \neq 0$, bank i and j are connected. Later, to construct $\mathbf{G}_t$ in the structural estimation we use interbank borrowing and lending data, which is likely to be most relevant for the daily variation of bank reserves that we focus on. Specifically, $g_{ij,t}$ will be measured by the historical fraction of borrowing by bank i from bank j in the month up to day t.[10] The network is therefore directed, and $\mathbf{G}_t$ is right stochastic.

The amount of accessible liquidity, $z_{i,t}+\eta \sum_{j\neq i} g_{ij,t} z_{j,t}$, is an *ex ante* measure of available liquidity. It is determined after banks simultaneously choose $z_{i,t}$ at the beginning of period t. As the period unfolds and payments take place, the actually used liquidity fluctuates, depending on the outflows from customers sending out payments and the inflows from customers receiving payments (e.g., Bech and Garratt, 2003). Here we do not explicitly model the intra-period payment flows and the interbank borrowing and lending *ex post*, but recognize that when the total accessible liquidity is larger, banks would allow depositors to conduct more payments throughout the period. Let $S_{i,t}$ denote bank i's supply of payment services. It increases in the total accessible liquidity at the beginning of period:

$$S_{i,t} = \kappa_b \left(z_{i,t} + \eta \sum_{j\neq i} g_{ij,t} z_{j,t} \right), \tag{3}$$

where $\kappa_b > 0$ (the subscript "b" for "bank"). In reality, banks introduce vari-

[10] Our estimation results are robust to alternative measurements of interbank relationships, such as bank i's lending to j and the gross amount of interbank borrowing and lending.

ous restrictions on customers' payment activities in order to limit the intraday liquidity used, such as restricting number of transfers from savings to checking accounts and limiting the value of electronic transfers that can be settled intraday. The parameter κ_b is the ratio of total payment volume to total accessible liquidity, a measure of liquidity *velocity* in the payment system. Given the velocity, holding more liquidity allows a bank to support more payments.

Bank optimization. Let $V(S_{i,t})$ denote bank i's revenues from providing payment services. In Appendix A.1, we provide a microfoundation of the function $V(\cdot)$ based on depositors' demand for payment services. Bank i's objective is

$$\begin{aligned}&\max_{z_{i,t}} \; u_i(z_{i,t}, \{z_{j,t}\}_{j\neq i} | \mathbf{G}_t) \\ =&V(S_{i,t}) - \left[\gamma\left(z_{i,t} + \eta\sum_{j\neq i} g_{ij,t} z_{j,t}\right) + \frac{\psi}{2}\left(z_{i,t} + \eta\sum_{j\neq i} g_{ij,t} z_{j,t}\right)^2 + \widetilde{\mu}_{i,t}\gamma' z_{i,t} + \frac{\psi'}{2} z_{i,t}^2\right]\end{aligned} \tag{4}$$

where $S_{i,t}$ is given in Eq. (3) and $\widetilde{\mu}_{i,t}$ is a random variable that is independent across banks and realized before banks decide on $z_{i,t}$. The objective function captures the costs of setting aside liquidity to support depositors' payment, which depend on the forgone investment opportunities and other usages of liquidity. The first two terms in the liquidity cost form a quadratic cost function, and the last two terms capture the fact that bank i's own reserves may cost differently from interbank borrowings.

We solve a Nash equilibrium where N banks simultaneously choose z, the reserves in the payment system. Specifically, bank i chooses the best response, $z_{i,t}$, to other banks' decisions, $\{z_{j,t}\}_{j\neq i}$. In the spirit of classic linear-quadratic games, we consider a linear marginal revenue function, in particular, $V'(S_{i,t}) =$

$\delta S_{i,t}$, so the first-order condition (F.O.C.) for $z_{i,t}$ yields

$$\delta \left(z^*_{i,t} + \eta \sum_{j \neq i} g_{ij,t} z_{j,t} \right) = \gamma + \psi \left(z^*_{i,t} + \eta \sum_{j \neq i} g_{ij,t} z_{j,t} \right) + \widetilde{\mu}_{i,t} \gamma' + \psi' z^*_{i,t}, \quad (5)$$

The parameter δ is decomposed into two economic forces and defined by[11]

$$\delta \equiv \delta_S \kappa_b \,. \quad (6)$$

As previously discussed, the parameter κ_b is the payment velocity – the volume of payments that one unit of reserves supports. When κ_b is large, one unit of liquidity can support more payments (i.e., a higher $S_{i,t}$) as shown in Eq. (3). The parameter δ_S determines how the increase of $S_{i,t}$ translates into more revenues. In Appendix A.1 we show that δ_S depends on the *payment multiplier*, i.e., how depositors' payments trigger economic activities and subsequent payments.

The main tradeoffs that a bank faces are captured by Eq. (5). The term on the left-hand side is the marginal revenue, which is a function of the level of the bank's supply of payment services ($S_{i,t}$). That is, as in a monopolist maximization problem, each bank internalises the effect of its own supply on marginal revenues. The right-hand side of Eq. (5) features the marginal costs of internal and external liquidity that are affected, respectively, by $\psi + \psi'$ and ψ.

For this problem to have a unique solution, we impose the parameter restriction that guarantees the concavity of bank's objective function in $z_{i,t}$:

$$\frac{\partial^2 u_i(z_{i,t}, \{z_{j,t}\}_{j \neq i} | \mathbf{G}_t)}{\partial z^2_{i,t}} = \delta - \psi - \psi' < 0 \,. \quad (7)$$

Equilibrium. All banks' first-order conditions imply a system of linear best response functions that jointly solve the set of optimal $\left\{ z^*_{i,t} \right\}_{i=1}^N$. Rearranging

[11] The microfoundation for these two forces is given in detail in the Online Appendix.

banks' F.O.C., we solve

$$z_{i,t}^{*}=\left(\frac{\delta-\psi}{\psi'-(\delta-\psi)}\right)\eta\sum_{j\neq i}g_{ij,t}z_{j,t}+\frac{(-\widetilde{\mu}_{i,t}\gamma'-\gamma)}{\psi'-(\delta-\psi)}. \tag{8}$$

From the condition Eq. (7), $\psi' > (\delta-\psi)$. To further simplify the notation, we define

$$\mu_{i,t}\equiv\frac{(-\widetilde{\mu}_{i,t}\gamma'-\gamma)}{\psi'-(\delta-\psi)}\,, \tag{9}$$

and, importantly, the parameter that captures the nature of network effects:

$$\phi\equiv\left(\frac{\delta-\psi}{\psi'-(\delta-\psi)}\right)\eta. \tag{10}$$

The solution to bank i's problem can thus be written as

$$z_{i,t}^{*}=\phi\sum_{j\neq i}g_{ij,t}z_{j,t}+\mu_{i,t}. \tag{11}$$

The bilateral network influences in our model are captured by the following cross-derivatives for $i\neq j$:

$$\frac{\partial^2 u_i(z_{i,t},\{z_{j,t}\}_{j\neq i}\,|\mathbf{G}_t)}{\partial z_{i,t}\partial z_{j,t}}=\phi g_{ij,t},$$

where the sign of ϕ determines whether the Nash equilibrium features strategic substitution ($\phi<0$) or complementarity ($\phi>0$). Note that the parameter restriction Eq. (7) implies that the denominator of Eq. (10) is always positive. Hence, the sign of ϕ and of the above cross-derivative depends on the sign of $\delta-\psi$. Strategic complementarity arises when δ is large, i.e., when either the payment velocity or the payment multiplier is large. Strategic substitution arises when ψ is high – i.e. in the presence of high marginal costs. Moreover, note that $sign(\partial\phi/\partial\psi)=-sign(\psi')$. Since internal funds are more flexible, it is natural to conjecture that they have higher opportunity cost than external ones, hence $\psi'>0$. In this case ϕ decreases in ψ: that is, as the overall marginal cost increases, the bilateral effect is pushed toward strategic substitution. This is quite intuitive: when internal liquidity has relatively higher opportunity cost, as the overall cost of holding liquidity increases, banks substitute internal liquidity with external one.

Proposition 1. *Suppose that $|\phi| < 1$. Then, there is a unique interior solution for the Nash equilibrium outcome given by*

$$z^*_{i,t}\left(\phi, \mathbf{G}_t\right) = \left\{\mathbf{M}\left(\phi, \mathbf{G}_t\right)\right\}_{i.}\, \mu_t, \tag{12}$$

where $\{\}_{i.}$ is the operator that returns the i-th row of its argument, $\mu_t \equiv \left[\mu_{1,t}, ..., \mu_{n,t}\right]^\top$, and

$$\mathbf{M}\left(\phi, \mathbf{G}_t\right) \equiv I + \phi\mathbf{G}_t + \phi^2\mathbf{G}_t^2 + \phi^3\mathbf{G}_t^3 + ... = \sum_{k=0}^{\infty} \phi^k \mathbf{G}_t^k = \left(I - \phi\mathbf{G}_t\right)^{-1}, \tag{13}$$

where I is the $N \times N$ identity matrix.

Proof. The first-order condition identifies the individual optimal response. Applying Theorem 1(b) in Calvo-Armengol et al. (2009) , we know the necessary equilibrium condition is $|\phi\lambda^{max}\left(\mathbf{G}_t\right)| < 1$ where the function $\lambda^{max}\left(\cdot\right)$ returns the largest eigenvalue. Since $\mathbf{G}_t$ is a right stochastic matrix, its largest eigenvalue is 1. Hence, the condition requires $|\phi| < 1$, and if so, the infinite sum in Eq. (13) is finite and equal to the stated result (Debreu and Herstein, 1953). ■

The condition $|\phi| < 1$ states that network externalities must be small enough in order to prevent the feedback triggered by such externalities to escalate without bounds. In vector form, $\mathbf{z}_t \equiv \left[z_{1,t}, ..., z_{N,t}\right]^\top$, and in equilibrium,

$$\mathbf{z}^*_t = \left(I - \phi\mathbf{G}_t\right)^{-1} \mu_t. \tag{14}$$

Note that in the Nash equilibrium, the aggregate level of bank reserves that support payments, $\sum_{i=1}^{N} z_{i,t}$, is not constrained by the supply of the central bank. It is fully determined by banks' reserve choices (the demand side). This assumption of perfectly elastic reserve supply is consistent with the empirical context – under the U.K. monetary policy framework, the Bank of England accommodates banks' reserve demand in order to maintain its policy rate.[12]

Note that Eq. (11), which leads to the equilibrium characterization in Proposition 1, is rather robust in that it could in principle be derived using different microfoundations other than the payment system dynamics. For instance, Eq. (11) can arise in an environment in which interbank relationships are driven by risk sharing motives as in Eisfeldt et al. (2020), or if banks have incentives to hold similar positions as in a beauty contest game à la Morris and Shin (2002). What changes across these different microfoundations is the economic interpretation of the network attenuation factor ϕ.[13] As we show in the empirical section below, the microfoundation of ϕ that we propose is supported by the data – the estimated ϕ has a strong positive correlation with the payment system velocity, which is part of δ, as postulated by our theory.

Network propagation. The matrix $\mathbf{M}(\phi, \mathbf{G}_t)$ has an important economic interpretation: it aggregates all direct and indirect links among banks using an attenuation factor, ϕ, that penalizes (as in Katz, 1953) the contribution of links between distant nodes at the rate ϕ^k, where k is the length of the path between nodes. In the infinite sum in Eq. (13), the identity matrix captures the (implicit) link of each bank with itself, the second term in the sum captures all the direct links between banks, the third term in the sum captures all the indirect links corresponding to paths of length two, and so on. The elements of $\mathbf{M}(\phi, \mathbf{G}_t)$, given by $m_{ij}(\phi, \mathbf{G}_t) \equiv \sum_{k=0}^{+\infty} \phi^k \left\{\mathbf{G}_t^k\right\}_{ij}$, aggregate all paths from j to i, where the kth step is weighted by ϕ^k.

In equilibrium, the matrix $\mathbf{M}(\phi, \mathbf{G}_t)$ contains information about the *centrality* of network players.[14] Multiplying the rows (columns) of $\mathbf{M}(\phi, \mathbf{G}_t)$ by

[12] For more details on the institutional background, please refer to the Online Appendix.

[13] We thank one of the referees for pointing this out.

[14] This centrality measure takes into account the number of both direct and indirect connections in a network. For more on the Bonacich centrality measure, see Bonacich (1987) and Jackson (2003). For other economic applications, see Ballester et al. (2006) and Acemoglu et al. (2012). For an excellent review of the literature, see Jackson and Zenou (2012).

a unit vector of conformable dimensions, we recover the indegree (outdegree) Katz–Bonacich centrality measure.[15] The indegree centrality measure provides the weighted count of the number of ties directed to each node (i.e., inward paths), while the outdegree centrality measure provides the weighted count of ties that each node directs to the other nodes (i.e., outward paths). That is, the i-th row of $\mathbf{M}(\phi, \mathbf{G}_t)$ captures how bank i loads on the network as whole, while the i-th column of $\mathbf{M}(\phi, \mathbf{G}_t)$ captures how the network as a whole loads on bank i.

The matrix $\mathbf{M}(\phi, \mathbf{G}_t)$ (which includes the network topology and the network attenuation factor ϕ) is *not* enough to determine the systemic importance of a bank. It governs the propagation of shocks. At the beginning of period t and before banks decide on reserve holdings, shocks to individual banks are realized, observed by banks and their neighbors, and encoded in $\mu_{i,t}$. Specifically, we can decompose $\mu_{i,t}$ into a time-invariant term, $\bar{\mu}_i$, and a shock specific to period t and bank i, $\nu_{i,t}$:

$$\mu_{i,t} = \bar{\mu}_i + \nu_{i,t}, \tag{15}$$

where $\nu_{i,t}$, the ultimate source of uncertainty, is a shock that is independent across banks and over time, with zero mean and variance equal to σ_i^2. The shock arrives at the beginning of period t, observed by all banks before the decision on reserve holdings is made.

To see clearly how the network propagates idiosyncratic shocks, we write Eq. (12) as

$$\mathbf{z}_t^* = \underbrace{\mathbf{M}(\phi, \mathbf{G}_t)\,\bar{\mu}}_{\text{level effect}} + \underbrace{\mathbf{M}(\phi, \mathbf{G}_t)\,\nu_t}_{\text{risk effect}}. \tag{16}$$

Regardless of $\mathbf{M}(\phi, \mathbf{G}_t)$, i.e., how shocks are propagated, banks with large liquidity shocks (i.e., large σ_i^2) have a large influence on other banks' reserve holdings.

[15] Newman (2004) shows that weighted networks can in many cases be analyzed using a simple mapping from a weighted network to an unweighted multigraph. Therefore, the centrality measures developed for unweighted networks apply also to the weighted cases.

The planner's solution. The model captures not only the shock amplification mechanism through the network but also the externalities. Individual banks make their own decisions without internalizing the impact on neighbors. We proceed to a formal analysis of the planner's problem in this interconnected system to highlight the wedge between decentralized equilibrium and social optimum. Specifically, we consider a planner that equally weights the utility of each bank and hence chooses liquidity holdings by solving the following problem:

$$\max_{\{z_{i,t}\}_{i=1}^{N}} \sum_{i=1}^{N} u_i(z_{i,t}, \{z_{j,t}\}_{j\neq i} | \mathbf{G}_t). \tag{17}$$

The planner's first-order condition for bank i's liquidity yields

$$\begin{aligned}
&\delta\left(z_{i,t} + \eta \sum_{j\neq i} g_{ij,t} z_{j,t}\right) + \eta \sum_{j\neq i} g_{ji,t} \delta \left(z_{j,t} + \eta \sum_{k\neq j} g_{jk,t} z_{k,t}\right) \qquad (18)\\
&= \left[\gamma + \psi\left(z_{i,t} + \eta \sum_{j\neq i} g_{ij,t} z_{j,t}\right) + \widetilde{\mu}_{i,t}\gamma' + \psi' z_{i,t}\right] + \eta \sum_{j\neq i} g_{ji,t}\left[\gamma + \psi\left(z_{j,t} + \eta \sum_{k\neq j} g_{jk,t} z_{k,t}\right)\right].
\end{aligned}$$

The first term on the left-hand side and the terms in the first square bracket on the right-hand side are the same as those in bank i's first-order condition in the decentralized equilibrium. The new terms reflect network externalities that bank i ignores in its own optimization. Specifically, the outdegree link, $g_{ji,t}$, prominently captures the impact of bank i's decision of $z_{i,t}$ on neighboring banks' decisions through the marginal revenue of payment services (the second term on the left) and the marginal cost of liquidity (the second term on the right).

We can write the first-order conditions for $\{z_{i,t}\}_{i=1}^{N}$ in vector form as:

$$\left(I + \eta \mathbf{G}_t^{\top}\right)(\delta \mathbf{z}_t + \delta\eta \mathbf{G}_t \mathbf{z}_t) = \left(I + \eta \mathbf{G}_t^{\top}\right)(\gamma \mathbf{1} + \psi \mathbf{z}_t + \psi\eta \mathbf{G}_t \mathbf{z}_t) + \widetilde{\mu}_t \gamma' + \psi' \mathbf{z}_t. \tag{19}$$

Thus, we obtain the following planner's solution:

$$\begin{aligned}\mathbf{z}_t^p &= \left[\psi' I - (\delta - \psi)\left(I + \eta \mathbf{G}_t^\top\right)(I + \eta \mathbf{G}_t)\right]^{-1}\left[-\widetilde{\mu}_t \gamma' - \gamma\left(I + \eta \mathbf{G}_t^\top\right)\mathbf{1}\right] \\ &= \left[I - \left(\frac{\phi/\eta}{1+\phi/\eta}\right)\left(I + \eta \mathbf{G}_t^\top\right)(I + \eta \mathbf{G}_t)\right]^{-1}\left[\left(\frac{1}{1+\phi/\eta}\right)\mu_t - \frac{\gamma\eta}{\psi'}\mathbf{G}_t^\top \mathbf{1}\right].\end{aligned} \tag{20}$$

This allows us to formally state the planner's solution, which will guide our empirical analysis, especially the comparison between the decentralized outcome and the planner's solution.

Proposition 2. *Let* $\mathbf{M}^p(\phi, \eta, \mathbf{G}_t) \equiv \left[I - \left(\frac{\phi/\eta}{1+\phi/\eta}\right)\left(I + \eta \mathbf{G}_t^\top\right)(I + \eta \mathbf{G}_t)\right]^{-1}$. *Suppose that the absolute value of the maximum eigenvalue of* $\mathbf{M}^p(\phi, \eta, \mathbf{G}_t)$, $|\lambda^{max}(\mathbf{M}^p(\phi, \eta, \mathbf{G}_t))|$, *is smaller than one. Then, the planner's optimal solution is uniquely defined and given by*

$$\mathbf{z}_t^p = \mathbf{M}^p(\phi, \eta, \mathbf{G}_t)\left[\left(\frac{1}{1+\phi/\eta}\right)\mu_t - \frac{\gamma\eta}{\psi'}\mathbf{G}_t^\top \mathbf{1}\right]. \tag{21}$$

Proof. The proof follows the same argument as in the proof of Proposition 1. ■

4. Empirical method

4.1. From model to data

In our model, banks hold reserves for two purposes: $q_{i,t}$ for reasons unrelated to interbank network and payment system, and $z_{i,t}$ to support the payment system. In the data, we only observe $l_{i,t} = q_{i,t} + z_{i,t}$, i.e., the total reserve holdings. In other words, unlike the banks in the network game, the econometrician cannot separately observe $q_{i,t}$ and $z_{i,t}$. However, we do observe bank characteristics ($x_{i,t}^m$) and macroeconomic variables (x_t^p) that drive $q_{i,t}$. Therefore, we can write the observed total reserve holdings as

$$l_{i,t} = \alpha_t^{week} + \alpha_i^{bank} + \sum_{m=1}^{M} \beta_m^{bank} x_{i,t}^m + \sum_{p=1}^{P} \beta_p^{macro} x_t^p + z_{i,t}, \tag{22}$$

where $i = 1, ..., n$, $t = 1, ..., T$, and according to our model we have that

$$z_{i,t} = \bar{\mu}_i + \phi \sum_{j=1}^{N} g_{ij,t} z_{j,t} + \nu_{i,t} \sim iid\left(0, \sigma_i^2\right). \tag{23}$$

Note that we also include week fixed effects to control for unobserved macro factors in $q_{i,t}$. Eq. (22) and Eq. (23) together constitute a spatial error model (SEM) (see e.g. Anselin, 1988; Elhorst, 2010b,a). Such models allow the joint estimation of the fixed effects and β coefficients in the observational Eq. (22), and $\bar{\mu}_i$, ϕ, and σ_i in the "error" Eq. (23). Therefore, even though the econometrician does not observe $z_{i,t}$ directly, the parameters of the network game can still be recovered. In the next subsection, we provide more details on the identification of these parameters.

We estimate the model using daily data. On day t, the network is predetermined; $g_{ij,t}$ is measured by the fraction of bank i's borrowing from bank j (average over the month up to t). As econometricians, we observe banks' characteristics, i.e., $\{x_{i,t}^m\}_{m=1}^M$ for bank i, and macro variables, i.e., $\{x_t^p\}_{p=1}^P$, which help us to separate, $q_{i,t}$, from the observed total liquidity holding, $l_{i,t}$, and thereby identify the impact of the network through the residual term, $z_{i,t}$. All control variables are lagged by one day for predeterminancy. The estimate of ϕ reveals the type of equilibrium on the network, i.e., strategic substitution or complementarity. To exhibit variation in ϕ and allow for changes in $\{\sigma_i\}_{i=1}^N$, we estimate the model in both subsamples and rolling samples.

4.2. Identification

The identification strategy, the likelihood function, and the estimation algorithm are discussed in detail in the Online Appendix. Nevertheless, to fix intuition about how the key network parameter, ϕ, is recovered from the data, it is useful to consider a simplified version of the spatial error model in Eq. (22) and Eq. (23). Let $L_t \in \mathbb{R}^N$ denote the vector containing the liquidity holdings of the individual banks at time t, and to simplify exposition let us disregard at first the fixed effects in Eq. (22) and Eq. (23) and assume that the spatial network matrix, $\mathbf{G}$, has constant weights. The spatial model can then be rewritten as

$$L_t = X_t\beta + z_t, \quad z_t \sim iid\left(0_N, \Omega\right), \tag{24}$$

where 0_N denotes a vector of zeros, $\Omega = M\Sigma_\nu M^\top$ with $M = \left(I_N - \phi\mathbf{G}\right)^{-1}$, and Σ_ν is a diagonal matrix with elements given by $\left\{\sigma_i^2\right\}_{i=1}^N$. In deriving the covariance Ω, we used Proposition 1, i.e., that in equilibrium we can rewrite z_t (having, for now, removed the fixed effects) as $z_t = \left(I_N - \phi\mathbf{G}\right)^{-1}\nu_t$, where ν_t has a normal distribution with zero mean and covariance Σ_ν.

Therefore, the likelihood of the model is given by

$$\ln\mathcal{L} \equiv -\frac{TN}{2}\ln\left(2\pi\right) - \frac{T}{2}\sum_{i=1}^N \ln\sigma_i^2 - \sum_{i=1}^N \frac{1}{2\sigma_i^2}\sum_{t=1}^T \nu_{i,t}^2. \tag{25}$$

The error term, $\nu_{i,t}$, contains the parameters and observables

$$\nu_{i,t} = \left\{\left(I_N - \phi\mathbf{G}\right)\left(L_t - X_t\beta\right)\right\}_{i.}, \tag{26}$$

where $\{\}_{i.}$ is the operator that returns the i-th row of its argument. In the likelihood, all the variables, L_t and X_t, and the network, $\mathbf{G}$, are observed, and z_t disappears because it is substituted out by $L_t - X_t\beta \equiv z_t$. We maximize the likelihood to obtain the parameter estimates using standard optimization methods.

The reduced form specification in Eq. (24) has the same structure and properties as the seemingly unrelated regressions (SUR model: see e.g. Zellner, 1962). Hence, one can consistently estimate the mean equation parameter, β (e.g., via linear projections), and use the fitted residuals to construct a consistent estimate of the covariance matrix Ω. However, can we recover the structural parameters ϕ and $\left\{\sigma_i^2\right\}_{i=1}^N$? Being symmetric, the estimated $\widehat{\Omega}$ gives $N(N+1)/2$ equations, while we have to recover $N+1$ parameters in $M\Sigma_\nu M^\top$ (ϕ plus the bank-specific volatilities). Therefore, as long as Ω is full-rank, the system is over-identified if we have three or more banks (with linearly independent links). In a nutshell, the identification of this spatial error formulation works like that of structural vector autoregressions (see, e.g., Sims and Zha, 1999) where the contemporaneous propagation of shocks among dependent variables (captured by ϕ in our setting) can be recovered from the reduced-form covariance structure.[16]

Note that what allows the identification of ϕ and $\{\sigma_i^2\}_{i=1}^N$ are exactly two key restrictions coming from the theoretical model: (1) the observed liquidity holdings, $l_{i,t}$, can be decomposed into $q_{i,t}$, driven by the control variables in X_t, and $z_{i,t}$, banks' liquidity contribution to the payment system; (2) Proposition 1 states how the network component $z_{i,t}$ depends on the bank-specific (structural) shocks in equilibrium. The first restriction defines the mean equation in Eq. (24), allowing us to recover $z_{i,t}$ as residuals.[17] The second restriction imposes a structure on the covariance matrix of $z_{i,t}$, allowing us to recover ϕ and $\{\sigma_i^2\}_{i=1}^N$.

To sharpen the intuition, let us consider a system of three banks and the simplest network, a chain: Bank 1 borrows from Bank 2, and 2 from 3, so

$$\mathbf{G} = \begin{bmatrix} 0 & 1 & 0 \\ 0 & 0 & 1 \\ 0 & 0 & 0 \end{bmatrix}, \text{ and } M\Sigma_\nu M^\top = \begin{bmatrix} \sigma_1^2 + \phi^2\sigma_2^2 + \phi^4\sigma_3^2 & \phi\sigma_2^2 + \phi^3\sigma_3^2 & \phi^2\sigma_3^2 \\ \phi\sigma_2^2 + \phi^3\sigma_3^2 & \sigma_2^2 + \phi^2\sigma_3^2 & \phi\sigma_3^2 \\ \phi^2\sigma_3^2 & \phi\sigma_3^2 & \sigma_3^2 \end{bmatrix}.$$

The volatility of z_1 is $\sigma_1^2 + \phi^2\sigma_2^2 + \phi^4\sigma_3^2$. The first term is the volatility of Bank 1's structural shock, ν_1. The second term is the volatility of Bank 2's structural shock transmitted by one step to Bank 1, i.e., ϕz_2, and the third term reflects Bank 3's shock transmitted by two steps (via Bank 2) to Bank 1, i.e., $\phi^2 z_3$. By the same logic, the volatility of z_2 is $\sigma_2^2 + \phi^2\sigma_3^2$, capturing Bank 2's exposure to its own shock and Bank 3's shock, while Bank 3 only

[16] For an extensive discussion of estimation and identification of spatial models see Anselin (1988), and chapter 8 in particular for the spatial error model.

[17] Ideally, if we were to observe $q_{i,t}$ and $z_{i,t}$ separately, we could estimate ϕ and $\{\sigma_i^2\}_{i=1}^N$ only using the data on $z_{i,t}$. But as econometricians we only observe $l_{i,t} = q_{i,t} + z_{i,t}$ and the control variables that drive $q_{i,t}$, so we estimate ϕ and $\{\sigma_i^2\}_{i=1}^N$ and the control variables' coefficients jointly.

loads on its own shock. The covariance between z_1 and z_2 is $\phi\sigma_2^2 + \phi^3\sigma_3^2$, reflecting Banks 1's and 2's exposure to Banks 2's and 3's shocks. The covariance between z_2 and z_3 is $\phi\sigma_3^2$ as it only arises from the one-step transmission of Bank 3's shock to Bank 2, i.e., ϕz_3. Such covariances are precisely due to network connections, and their estimates identify the network effect parameter, ϕ. Given $\sigma_3^2 = \{\widehat{\Omega}\}_{3,3}$, we can solve for ϕ using either the covariance between z_1 and z_3, i.e., $\{\widehat{\Omega}\}_{1,3} = \phi^2\sigma_3^2$, or the covariance between z_2 and z_3, i.e., $\{\widehat{\Omega}\}_{2,3} = \phi\sigma_3^2$, so the system is clearly over-identified. Moreover, given the estimates of σ_3^2 and ϕ, either the volatility of z_2, i.e., $\{\widehat{\Omega}\}_{2,2} = \sigma_2^2 + \phi^2\sigma_3^2$, or the covariance between z_1 and z_2, i.e., $\{\widehat{\Omega}\}_{1,2} = \phi\sigma_2^2 + \phi^3\sigma_3^2$, give a solution for σ_2^2. Finally, given ϕ, σ_2^2, and σ_3^2, $\{\widehat{\Omega}\}_{1,1}$ pins down σ_1^2.

A key identifying assumption is that the structural shocks, ν_i, are independent across banks, and thus, after controlling for the observed bank characteristics and macro variables, the residuals' (i.e., z_i's) correlations only arise from the network linkages. Therefore, the impact of the network, ϕ, is identified by such correlations. Accordingly, in the estimation, we saturate the mean equation by controlling for a rich set of bank characteristics and macro variables, so the residual correlations are driven by the network linkages instead of missing variables that induce comovement among banks' liquidity choices.

Note that, in general, if we knew the parameters ϕ and $\left\{\sigma_i^2\right\}_{i=1}^N$ we could actually premultiply the specification in Eq. (24) by the Cholesky decomposition of Ω^{-1}, obtaining a transformed system with spherical errors, and therefore gaining efficiency of the estimates – e.g., we could do the canonical GLS transformation. For this reason, rather than employing a two-step procedure, we jointly estimate the mean equation and covariance parameters by maximizing the quasi-maximum likelihood function (as described in detail in the Appendix).

The above identification argument is not affected by time variation in $\mathbf{G}$ as long as we have a well-defined unconditional variance.[18] Furthermore, the iden-

[18] The identification is in this case analogous to that of S-VARs with time varying volatility as, e.g., in Primiceri (2005).

tification of ϕ does not depend on whether we can *separately* identify network fixed effects (the $\bar{\mu}_i$) from the bank fixed effects (the α_i^{bank}). Adding these fixed effects, Eq. (24) becomes

$$L_t = \alpha^{bank} + X_t\beta + (I_N - \phi\mathbf{G})^{-1}\bar{\mu} + \epsilon_t, \quad \epsilon_t \sim iid\,(0_N, \Omega)\,, \tag{27}$$

where α^{bank} is the vector of bank specific fixed effect, $\bar{\mu}$ is the vector of bank specific $\bar{\mu}_i$, $\epsilon_t \equiv (I_N - \phi\mathbf{G})^{-1}\nu_t$ is orthogonal to X_t, and as before, $\Omega = MVM^{\top}$ with $M = (I_N - \phi\mathbf{G})^{-1}$. Once again, the above is an SUR; hence, the logic for the identification of ϕ stays unchanged, independent from whether we can *separately* identify $\bar{\mu}$ and α^{bank}.

It is clear that in the above equation, α^{bank} and $\bar{\mu}$ are in general not separately identified, even with time variation in the network matrix – i.e., if we replace $\mathbf{G}$ with $\mathbf{G}_t$ in the above equation. This is because $\mathbf{I}_N$ (the identity matrix and regressor associated with α^{bank}) and $(I_N - \phi\mathbf{G}_t)^{-1}$ (the regressor associated with $\bar{\mu}$ in Eq. (24)) are not linearly independent when $\mathbf{G}_t\mathbf{1}_N = \mathbf{1}_N$ for all t, i.e., when $\mathbf{G}_t$ is always a right stochastic matrix.[19] Fortunately, our sample has an interesting feature: banks 7 and 11 were not connected with other banks in 14 and 145 days, respectively. These 159 days do not overlap. They cover 13.5% of the time and spread across our subsamples. On such days, one row of $\mathbf{G}_t$ has all elements equal to zero, and thus, $\mathbf{G}_t\mathbf{1}_N \neq \mathbf{1}_N$. Therefore, we can separately identify $\bar{\mu}$ and α^{bank} using the time variation in $\mathbf{G}_t$.

4.3. Systemic risk

The empirical model in Eq. (22) and Eq. (23) highlights that the network is a shock propagation mechanism: a shock to bank j is transmitted to bank i through $\phi g_{ij,t}$, so if $\phi > 0$ (strategic complementarity), the network amplifies shocks, and if $\phi < 0$ (strategic substitution), the network buffers shocks.

[19] To see this, note that $(I_N - \phi\mathbf{G}_t)^{-1}\mathbf{1}_N = \sum_{k=0}^{\infty}\phi^k\mathbf{G}_t^k\mathbf{1}_N = \left(\frac{1}{1-\phi}\right)\mathbf{1}_N = \left(\frac{1}{1-\phi}\right)\sum_{i=1}^{N}\{I_N\}_i$, i.e., a linear combination of the columns of $(I_N - \phi\mathbf{G}_t)^{-1}$ is equal to a linear combination of the columns of $\mathbf{I}_N$.

The ultimate impact of shocks to all banks is

$$\epsilon_t = (I - \phi \mathbf{G}_t)^{-1} \nu_t = \mathbf{M}(\phi, \mathbf{G}_t) \nu_t, \tag{28}$$

where $\nu_t = [\nu_{1,t}, ..., \nu_{n,t}]^\top$ denotes the structural bank shocks and, as shown by Eq. (13), $\mathbf{M}(\phi, \mathbf{G}_t)$ records the routes that propagate ν_t with the direction governed by ϕ. We can define $(1-\phi)^{-1}$ as the "average network multiplier". If $\mathbf{G}_t$ is a right stochastic matrix (i.e., $\mathbf{G}_t \mathbf{1}_N = \mathbf{1}_N$), then a unit shock to the system equally spread across banks (i.e., $\nu_t = (1/n)\mathbf{1}_N$) has an ultimate impact on aggregate liquidity equal to $(1-\phi)^{-1}$.[20]

With the estimated parameters at hand, we identify the key contributors of systemic risk (the "risk key players"). First, we can decompose the *aggregate* network-induced liquidity, $Z_t \equiv \sum_i z_{i,t}$, as

$$Z_t^* = \underbrace{\mathbf{1}^\top \mathbf{M}(\phi, \mathbf{G}_t)\bar{\mu}}_{\text{level effect}} + \underbrace{\mathbf{1}^\top \mathbf{M}(\phi, \mathbf{G}_t)\nu_t}_{\text{risk effect}}, \tag{29}$$

where $\bar{\mu} \equiv [\bar{\mu}_1, ..., \bar{\mu}_n]^\top$. The first term captures the network level effect, and the second captures the risk effect by aggregating idiosyncratic shocks. Note that even when N is large, idiosyncratic shocks may not vanish in aggregation because of the network effects in $\mathbf{M}(\phi, \mathbf{G}_t)$ (similar to Acemoglu et al., 2012).

We measure risk by the conditional volatility of the aggregate liquidity, so we simply work with the demeaned liquidity:

$$Var_t(Z^*) = \mathbf{1}^\top \mathbf{M}(\phi, \mathbf{G}_t)\Sigma_\nu \mathbf{M}(\phi, \mathbf{G}_t)^\top \mathbf{1}, \tag{30}$$

where Σ_ν is the covariance matrix of ν_t, a diagonal matrix whose i-th diagonal element is σ_i^2. Here we have used the fact that $\mathbf{G}_t$ is predetermined with respect to time-t information. To identify risk key players, we define the network impulse response function as follows.

[20] From $\mathbf{1}_N = (I_N - \phi\mathbf{G}_t)^{-1}(I_N - \phi\mathbf{G}_t)\mathbf{1}_N = (I_N - \phi\mathbf{G}_t)^{-1}\mathbf{1}_N(1-\phi)$, we have $\mathbf{M}(\phi, \mathbf{G}_t)\mathbf{1}_N = (1-\phi)^{-1}\mathbf{1}_N$.

Definition 1 (Network Impulse Response Function). *The network impulse response function of aggregate liquidity, Z_t^*, to a one standard deviation shock to a bank i, is given by*

$$NIRF_i\left(\phi, \sigma_i, \mathbf{G}_t\right) \equiv \frac{\partial Z_t^*}{\partial \nu_{i,t}} \sigma_i = \mathbf{1}^\top \left\{\mathbf{M}\left(\phi, \mathbf{G}_t\right)\right\}_{.i} \sigma_i, \tag{31}$$

where the operator $\{\}_{.i}$ returns the i-th column of its argument.

The network impulse response is the shock-size weighted *outdegree* centrality of bank i. As a reminder, for $|\phi| < 1$,

$$\mathbf{1}^\top \left\{\mathbf{M}\left(\phi, \mathbf{G}_t\right)\right\}_{.i} = \mathbf{1}^\top \left\{I + \phi \mathbf{G}_t + \phi^2 \mathbf{G}_t^2 + ...\right\}_{.i} = \mathbf{1}^\top \left\{\sum_{k=0}^{\infty} \phi^k \mathbf{G}_t^k\right\}_{.i},$$

where the initial element in the series captures direct effects of a unit shock to bank i, the next element is the sum of first-order outbound links, the third element is the sum of second-order outbound links, and so on. $NIRF_i\left(\phi, \sigma_i, \mathbf{G}_t\right)$ measures a bank's contribution to the volatility of aggregate liquidity and thus identifies the risk key player by providing a clear ranking of the riskiness of each bank from a systemic perspective.

Definition 2 (Risk Key Player). *The risk key player i_t^*, given by the solution of*

$$i_t^* = \underset{i=1,\ldots,N}{\arg\max} \;\; NIRF_i\left(\phi, \sigma_i, \mathbf{G}_t\right), \tag{32}$$

is the one that contributes the most to the conditional volatility of aggregate network liquidity.

A bank's risk contribution depends on the size of its own shock σ_i, the network attenuation factor, ϕ, and all the direct and indirect network links. The network impulse response functions offer a natural decomposition of volatility, since

$$Var_t\left(Z^*\right) \equiv vec\left(\left\{NIRF_i\left(\phi, \sigma_i, \mathbf{G}_t\right)\right\}_{i=1}^N\right)^\top vec\left(\left\{NIRF_i\left(\phi, \sigma_i, \mathbf{G}_t\right)\right\}_{i=1}^N\right), \tag{33}$$

where "vec" is the vectorization operator.

We can isolate the purely network-driven part of the impulse response, that is, the impact beyond direct effects of bank-level shocks, which we call the "excess NIRF":

$$NIRF_i^e\left(\phi, \sigma_i, \mathbf{G}_t\right) \equiv NIRF_i\left(\phi, \sigma_i, \mathbf{G}_t\right) - \sigma_i. \tag{34}$$

The sign of $NIRF_i^e\left(\phi, \sigma_i, \mathbf{G}_t\right)$ depends on the type of equilibrium (strategic substitution or complementarity), i.e., the sign of ϕ. Note that it is straightforward to compute confidence bands for the estimated $NIRF$s using the delta method, since they are functions of $\hat{\phi}$ and $\{\hat{\sigma_i}\}_{i=1}^N$ that have canonical asymptotic Gaussian distribution (see the Online Appendix).

After we obtain the estimates of ϕ and $\{\sigma_i\}_{i=1}^N$, we compare the volatility of aggregate liquidity from the decentralized equilibrium, i.e., $Var_t\left(Z^*\right)$ defined in Eq. (30), and the volatility of aggregate liquidity from the planner's solution given by

$$Var_t\left(Z^p\right) = \left(\frac{1}{1+\phi/\eta}\right)^2 \mathbf{1}^\top \mathbf{M}^p\left(\phi, \eta, \mathbf{G}_t\right) \Sigma_\nu \mathbf{M}^p\left(\phi, \eta, \mathbf{G}_t\right)^\top \mathbf{1}, \tag{35}$$

where $Z^p \equiv \sum_i z_{i,t}^p$ and $\mathbf{M}^p\left(\phi, \eta, \mathbf{G}_t\right)$ is defined in Proposition 2.

Finally, we also identify the "systemic level key player", whose removal from the system causes the largest reduction of aggregate liquidity level in expectation.[21] A key input is the average liquidity valuation, i.e., $\bar{\mu}$. Since our empirical analysis focuses on shock propagation through the network instead of the sample average of liquidity level, we present the theoretical results on the level key players in Appendix A.3.

[21] This definition is in the same spirit as the concept of the key player in the crime network literature, e.g., Ballester et al. (2006), where targeting key players is important for crime reduction.

4.4. Alternative specification

As a specification test of our model, we consider a more general formulation that allows for richer network interactions. That is, we model the liquidity holding game as a spatial Durbin model (SDM – see, e.g. LeSage and Pace, 2009) where a bank's liquidity depends directly on other banks' liquidity and pairwise control variables

$$l_{i,t} = \phi \sum_{j \neq i} g_{ij,t} l_{j,t} + \sum_{m=1}^{M} \beta_m^{bank} x_{i,t}^m + \sum_{p=1}^{P} \chi_p x_t^p + \sum_{j=1}^{N} g_{ij,t} \sum_{m=1}^{M} \theta_m x_{j,t}^m + \bar{\mu}_i + \nu_{i,t} \sim iid\left(0, \sigma_i^2\right).$$

In Appendix A.2, we show that the above formulation is the equilibrium outcome of a network game in which banks can borrow both the neighbors' liquidity held for their depositors' payments (i.e., $z_{i,t}$) and, up to a fraction ρ, the neighbors' liquidity held for their own payments (i.e., $q_{i,t}$). The coefficients χ_p and θ_m are related to the main model as follows: $\chi_p \equiv \left[1 - \phi\left(1-\rho\right)\right] \beta_p^{macro}$ and $\theta_m \equiv -\phi\left(1-\rho\right) \beta_m^{bank}$. Therefore, this formulation nests the main model as a special case: when $\rho = 0$, i.e., banks can only access neighbors' $z_{i,t}$, we can rearrange the equation and get back to the main model,

$$\underbrace{l_{i,t} - \sum_{m=1}^{M} \beta_m^{bank} x_{i,t}^m - \sum_{p=1}^{P} \beta_p^{macro} x_t^p}_{z_{i,t}} = \phi \sum_{j \neq i} g_{ij,t} \underbrace{\left[l_{j,t} - \sum_{m=1}^{M} \beta_m^{bank} x_{j,t}^m - \sum_{p=1}^{P} \beta_p^{macro} x_t^p \right]}_{z_{j,t}} + \bar{\mu}_i + \nu_{i,t}.$$

Note that our baseline SEM is a conservative approach, leaving a minimal amount of variation in liquidity holdings to be driven by the network. In contrast, the SDM allows the network to play a larger role since banks' reserve holdings in this case depend not only on shocks to other banks but also on other banks' characteristics. In Section 6, we compare the estimates of SDM with those of our benchmark model (SEM) in rolling windows. Given that the SDM nests the SEM, the comparison can be viewed as a specification test of the main model. In the Online Appendix, we discuss identification and estimation of the SDM parameters.

5. Data description

We study the liquidity holdings of banks that are members of CHAPS, the U.K. large-value payment system. These eleven banks are at the core of the U.K. banking system, conducting transactions for their own purpose and on behalf of their clients and hundreds of nonmember banks.[22] Their liquidity holdings serve the critical purpose of buffering intraday flow imbalances, ensuring the functioning of the transaction system for the whole economy. Our sample covers the period from January 2006 to September 2010, which allows us to estimate the network effect in the pre-crisis period, during the financial crisis, and later in the era of quantitative easing. We focus on the daily variation of liquidity holdings, so the model is estimated at daily frequency while incorporating variables constructed from higher frequency data.

Liquidity holdings. To measure the dependent variable $l_{i,t}$, that is, the liquidity holdings of each bank, we use central bank reserve holdings (logarithm). We supplement this with the collateral assets that are posted at the Bank of England and allow banks to access intraday liquidity from the Bank of England (these repos are unwound at the end of each day).

The weekly average of aggregate liquidity in the system (the sum of banks' holdings) is reported in Fig. 1. The figure shows a substantial upward trend in the period after the U.S. subprime mortgage crisis that saw several market disruptions. This trend is consistent with the evidence that banks hoard liquidity in crisis (e.g., Acharya and Merrouche, 2010), but this upward trend

[22] The banks are Halifax Bank of Scotland (owned by Lloyds Banking Group), Barclays, Citibank, Clydesdale (owned by National Australia Bank), Co-operative Bank (owned by The Co-operative Group), Deutsche Bank, HSBC (which acquired Midland Bank – one of the historical "big four" sterling clearing banks, in 1999), Lloyds TSB, Royal Bank of Scotland (including NatWest), Santander (formerly Abbey, Alliance & Leicester and Bradford & Bingley, owned by Banco Santander of Spain), and Standard Chartered. For most of the 20th century, the phrase "the Big Four" referred to the four largest sterling banks, which acted as clearing houses for bankers' cheques. These were Barclays Bank, Midland Bank (now part of HSBC), Lloyds Bank (now Lloyds TSB Bank and part of Lloyds Banking Group), and National Westminster Bank ("NatWest", now part of The Royal Bank of Scotland Group). Currently, the largest four U.K. banks are Barclays, HSBC, Lloyds Banking Group, and The Royal Bank of Scotland Group, closely followed by Standard Chartered – and all of these banks are in our sample.

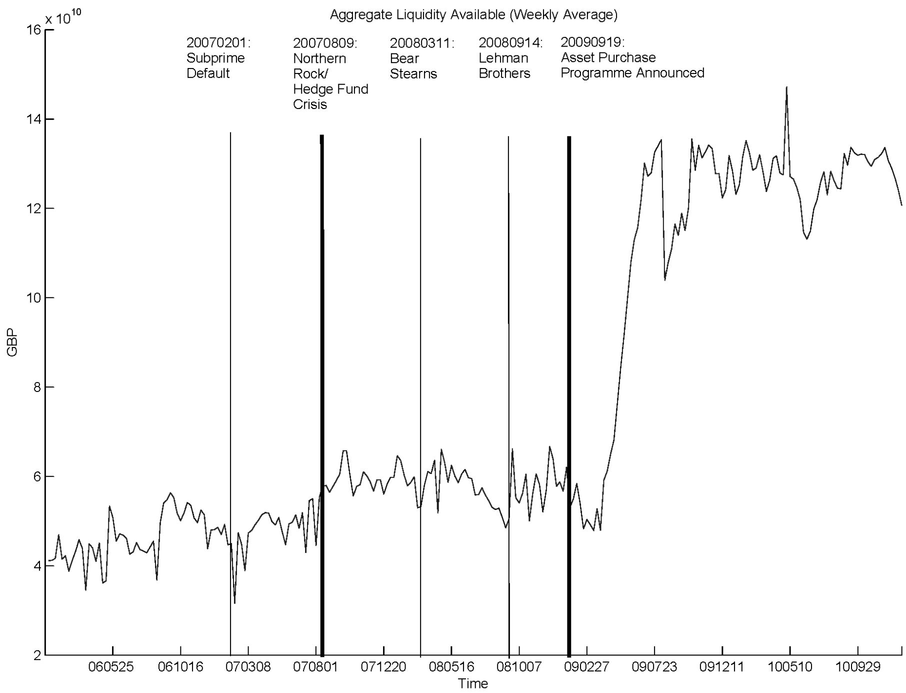

Fig. 1. Weekly rolling average of aggregate liquidity holdings of eleven CHAPS member banks at the beginning of the day (Unit: £1).

is dwarfed by the steep run-up in response to the Asset Purchase Programme (also known as quantitative easing) that almost tripled the aggregate liquidity. Note that since we include week fixed effects and macro control variables, this trend is unlikely to affect our estimate of ϕ, and in particular, induce a positive bias in $\hat{\phi}$ that is due to trend-induced comovement (i.e., spurious strategic complementarity in banks' liquidity holdings).

Interbank network. We construct the interbank network G_t using interbank borrowing data that we extract from overnight interbank payments using the Furfine (2000) algorithm. This algorithm is a common approach in the literature on the interbank money market, identifying pairs of payments between two banks where the outgoing payments are loans and the incoming payments are repayments (equal to the outgoing payment plus an interest rate). It has been tested thoroughly and accurately tracks the LIBOR rate.[23] Furfine (2000) showed that when applied to Fedwire data, the algorithm accurately identifies the Fed Funds rate.[24]

The loan data are compiled to form an interbank lending and borrowing network. In particular, the element $g_{ij,t}$ of the adjacency matrix $\mathbf{G}_t$ is given by the *average* fraction of bank's i overnight loans from bank j in the previous month ending on day $t-1$.

By construction, $\mathbf{G}_t$ is a square right stochastic matrix. Its largest eigenvalue is therefore equal to one. This implies that the strength of shock propagation on the network depends on the second largest eigenvalue of $\mathbf{G}_t$, which is plotted in Fig. 2.[25] There was a substantial increase in the crisis period, but what is striking is the large variation of network topology after QE. The variation of G_t is critical for us to empirically identify the network parameters.

Another way to exhibit the variation of G_t is to plot a measure of network cohesiveness, for which we use the average clustering coefficient (ACC – see Watts and Strogatz, 1998)

$$ACC_t = \frac{1}{N}\sum_{i=1}^{N} CL_i(\mathbf{G_t}), \quad CL_{i,t} = \frac{\#\{jk \in \mathbf{G}_t \mid k \neq j,\, j \in n_i(\mathbf{G_t}),\, k \in n_i(\mathbf{G}_t)\}}{\#\{jk \mid k \neq j,\, j \in n_i(\mathbf{G}_t),\, k \in n_i(\mathbf{G}_t)\}}$$

[23] The data are only available for CHAPS banks. Thus, some loans may be attributed to a settlement bank when in fact the payments are made on behalf of its customers. Moreover, where a loan is made between one customer of a settlement bank and another, this transaction will not be settled through the payment system but rather across the books of the settlement bank (internalization). Internalized payments are invisible to the BoE, so they are a part of the overnight money market that is not captured here.

[24] As documented in Armantier and Copeland (2012), Furfine's algorithm can be affected by Type I and, to a lesser extent, Type II, errors. Nevertheless, this is less of a concern in our application because of the following: first, as documented in Kovner and Skeie (2013), at the overnight frequency that we focus on, interbank exposures measured by the algorithm are highly correlated with the Fed funds borrowing and lending reported in bank quarterly regulatory filings; second, and more importantly, instead of using the daily borrowing and lending data, we smooth these exposures by computing rolling monthly averages, therefore greatly reducing the relevance of false positives and negatives in the identification of interbank relationships. Furthermore, we apply several robustness checks on our measure of interbank linkages (results available upon request).

[25] This is because $\mathbf{G}^k$ can be rewritten in Jordan normal form as $\mathbf{P}\mathbf{J}^k\mathbf{P}^{-1}$, where $\mathbf{J}$ is the (almost) diagonal matrix with eigenvalues (or Jordan blocks in case of repeated eigenvalues) on the main diagonal.

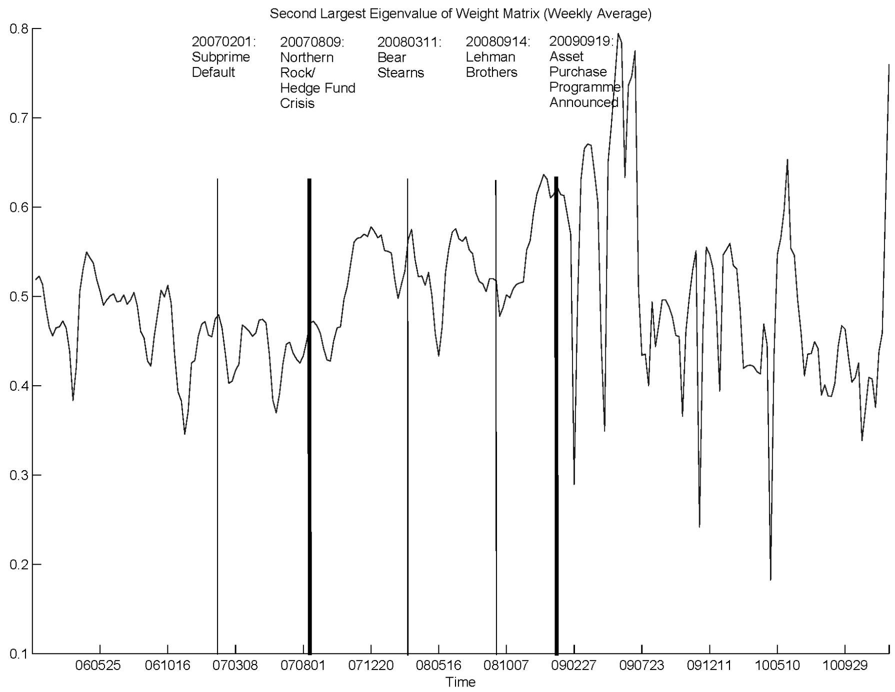

Fig. 2. Second largest eigenvalue of the matrix $\mathbf{G}_t$ with elements $g_{ij,t}$ given by the average share of bank's i overnight loans from bank j in the previous month ending on day $t-1$.

where $n_i(\mathbf{G}_t)$ is the set of players that have a direct link with i and $\#\{.\}$ is the count operator. The numerator is the number of pairs linked to i that are also linked to each other, while the denominator is simply the number of pairs linked to i. Therefore, ACC measures the average proportion of banks that are connected to i and also connected with each other. By construction, it ranges from 0 to 1. A higher value means that the network is more dense.

The time series of ACC is shown in Fig. 3. At the beginning of our sample, the network is highly cohesive since, on average, approximately 80% of pairs of banks connected to any given bank are also connected to each other. The degree of connectedness appears to have a decreasing trend during 2007–2008, and a substantial and sudden decrease following the Asset Purchase Programme, when ACC dropped by approximately one-quarter of its pre-crises average. This is

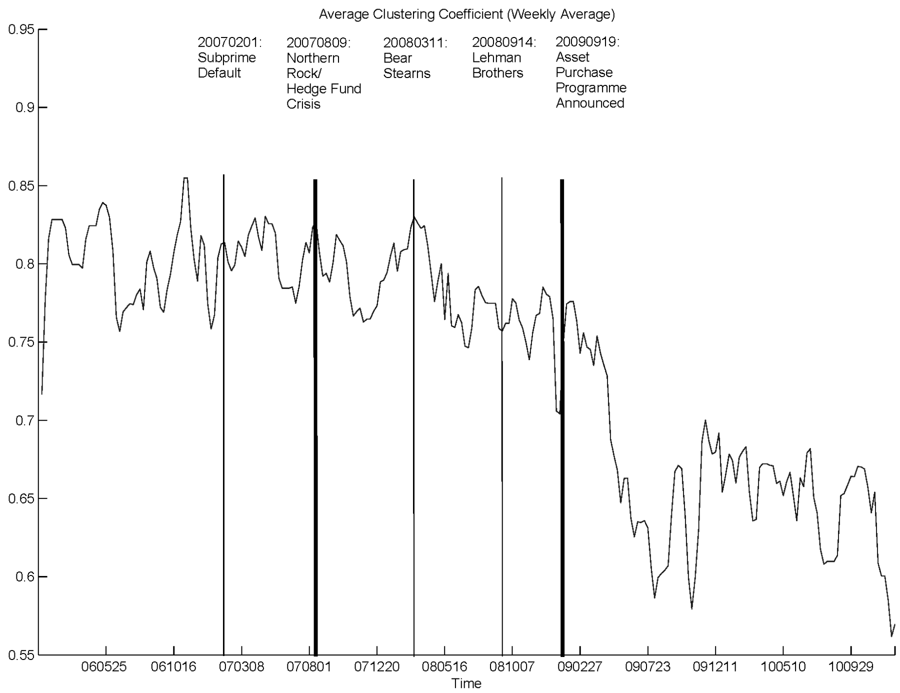

Fig. 3. Average clustering coefficient (see Watts and Strogatz, 1998) of the interbank network.

related to the reduced interbank borrowing needs during the QE period owing to the availability of additional reserves from the Bank of England (combined with a move towards increased collateralization of borrowing and an overall deleveraging; see, e.g., Westwood, 2011). This interpretation is consistent with dynamics of gross borrowing value in the interbank network.[26]

Macro control variables. To control for the aggregate liquidity condition, we use the LIBOR rate as a proxy for funding cost together with the interbank rate premium (the average overnight borrowing rate of the CHAPS banks minus the LIBOR rate).[27] All control variables are lagged by one day so that they are

[26]We report the monthly rolling average of daily sterling value of gross borrowing in the Online Appendix.

[27]LIBOR is the average of borrowing rates reported by selected banks, not CHAPS banks. The interbank rate premium can be positively or negatively correlated with banks' liquidity holdings. First, when CHAPS banks face more risks, they may hold more liquidity and face

predetermined with respect to time t shocks.

Since banks' decisions to hold liquidity are likely to be influenced by the volatility of their daily payment outflows, we construct a measure of intraday payment volatility as

$$VolPay_t = \sqrt{\frac{1}{88}\sum_{\tau=1}^{88}\left(P_{t,\tau}^{out}\right)^2}. \tag{36}$$

where P^{out} denotes payment outflows and 88 is the number of ten-minute time intervals (the unit of time for payment recording in our sample) within a day. The time series is plotted in the Online Appendix. Outflow volatility declined steadily throughout the crisis, suggesting that banks in aggregate smoothed intraday outflow.

We also control for the turnover rate in the payment system. This variable is defined as

$$TOR_t = \frac{\sum_{i=1}^{N}\sum_{\tau=1}^{88} P_{i,t,\tau}^{out}}{\sum_{i=1}^{N}\max\left\{\max_{\tau\in[1,88]}\left[CNP(\tau;i,t)\right],0\right\}},$$

where the cumulative net debit position (CNP) is defined as the difference between payment outflows and inflows (see also Benos et al., 2010). The numerator is the total payments in day t, while the denominator is the sum of maximum intraday net debt positions of all banks. The time series is plotted in the Online Appendix. The turnover rate increased during the crisis period and declined after the introduction of QE.

Since banks have some discretion on the timing of intraday outflows, they could behave strategically – to preserve liquidity, banks may expedite inflows and delay outflows. Therefore, we control for the right kurtosis (rK_t) of intraday payment time.[28] The time series is plotted in the Online Appendix, showing a

higher borrowing costs. Second, interbank rate premium measures an opportunity cost – CHAPS banks can borrow to lend at the LIBOR rate rather than hold reserves. So, when LIBOR is high (interbank rate premium low), banks prefer to hold less liquidity.

[28] We define right and left kurtosis (denoted, respectively, by rK_t and lK_t) as the part of

substantial increase in the QE period.

Beyond these control variables at daily frequency, we add week fixed effects to account for potential missing variables that fluctuate at lower frequencies, such as monetary policy conditions beyond the interbank rates and real economic activities that drive payment flows.

Bank characteristics. Despite the fact that we control for average interest rates, we also control for the bank-specific overnight borrowing rate, which is a daily volume-weighted average. As we report in the Online Appendix, there was a substantial increase in the cross-sectional dispersion of the overnight borrowing rates during turmoil periods, such as the collapse of Northern Rock and Lehman Brothers. This cross-sectional dispersion persisted during the QE period. Therefore, it is critical to account for the heterogeneity in banks' overnight borrowing rates. As macro variables, all bank-level control variables are lagged by one day.[29]

We also control for other bank-level variables: the level of intraday payment outflow ($LevPay_{i,t} \equiv \sum_{\tau=1}^{88} P_{i,t,\tau}^{out}$); the right kurtosis of intraday payment inflow time ($rK_{i,t}^{in}$) and outflow time ($rK_{i,t}^{out}$); the volatility of intraday payment outflow ($VolPay_{i,t}$, constructed as in Eq. (36) using bank-level flows); the liquidity used ($LU_{i,t}$, as in Benos et al., 2010 and defined in the Appendix); total assets; the repo liabilities to total assets ratio; the retail deposits to total assets ratio; the interbank borrowing rate; total interbank lending and borrowing; the

kurtosis generated by payment times, respectively, above and below the average payment time of the day:

$$rK_t = \frac{\sum_{\tau > m_s} (\frac{\tau - m_t}{\sigma_t})^4}{\sum_{\tau=1}^{88} (\frac{\tau - m_t}{\sigma_t})^4}, \text{ and } lK_t = \frac{\sum_{\tau < m_t} (\frac{\tau - m_t}{\sigma_t})^4}{\sum_{\tau=1}^{88} (\frac{\tau - m_t}{\sigma_t})^4};$$

where m_t and σ_t are defined as flow-weighted average payment time and standard deviation, i.e.,

$$m_t = \frac{1}{88} \sum_{\tau=1}^{88} \tau \left(\frac{P_{t,\tau}^{OUT}}{\sum_{t=1}^{T} P_{t,\tau}^{OUT}} \right), \text{ and } \sigma_t^2 = \frac{1}{88-1} \sum_{\tau=1}^{88} \left[\tau \left(\frac{P_{t,\tau}^{OUT}}{\sum_{t=1}^{88} P_{t,\tau}^{OUT}} \right) - m_t \right]^2.$$

[29] For variables available at lower than daily frequency (monthly), we use the latest lagged observation. These variables are total assets, the ratio of repo liabilities to assets, and the ratio of retail deposits to total assets.

5-year credit default swap (CDS) spread; and daily stock returns.

6. Estimation results

6.1. Subsample estimation

We estimate our model [Eq. (22) and Eq. (23)] in three subsamples of roughly equal size: the period before the Northern Rock and BNP Paribas Fund crisis (August 9, 2007), the period after it and before QE (January 19, 2009), and the QE period. These three periods are marked by distinct liquidity conditions, and as documented in Section 5, different behavior of the network and other variables. Period 1 was a relatively tranquil period. Period 2 saw several significant events, such as the subprime mortgage fund crisis (e.g., BNP Paribas fund freezing on August 9, 2007), the run on Northern Rock (the U.K.'s first in 150 years), the Federal Reserve intervention in Bear Stearns and its subsequent sale to JPMorgan Chase, and the bankruptcy of Lehman Brothers. Period 3 began with a regime switch in monetary policy. The announcement of the Bank of England on January 19, 2009 marked the beginning of quantitative easing in the U.K.

The network multiplier. The estimation results for these three subsamples are reported in Panel A of Table 1, where we report only the estimates of the spatial dependency parameter ϕ (first row), the R^2 of the regression (second row), the implied average network multiplier (third row) $1/(1-\phi)$ that was discussed in Section 4, as well as the ratio of the volatility of network liquidity to the counterfactual volatility when $\phi = 0$. Omitted from the table are the coefficient estimates of control variables, which are reported in the Online Appendix.

Recall that $\phi > 0$ (< 0) implies that banks' liquidity holding decisions are strategic complements (substitutes) and that this tends to amplify (reduce) the impact of bank-level shocks to aggregate liquidity. In the first period, the estimate of ϕ is 0.8137 and highly significant, indicating a substantial network

Table 1
Spatial Error Model Estimation. Estimation results for Eq. (22) and Eq. (23). Periods 1, 2, and 3 correspond, respectively, to: before the Northern Rock/BNP Paribas Fund crisis, after it but before the first BoE announcement of Asset Purchase Programme, and the QE period. The t-statistics are reported in parentheses under the estimated coefficients. Standard errors are QMLE-robust ones, and the delta method is used for the average network multiplier, $1/(1-\hat{\phi})$. In Panel A, the adjacency matrix is computed using the interbank borrowing data, while in Panels B and C, we respectively use lending and borrowing plus lending (all row-normalized).

	Period 1	*Period 2*	*Period 3*
Panel A: G_t based on borrowing			
$\hat{\phi}$	0.8137	0.3031	-0.1794
	(21.47)	(1.90)	(-4.96)
R^2	66.01%	92.09%	91.53%
$1/\left(1-\hat{\phi}\right)$	5.3677	1.4349	0.8479
	(4.92)	(4.37)	(32.61)
$\sqrt{\frac{Var(Z_t\|\hat{\phi})}{Var(Z_t\|\phi=0)}}$	5.59	1.25	0.89
Panel B: G_t based on lending			
$\hat{\phi}$	0.8209	0.2573	-0.3925
	(20.38)	(1.23)	(-7.18)
R^2	66.02%	91.63%	91.61%
$1/\left(1-\hat{\phi}\right)$	5.5835	1.3464	0.7181
	(4.45)	(3.54)	(25.49)
$\sqrt{\frac{Var(Z_t\|\hat{\phi})}{Var(Z_t\|\phi=0)}}$	5.71	1.45	0.85
Panel C: G_t based on borrowing and lending			
$\hat{\phi}$	0.8204	0.3258	-0.2824
	(19.36)	(1.89)	(-6.10)
R^2	63.98%	92.22%	91.70%
$1/\left(1-\hat{\phi}\right)$	5.5679	1.3464	0.7181
	(4.24)	(3.91)	(26.74)
$\sqrt{\frac{Var(Z_t\|\hat{\phi})}{Var(Z_t\|\phi=0)}}$	5.94	1.15	0.74

amplification effect: a £1 shock equally spread across banks would result in a $1/\left(1-\hat{\phi}\right)$ = £5.3677 shock to the aggregate liquidity.

In the second period, the coefficient ϕ is substantially lower in magnitude and marginally significant, implying weak strategic complementarity and an average network multiplier of approximately $1/(1-0.3031) = 1.4349$. This finding suggests that in response to the turbulence in financial markets that have characterized the second period, banks' marginal cost of holding liquidity increased significantly (i.e., ψ became large), so strategic substitution gained strength.

In the third period, $\hat{\phi}$ becomes negative, -0.1794, and statistically significant, implying an average network multiplier of 0.8479. This result is particularly interesting since strategic substitution became the dominant force in banks' liquidity holding decisions, as in Bhattacharya and Gale (1987). As a result, the network buffers the impact of shocks from individual banks on aggregate liquidity. This finding also sheds light on how the massive liquidity injection by the central bank affects the network effect. Overall, the model fits the data fairly well in the three subsamples, with R^2 in the range of 66%–92%.

The last row of Panel A reports $\sqrt{Var(Z_t|\hat{\phi})/Var(Z_t|\phi=0)}$, i.e., the ratio of the volatility of aggregate liquidity implied by our estimate of ϕ to the counterfactual volatility if there were no network externalities. In the first period, the network multiplier generates a 459% increase in volatility. The excess volatility from network effects dropped to 25% in the crisis period, and turned negative, -11%, in the QE period. The Online Appendix reports $\sqrt{Var(z_{i,t}|\hat{\phi})/Var(z_{i,t}|\phi=0)}$, the network volatility multiplier for each bank.

For robustness, in Panels B and C, we estimate our network model with two alternative constructions of the adjacency matrix G_t. In Panel B, we use the lending flows, while in Panel C, we use the combined borrowing and lending flows. In both cases, the adjacency matrix is row-normalized (right stochastic). Such an exercise is meaningful because, as we emphasized when constructing the theoretical model, network linkages reflect the interbank relationships. Thus, a linkage is not necessarily just about borrowing. If a bank lends to another bank, a relationship formed through this transaction may facilitate future borrowing. Overall, the estimates in Panels B and C are very similar to those in Panel A.

Additionally, we also consider a counterparty-adjusted version of the $\mathbf{G}_t$ used in Panel A. That is, after obtaining the average fraction of bank's i overnight loans from bank j in the previous month ending on day $t-1$, we divide this fraction by one plus the number of banks that bank j lends to in that month since some banks have zero borrowers in some subsample periods.[30] As in the other specifications, we normalize by rows so that the new adjacency matrix is still right stochastic. Doing such an adjustment captures the possibility that if bank j lends to many banks, this might reduce the likelihood of it being able to lend to bank i. This counterparty-adjusted $\mathbf{G}_t$ essentially re-weights the baseline $\mathbf{G}_t$ to deliver an "effective" measure of access to network liquidity. Such re-weighting is consistent with our theoretical model since therein the entries of $\mathbf{G}_t$ are meant to capture the availability of funds through network connections. The Online Appendix reports the estimation results obtained with this adjacency matrix. The point estimates of ϕ are very similar to the ones in Panel A of Table 1 and the estimates of coefficients of control variables are close to the ones obtained from using the baseline $\mathbf{G}_t$ (reported in the Online Appendix).

Network impulse response and key players. Next, using the estimates, we compute the network impulse response functions to identify risk key players in each subsample. The results are reported together with banks' net borrowing amount and the network graph.

In the upper panel of Fig. 4, we report each bank's excess network impulse response to a unit shock, i.e., $NIRF_i^e\left(\hat{\phi}, 1, \bar{\mathbf{G}}_1\right) = NIRF_i\left(\hat{\phi}, 1, \bar{\mathbf{G}}_1\right) - 1$, defined in Eq. (34), where $\bar{\mathbf{G}}_1$ denotes the average $\mathbf{G}_t$ in Period 1. It measures Bank i's contribution to systemic risk – the network-induced reaction of aggregate liquidity to a unit shock to Bank i. Note that if either $\phi = 0$ or there are no network linkages ($\bar{\mathbf{G}}_1 = \mathbf{0}$), a unit shock to Bank i is a unit shock to the aggregate liquidity, and thus, the excess response is zero. We also plot one and two standard deviation bands. As a point of reference, we show the *average* excess network multiplier, $\left(1 - \hat{\phi}\right)^{-1} - 1 = 4.3677$ (Panel A of Table 1), i.e., how the network as the whole amplifies a unit shock equally spread across banks.

[30]We have also constructed another adjusted adjacency matrix $\mathbf{G}_t$ which re-weights $g_{ij,t}$ by dividing the number of bank j's borrowers except for the banks with zero borrowers. In the latter case, we leave the entries in $\mathbf{G}_t$ unchanged. Estimation results are very similar so we choose to report only one of the two in the paper.

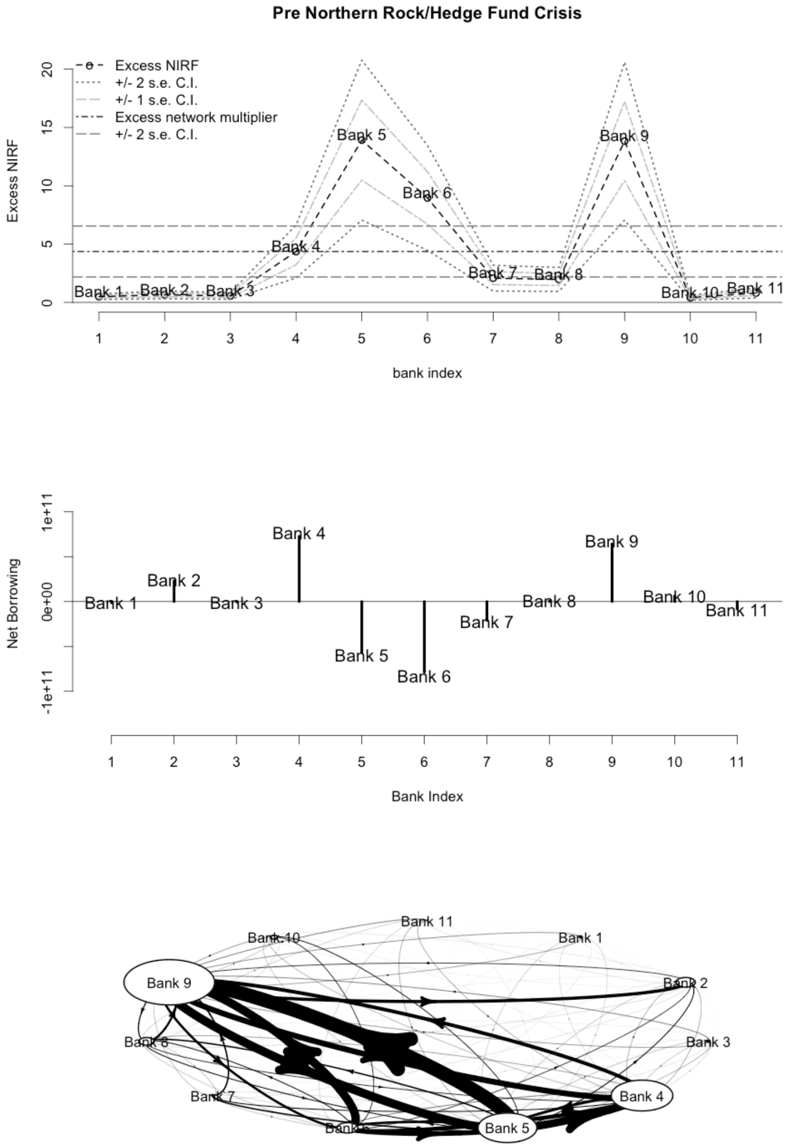

Fig. 4. The period before the Northern Rock/Hedge Fund Crisis: Network excess impulse response functions to a unit shock (upper panel); average net borrowing per month (central panel; unit: £1); borrowing and lending flows (lower panel) where the ellipses identifying individual banks are (log) proportional to their average gross borrowing per month, incoming arrows to a node indicate borrowing flows, outgoing arrows indicate lending flows, and the thickness of arrows is (log) proportional to the sterling value of the flows.

Since (as per Eq. (33)), a large NIRF for a given bank implies a larger contribution to the volatility of total liquidity, a key message from the upper panel of Fig. 4 is that a handful of key players (banks 5, 6, and 9) are responsible for most of the systemic risk. For instance, a shock of £1 to Bank 5, 6, or 9 would generate an excess response of aggregate liquidity equal to £13.9, £8.9, and £13.8, respectively. A shock to Bank 4 would induce an excess response similar to the network average, while the remaining seven banks contribute relatively little to shock amplification.

The comparison between the upper and central panels makes clear that risk key players are not necessarily large net borrowers – large net borrowers and lenders are both likely to be key risk contributors. This is intuitive: a negative shock to a bank that lends to a large part of the network (high outdegree centrality) can be, for the aggregate liquidity buffer, as bad as a negative shock to a bank that borrows from many banks (high indegree centrality).

However, even if we consider both borrowing and lending amounts, it is still not enough to identify key players. For example, the risk contribution of Bank 5 would be underestimated. The reasons behind this can be understood by looking at the lower panel of Fig. 4, where we present the average network structure in Period 1. The sizes of ellipses identifying individual banks are (log) proportional to their average gross borrowing, incoming arrows to a node indicate borrowing flows, outgoing arrows indicate lending flows, and the thickness of arrows is (log) proportional to the sterling value. This shows that key risk contributors tend to be banks with high centrality (e.g., Bank 5), i.e., with thick and numerous links, especially links to other well-connected banks, but not necessarily the large players by size.

Fig. 5 reports excess impulse response functions (upper panel), average net borrowing (central panel), and network flows (lower panel) for Period 2 – the period characterized by a high degree of stress in the financial market. The first thing to notice is that despite the overall increase in borrowing and lending activities in the interbank market (reported in the Online Appendix), there is a drastic reduction in the average network multiplier reported in the

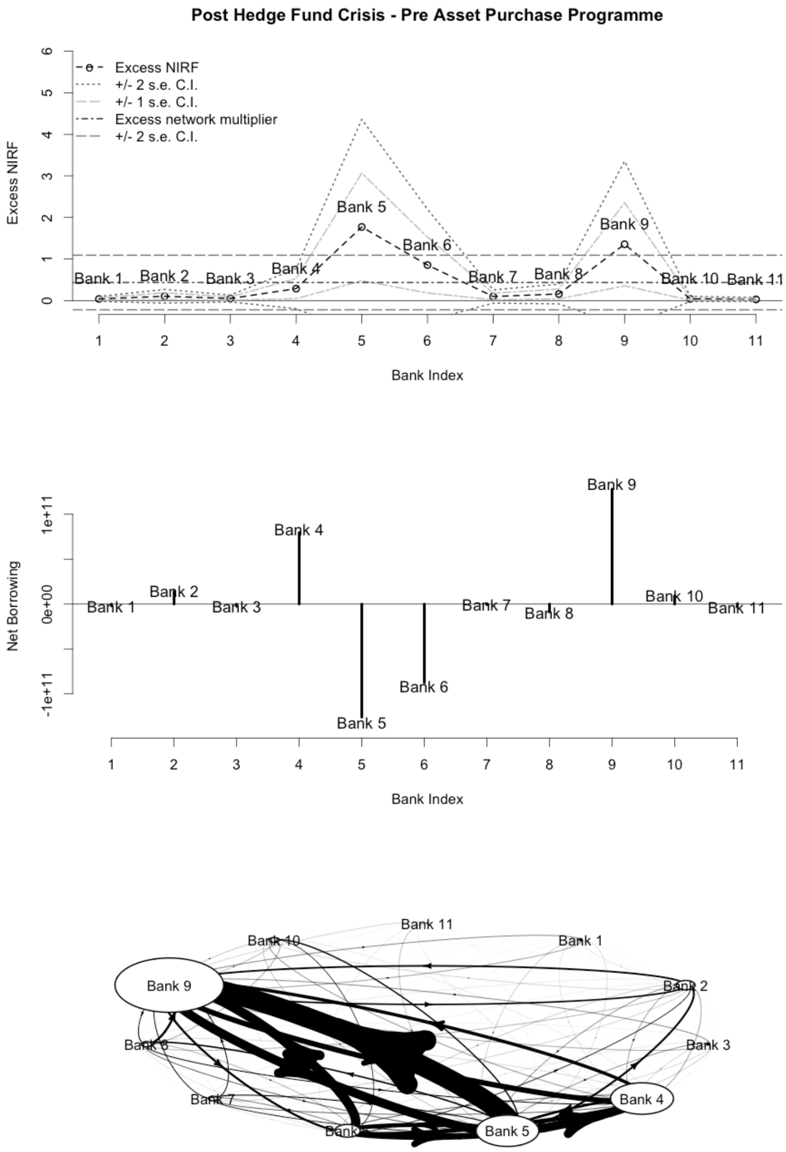

Fig. 5. The period after the Northern Rock/Hedge Fund Crisis but before QE: Network excess impulse response functions to a unit shock (upper panel); average net borrowing per month (central panel; unit: £1); borrowing and lending flows (lower panel) where the ellipses identifying individual banks are (log) proportional to their average gross borrowing per month, incoming arrows to a node indicate borrowing flows, outgoing arrows indicate lending flows, and the thickness of arrows is (log) proportional to the sterling value of the flows.

top panel: the network-induced excess reaction to a unit shock is only about 0.44. In a crisis period, banks seem to have radically adjusted their liquidity management objectives, reflected by the estimate of ϕ, and they have done so despite having increased the utilization of the interbank network to transfer liquidity. Nevertheless, systemic risk, even though substantially reduced, is still quite high and driven by a couple of key players. In particular, a unit shock to Bank 5, Bank 9, and Bank 6 triggers an excess reaction of aggregate liquidity equal to 1.77, 1.36, and 0.85, respectively, while a shock to Bank 4 has an average effect, and the remaining banks contribute little.

The results for Period 3 – the one starting at the onset of QE – are reported in Fig. 6 and are radically different from those of the previous two periods. First, banks' liquidity holdings exhibit strategic substitution ($\hat{\phi} < 0$), and as a result, the network buffers shocks to individual banks, reflected in an average excess multiplier of -0.15: a unit shock equally spread across banks would result in a shock of $1 - 0.15 = 0.85$ to the aggregate liquidity. However, once again, there is substantial heterogeneity among the banks in the sense that most banks (1, 3, 7, 8, 10, and 11) contribute little to shock propagation, while a few key players (4, 5, 6, and 9) are responsible for the network buffering effect.

This behavior arises in a period in which the degree of connectedness of the network was substantially reduced (see Fig. 3 and the lower panel of Fig. 6), most banks held net borrowing positions close to zero (central panel of Fig. 6), and the total borrowing had been substantially reduced (see the Online Appendix), but at the same time, the overall liquidity in the system had substantially increased, which is likely due to QE (Fig. 1).

What is also interesting to notice is that the same banks that were the riskiest players in the previous two periods (Banks 5, 6, and 9) are now the least risky ones for the system. Owing to their network centrality, and more importantly, the overall strategic substitution behavior on the network, these banks become the biggest shock absorbers.

A natural question is whether we can explain the large heterogeneity of individual banks' contribution to systemic risk using banks' characteristics, and

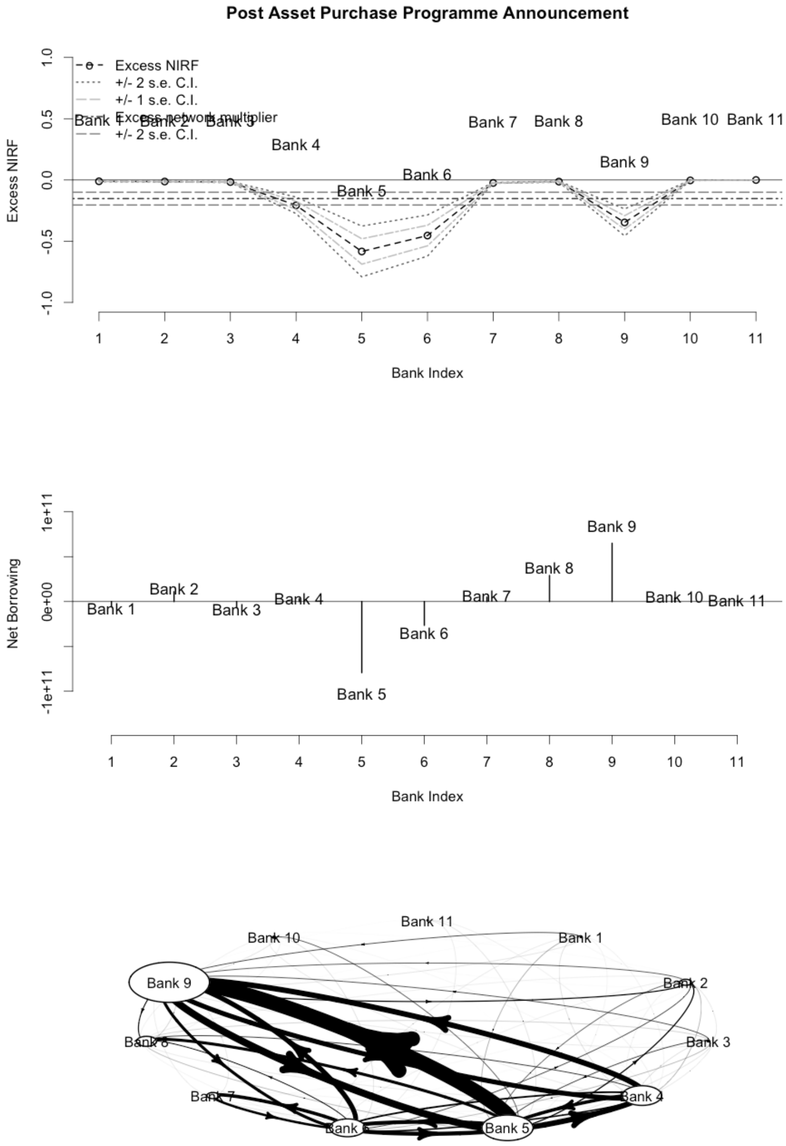

Fig. 6. The QE period: Network excess impulse response functions to a unit shock (upper panel); average net borrowing per month (central panel; unit: £1); borrowing and lending flows (lower panel) where the ellipses identifying individual banks are (log) proportional to their average gross borrowing per month, incoming arrows to a node indicate borrowing flows, outgoing arrows indicate lending flows, and the thickness of arrows is (log) proportional to the sterling value of the flows.

Table 2
Bank Characteristics and Network Impulse-Respose Functions. The table reports the rank correlations between Network excess impulse response ($NIRF_i^e$) of banks and their characteristics. Periods 1, 2 and 3 correspond, respectively, to: before the Northern Rock/BNP Paribas Fund Crisis, after it but before the first BoE announcement of Asset Purchase Programme, and the QE period. * represents 10% significance, ** 5% significance, and *** 1% significance.

	Period 1	*Period 2*	*Period 3*
Interbank Rate	20.91%	37.27%	-64.55%
$\ln LevPay_{i,t-1}$	$82.73\%^{***}$	$95.45\%^{***}$	$-85.45\%^{***}$
$rK^{in}_{i,t-1}$	20.00%	-34.55%	10.91%
$rK^{out}_{i,t-1}$	-45.45%	$-89.09\%^{***}$	$73.64\%^{**}$
$\ln VolPay_{i,t-1}$	48.18%	$56.36\%^{*}$	$-54.55\%^{*}$
$\ln LU_{i,t-1}$	21.82%	35.45%	-23.64%
Total Assets (log)	12.73%	25.45%	4.55%
$\frac{\text{Repo Liability}}{\text{Assets}}$	39.45%	48.18%	-37.27%
$\frac{\text{Deposits}}{\text{Assets}}$	12.73%	-50%	$68.18\%^{**}$
CDS Spread	38.18%	18.18%	-40.00%
Stock Return	13.64%	-17.27%	$-56.36\%^{*}$
Total Lending and Borrowing (log)	$86.36\%^{***}$	$95.45\%^{***}$	$-89.09\%^{***}$
Total Lending (log)	$97.27\%^{***}$	$99.09\%^{***}$	$-89.09\%^{***}$
Total Borrowing (log)	$66.36\%^{**}$	$91.82\%^{***}$	$-76.36\%^{***}$
Net Borrowing (log)	-17.27%	10.91%	$54.55\%^{*}$

perhaps find some proper indicators. Table 2 reports the rank correlations of individual bank characteristics with banks' network impulse response functions in the subsamples. Only a few characteristics appear to correlate significantly with the magnitude of $NIRF_i^e$. Several observations are in order.

For the total payments channeled by a bank, in periods 1 and 2, the rank correlations for this variable are, respectively, 82.73% and 95.45%, while in period 3, we have -85.45%, suggesting that banks that channel a larger amount of payments are likely to be central in the interbank credit network but that the implications of its centrality depend on the type of equilibrium, i.e., strategy complementarity ($\phi > 0$) or substitution ($\phi < 0$). In the first two periods, when $\phi > 0$, banks with large payment flows contribute to the volatility of aggregate liquidity, while in the third period, when $\phi < 0$, they dampen the effect of shocks.

The last row of Table 2 shows that *net* borrowing has no significant rank correlation with banks' $NIRF_i^e$, consistent with Fig. 4–6. Nevertheless, *gross* lending and gross borrowing, and their sum, are all highly correlated with banks' $NIRF_i^e$. That is, banks that borrow and/or lend substantially (in gross terms) tend to be key players in our network. Once again, the sign of correlation depends on the sign of ϕ: large banks, in terms of gross borrowing or lending, can be key risk contributors or absorbers depending on the type of equilibrium on the network. How to measure bank size is important. For example, size measured by total assets is only weakly correlated with $NIRF_i^e$ – instead, the total level of payment activity intermediated by a bank ($\ln LevPay_i$) seems to be a more salient metric to identify risk key players, as it strongly correlates with the $NIRF_i^e$. Interestingly, the rank correlations are, in absolute terms, marginally larger for total lending than for total borrowing, suggesting outdegree links are more important for shock propagations. As we have shown in the theoretical model, outbound routes are responsible for the discrepancy between the planner's solution and decentralized equilibrium outcome. Next, we use our estimates to quantify this discrepancy.

6.2. Planner's solution vs. decentralized equilibrium

Using the estimated structural parameters, we assess the difference between the aggregate liquidity in the decentralized equilibrium and the aggregate liquidity that a benevolent planner would have chosen in the payment system. The difference arises because the planner internalizes the network effects of individual banks' liquidity, while in the decentralized equilibrium individual banks ignore such network externalities.

Specifically, conditional on the network structure, we examine how the decentralized equilibrium propagates shocks differently from the planner's solution by computing the percentage difference between $Var\left(Z_t^p \,|\, \mathbf{G}_t = \bar{\mathbf{G}}\right)$, the volatility of aggregate liquidity from the planner's solution, and $Var\left(Z_t^* \,|\, \mathbf{G}_t = \bar{\mathbf{G}}\right)$, the volatility in decentralized equilibrium, where $\bar{\mathbf{G}}$ denote the average of $\mathbf{G}_t$ in a subsample. For each subsample, we compute

$$\frac{\sqrt{Var\left(Z_t^p \,|\, \mathbf{G}_t = \bar{\mathbf{G}}\right)} - \sqrt{Var\left(Z_t^* \,|\, \mathbf{G}_t = \bar{\mathbf{G}}\right)}}{\sqrt{Var\left(Z_t^* \,|\, \mathbf{G}_t = \bar{\mathbf{G}}\right)}} \tag{37}$$

where the variances are $Var\left(Z_t^* \,|\, \mathbf{G}_t = \bar{\mathbf{G}}\right) = \mathbf{1}^\top \mathbf{M}\left(\phi, \bar{\mathbf{G}}\right) \Sigma_\nu \mathbf{M}\left(\phi, \bar{\mathbf{G}}\right)^\top \mathbf{1}$ from Eq. (30) and $Var\left(Z_t^p \,|\, \mathbf{G}_t = \bar{\mathbf{G}}\right) = \left(\frac{1}{1+\phi/\eta}\right)^2 \mathbf{1}^\top \mathbf{M}^p\left(\phi, \eta, \bar{\mathbf{G}}\right) \Sigma_\nu \mathbf{M}^p\left(\phi, \eta, \bar{\mathbf{G}}\right)^\top \mathbf{1}$ from Eq. (35). The variance operator is taken over the structural shocks ν_t, i.e., we condition on the parameter and the network topology.

We also compute the difference in the expected level of aggregate liquidity (conditional on the network structure) between the planner's solution [Eq. (21)] and the decentralized equilibrium [Eq. (14)]:

$$\mathbb{E}\left[Z_t^p - Z_t^* \,|\, \mathbf{G}_t = \bar{\mathbf{G}}\right] = \mathbf{1}^\top \left\{\mathbf{M}^p\left(\phi, \eta, \bar{\mathbf{G}}\right)\left[\left(\frac{1}{1+\phi/\eta}\right)\bar{\mu} - \frac{\gamma\eta}{\psi'}\bar{\mathbf{G}}^\top \mathbf{1}\right] - \mathbf{M}\left(\phi, \bar{\mathbf{G}}\right)\bar{\mu}\right\}, \tag{38}$$

where the expectation is taken over the structural shocks, i.e., ν_t.

We use the estimates of ϕ, $\Sigma_\nu = diag\left(\left\{\sigma_i^2\right\}_{i=1}^N\right)$, and $\bar{\mu}$, and calculate $\bar{\mathbf{G}}$ for each subsample. To calculate the percentage volatility wedge in Eq. (37), we also need η, and, to calculate the level difference in Eq. (38), we need ψ', η, and γ. By inspecting bank i's objective function given by Eq. (4), we can see that dividing Eq. (4) by ψ' does not affect the bank i's preference. Therefore, we normalize ψ' to one. While we cannot estimate η and γ directly, we calibrate them to natural benchmark values.

First, we calibrate η. In our model, $z_{i,t} + \eta \sum_{j \neq i} g_{ij,t} z_{j,t}$ gives the *maximum* amount of liquidity that bank i can access. The component from interbank borrowing, $\eta \sum_{j \neq i} g_{ij,t} z_{j,t}$, cannot exceed the aggregate liquidity $\sum_{j \neq i} z_{j,t}$ of i's neighbors, i.e., $\eta \sum_{j \neq i} g_{ij,t} z_{j,t} \leq \sum_{j \neq i} z_{j,t}$, which implies an upper bound for η: $\left(\sum_{j \neq i} z_{j,t}\right) / \left(\sum_{j \neq i} g_{ij,t} z_{j,t}\right)$. In our sample, this upper bound of η

Table 3
Planner's Solution vs. Decentralized Equilibrium. This table reports the percentage difference between the volatility of aggregate liquidity of the planner's solution and that of the decentralized equilibrium, conditional on the network structure. Periods 1, 2, and 3 correspond, respectively, to: before the Northern Rock/BNP Paribas Fund crisis, after it but before the first BoE announcement of Asset Purchase Programme, and the QE period.

	γ	*Period 1*	*Period 2*	*Period 3*
$\frac{\sqrt{Var\left(Z_t^p \mid \mathbf{G}_t=\bar{\mathbf{G}}\right)}-\sqrt{Var\left(Z_t^* \mid \mathbf{G}_t=\bar{\mathbf{G}}\right)}}{\sqrt{Var\left(Z_t^* \mid \mathbf{G}_t=\bar{\mathbf{G}}\right)}}$		-89.6%	-35.6%	-12.4%
$\mathbb{E}\left[Z_t^p - Z_t^* \mid \mathbf{G}_t = \bar{\mathbf{G}}\right]$ (unit: £billion)	-0.36	-60.4	51.6	-100.0
	-0.30	-54.0	62.5	-200.0
	-0.27	-50.2	68.9	-300.0

varies tightly around 10 over time and across banks, so we set η to 10. In the Online Appendix, we report our results with $\eta = 9$ and 11.

Next, we calibrate γ. Note that to compute the percentage volatility wedge in Eq. (37), we do *not* need this parameter, but we do for the level wedge in Eq. (38). In our third subsample period, the Bank of England supplied around £125 billion of reserves through the quantitative easing (QE) program, and then another £50 billion two months later by the end of November 2010. By the end of 2012, the total QE amount reached £375 billion. Through the lens of our model, liquidity injection is to address the inefficiencies in the interbank network, which are in turn due to banks' not internalizing their impact on neighboring banks. Without such inefficiencies, liquidity injection via QE would not be necessary, so the social optimum should feature less liquidity than the decentralized outcome. Therefore, we consider three values of γ, -0.41, -0.36, and -0.30, which imply respectively a level wedge of £-100 billion, £-200 billion, and £-300 billion in Period 3, i.e., different levels of liquidity required in the decentralized equilibrium to correct inefficiencies.

Table 3 reports the results. In Period 1, when the network multiplier is large, the decentralized equilibrium features excessive risk: the planner would prefer the volatility of aggregate liquidity to be reduced by 89.6%. Moreover, the liquidity level in the system is also excessive. The wedge ranges from £50 billion to £60 billion higher than the planner's solution depending on the value of γ. Because the planner and individual banks face the same $\{\bar{\mu}_i\}_{i=1}^N$ and $\{\sigma_i^2\}_{i=1}^N$, the discrepancy between the planner's solution and the decentralized outcome lies in the fact that individual banks do not internalize their impact on each other (via the outdegree linkages), as shown by Eq. (18).

In Period 2, the decentralized equilibrium produces less volatility in the aggregate liquidity than in Period 1 relative to the volatility from the planner's solution. Nevertheless, the volatility is still too large (by 35.6%) from the planner's perspective. In comparison with Period 1, the network is less cohesive (see Fig. 3), and the network multiplier declines since ϕ is closer to zero. However, this does not mean that the network externalities are eliminated. Quite the opposite, such externalities through the outdegree linkages lead to an expected level of aggregate liquidity buffer that is lower than the social optimum by the amount of £52 to £69 billion depending on γ. That is, the crisis period is characterized by too much risk and too little liquidity.

In the last period, the network multiplier is smaller than 1; hence, overall the decentralized equilibrium produces a volatility of aggregate liquidity that is lower than a system without any network connections (i.e., a diagonal $\mathbf{G}$). However, given the network connections, the decentralized equilibrium still produces a volatility that is 12.4% higher than the volatility of aggregate liquidity in the planner's solution. As previously discussed, the level wedges in this subsample are set to calibrate γ.

6.3. The role of the network topology

So far our analysis on banks' contribution to the aggregate liquidity risk assumes a unit shock to each bank. We examine how shocks of the same size, originated in different banks, can be propagated differently on the network. In the following, we feed a shock of $\hat{\sigma}_i$ to bank i. By doing so, we recognize banks differ in their contributions to the aggregate liquidity risk because (1) their structural shocks are of different sizes and (2) banks are located differently on

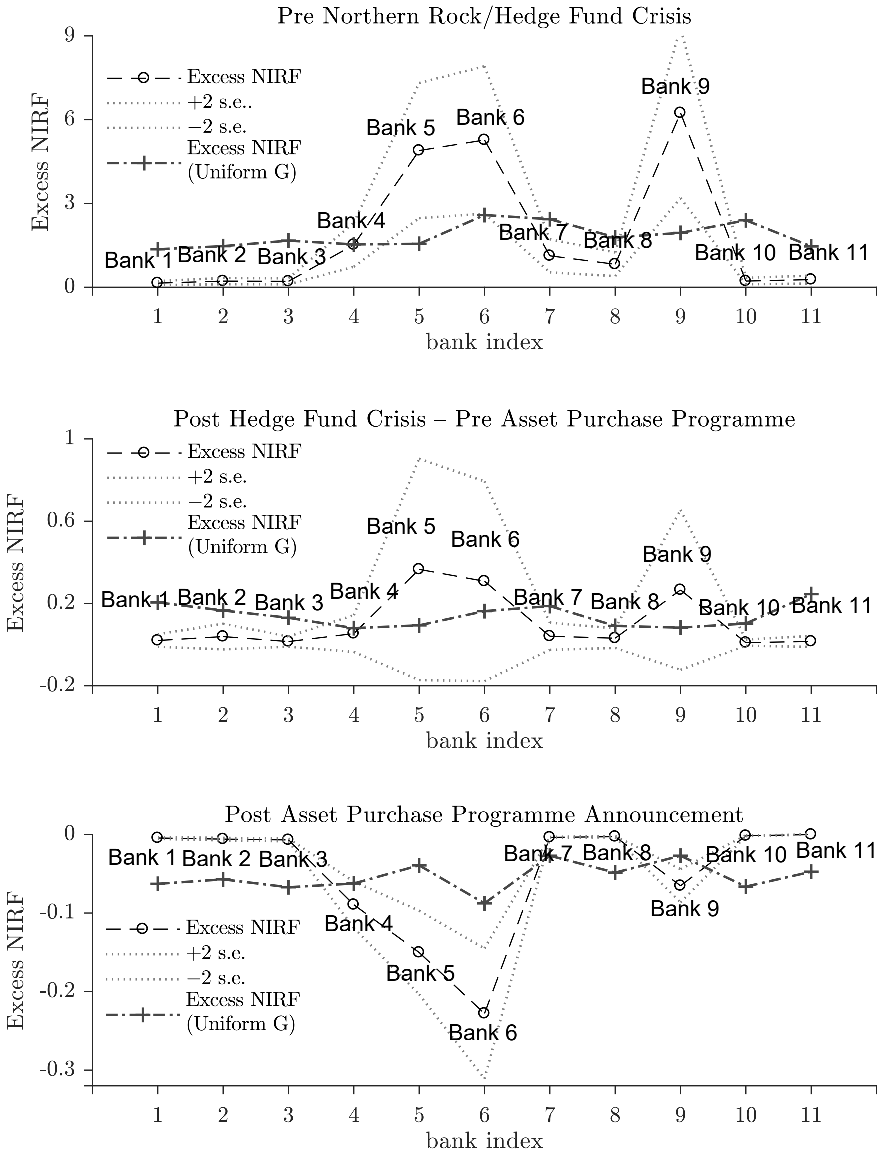

Fig. 7. The figure plots the excess network impulse response function $NIRF_i^e$ (long dashed line with circle markers), defined in Eq. (31), and its two standard error band (dotted lines) for the period before the Northern Rock/Hedge Fund crisis (upper panel), the period after the Northern Rock/Hedge Fund crisis but before QE (central panel), and the QE period (lower panel). A bank i receives a σ_i shock. The adjacency matrix of the interbank network is the average in each subsample period. In each panel, the excess network impulse response function of a uniform network is also plotted for comparison (dot-dashed line with cross markers).

the network.

In Fig. 7, we plot the excess network impulse response function, $NIRF_i^e\left(\hat{\phi}, \hat{\sigma_i}, \mathbf{G}_t\right) = NIRF_i\left(\hat{\phi}, \hat{\sigma_i}, \mathbf{G}_t\right) - \sigma_i$, defined in Eq. (34) for each bank (dashed line) and the two standard error band (dotted lines). In each subsample period, we use the average $\mathbf{G}_t$. In the pre-crisis period (upper panel), banks 5, 6, and 9 contribute the most to the risk of aggregate liquidity in the payment system. As the crisis unfolds, the level of risk declines but these banks remain the key contributors (central panel). In the QE period, these banks become the main risk absorbers as ϕ turns negative and the network becomes a risk buffer under strategic substitution in banks' liquidity decisions.

Next, to highlight the role of the network in creating the cross-sectional variation in banks' risk contribution, we compare $\left\{NIRF_i^e\left(\hat{\phi}, \hat{\sigma_i}, \mathbf{G}_t\right)\right\}_{i=1}^N$ with those generated by a counterfactual network where banks are equally connected, i.e., :

$$\mathbf{U} = \begin{bmatrix} 0 & \frac{1}{N-1} & \cdots & \frac{1}{N-1} \\ \frac{1}{N-1} & 0 & \ddots & \vdots \\ \vdots & \ddots & \ddots & \frac{1}{N-1} \\ \frac{1}{N-1} & \cdots & \frac{1}{N-1} & 0 \end{bmatrix}, \tag{39}$$

the "uniform" network. The dashed line marked by crosses shows $\left\{NIRF_i^e\left(\hat{\phi}, \hat{\sigma_i}, \mathbf{U}\right)\right\}_{i=1}^N$. Because banks do not differ in their position on the network, the only source of cross-sectional difference in $NIRF_i^e$ is σ_i, the size of bank-specific structural shocks. In each subsample period, the counterfactual $NIRF_i^e$ exhibits a different pattern in the cross section of banks. Therefore, given the nature of strategic interactions on the network, i.e., ϕ, a bank's position on the network is an important determinant of the risk that it contributes to the whole system. Indeed, on the real network a couple of banks stand out as the main risk contributors (absorbers) when $\phi > 0$ (< 0), but on the counterfactual network of equal connections the risk contributions are largely flat in the cross section.

6.4. Time-varying network effects

The results presented so far indicate a substantial change over time in the role played by the network interactions in determining aggregate liquidity level and risk. Specifically, the network impulse response functions depicted in Fig. 4–6 show substantial time variation across periods. This could be caused by either the time variation in the network topology $\mathbf{G}$ or in the network multiplier ϕ. To examine the relative contributions, we compute the changes in the network impulse response functions across the three periods.

In particular, Panel A of Fig. 8 reports the change in NIRFs between Periods 1 and 2 due to the variation of $\mathbf{G}$ [$NIRF_i(\hat{\phi}_1, 1, \bar{\mathbf{G}}_2) - NIRF_i(\hat{\phi}_1, 1, \bar{\mathbf{G}}_1)$, dotted line with triangles], and the change due to the variation of ϕ [$NIRF_i(\hat{\phi}_2, 1, \bar{\mathbf{G}}_1) - NIRF_i(\hat{\phi}_1, 1, \bar{\mathbf{G}}_1)$, dash-dotted line with +]. Note that the total change is not the sum of the ceteris paribus change due to variation in $\mathbf{G}$ and the ceteris paribus change due to variation in ϕ, but as a point of reference the total change is also plotted [$NIRF_i(\hat{\phi}_2, 1, \bar{\mathbf{G}}_2) - NIRF_i(\hat{\phi}_1, 1, \bar{\mathbf{G}}_1)$, dashed line with circles].

A striking feature of the graph is that most of the total change comes from the reduction in the network multiplier ϕ for all banks. In fact, ceteris paribus, the NIRF of Bank 5 would have increased from Period 1 to 2 because of the change in $\mathbf{G}$. However, this effect is dwarfed by the reduction of its NIRF caused by the change in ϕ.

Panel B reports the same decomposition of the change in NIRFs between Periods 2 and 3. Once again the changes are mostly driven by the change in the network multiplier rather than the change in network topology. Overall, Fig. 8 shows that the time variation of the network multiplier, i.e., the type of equilibrium on the network (strategic complementarity vs. substitution), has a first-order effect on the network amplification mechanism.

The results in Fig. 8 indicate the importance of variation of ϕ in determining the network effects. To capture this time variation, we also estimate the struc-

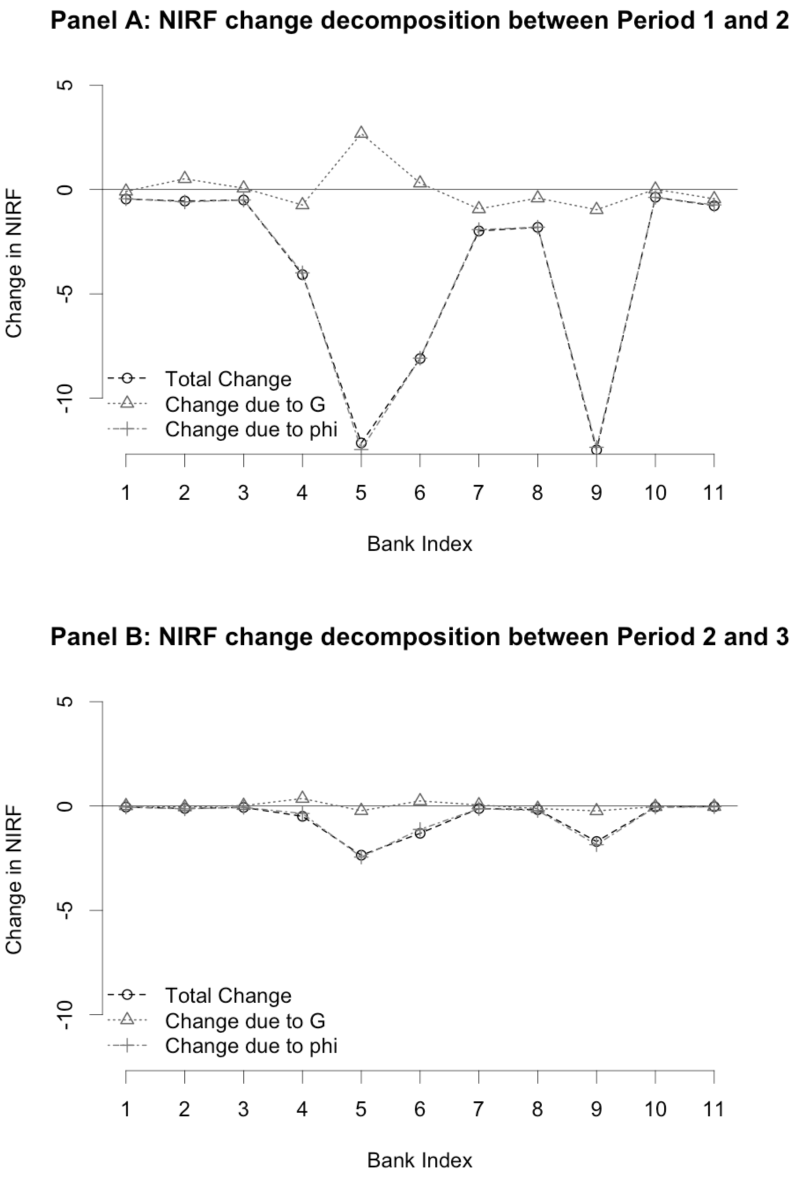

Fig. 8. Attribution of the change in NIRFs across periods: the ceteris paribus change due to variation of $\mathbf{G}$ [$NIRF_i(\hat{\phi}_1, 1, \bar{\mathbf{G}}_2) - NIRF_i(\hat{\phi}_1, 1, \bar{\mathbf{G}}_1)$, dotted line with triangle markers]; the ceteris paribus change due to variation of ϕ [$NIRF_i(\hat{\phi}_2, 1, \bar{\mathbf{G}}_1) - NIRF_i(\hat{\phi}_1, 1, \bar{\mathbf{G}}_1)$, dashed line with cross markers]; the total change [$NIRF_i(\hat{\phi}_2, 1, \bar{\mathbf{G}}_2) - NIRF_i(\hat{\phi}_1, 1, \bar{\mathbf{G}}_1)$, dashed line with circle markers]. Periods 1, 2, and 3 correspond, respectively, to before the Northern Rock/BNP Paribas Fund crisis, after it but before the first BoE announcement of the Asset Purchase Programme, and the QE period.

tural model in Eq. (22) and Eq. (23) using a 6-month rolling window.[31] These rolling estimates of the network coefficient ϕ are reported (solid line), together with 95% confidence bands (dotted lines), in Fig. 9. The figure also depicts the rolling point estimates of the coefficient ϕ implied by the spatial Durbin model (dashed line) in Eq. (36) which, as a more general empirical formulation, serves as a specification test of our benchmark spatial error model. If the two estimated ϕ are close to each other, as shown in Fig. 9, this indicates that our theory-driven spatial error specification of the interbank network cannot be rejected in favour of a more general specification.[32] Specifically, we find that, at the 5% confidence level, two estimates are statistically different less than 95% of the time.

At the beginning of the sample, the estimate of ϕ implies an extremely large network multiplier, and thus, the interbank system is a powerful shock amplifier. According to our model, this reflects that the forces behind strategic complementarity, i.e., the high values of payment multiplier and velocity, dominate the force of strategic substitution. The estimate has its first sharp reduction around the 18th of May 2006 when the Bank of England introduced the reserve averaging system (see details in the Online Appendix). The network multiplier is relatively stable after that except for a temporary decrease during the 2007 subprime mortgage default, until the Northern Rock bank run when the network multiplier is drastically reduced for several months. After this reduction, the coefficient goes back to roughly the previous average level but exhibits a

[31]Recall that when $\mathbf{G}_t$ is a right stochastic matrix, separate identifications of the bank (α^{bank}) and network ($\bar{\mu}$) fixed effects require a subset of banks that do not borrow at least at one point in time in each subsample (see footnote 25 and the discussion on our emprical methodology in the Online Appendix). This condition is not satisfied in every rolling window. However, since the separate identification of these fixed effects does not affect the identification of ϕ, we normalize the bank fixed effects to zero. Moreover, given the very short length of the rolling window, we drop time fixed effects from the specification and heteroskedastic specification of shocks. Estimates with the full sets of fixed effects and heteroskedasticity show a very similar behavior, but with somewhat larger confidence intervals, owing to the increase in the number of parameters. We focus on the more parsimonious specification, but the results of the full specifications are available upon request.

[32]The likelihood ratio test cannot reject the spatial error model in most parts of our sample (i.e., except rolling windows ending from May 2009 to May 2010). Results are available upon request.

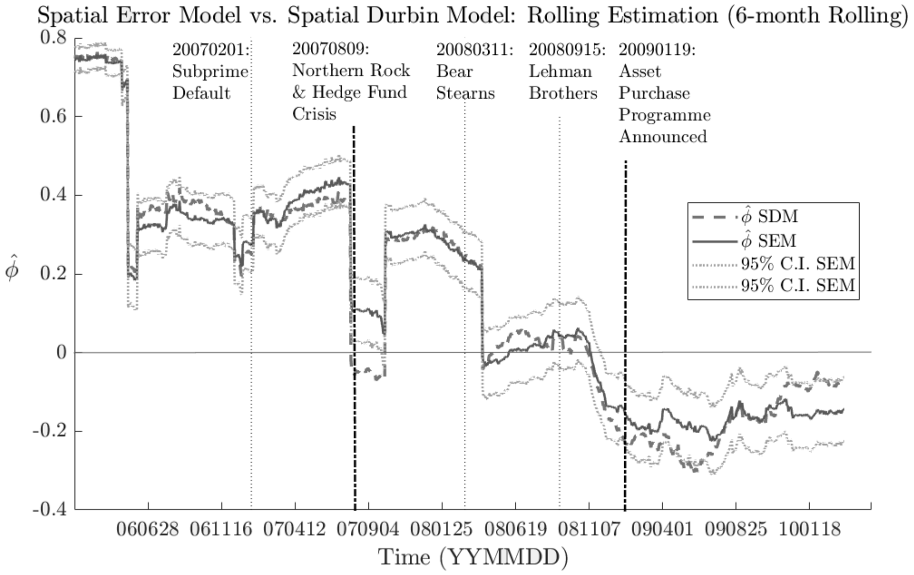

Fig. 9. Spatial error (solid line) and Durbin (dashed line) models: Rolling estimates of ϕ with a 6-month window. SEM (spatial error model) corresponds to the baseline specification in Eq. (22) and Eq. (23). Its 95% confidence intervals are marked by the dotted lines. SDM (spatial Durbin model) corresponds to the specification in Eq. (36).

declining trend that culminates in a slump following the Bear Stearns collapse. From this period onward, and until long after the Lehman Brothers bankruptcy, the coefficient is statistically indistinguishable from zero.

Our estimation suggests that banks' liquidity management objectives change in response to market-wide crisis in a way that reduces the domino effect of shock propagation and amplification on the interbank network. Interestingly, the coefficient $\hat{\phi}$ becomes negative right before the announcement of the Asset Purchase Programme and remains negative throughout the QE period. This result indicates that during the active liquidity injection by the Bank of England (and also in expectation of it), banks' liquidity holding decisions exhibit strategic substitution. The sign of ϕ depends on the relative strength of strategic complementarity and substitution forces, while its magnitude depends on the overall accessibility of interbank credit [captured by η in Eq. (10)]. The downward trend of magnitude during the crisis can be attributed to the stress in the interbank credit market, while the increase in absolute magnitude post-QE suggests that the policy intervention alleviated such stress and partly restored interbank credit.

Our results are unlikely to be driven by the direct or mechanical impact of QE on the interbank market of reserves for the following reasons: *a*) our estimation controls for variation in many prices (e.g., interbank rates), quantities (e.g., payment patterns, repo, deposits), and time (weekly) fixed effects, so our estimated response functions of individual banks are already conditional on such information; *b*) as shown in Fig. 1, overall, banks hold more liquidity after QE, which favors strategic complementarity (i.e., correlated liquidity holdings) instead of strategic substitution; *c*) the drop in ϕ actually occurred before the announcement of QE; and *d*) as previously emphasized, the Bank of England followed an accommodative reserve supply policy throughout our sample period, so the impact of QE is not through the alleviation of reserve scarcity. Therefore, our finding of a strong QE impact on banks' liquidity management objectives (i.e., our structural parameters) posits a challenge for theoretical research on how monetary policy affects the banking system.

The role of payment system velocity. Next we explore the economic forces driving the dynamics of ϕ shown in Fig. 9. Defined in Eq. (10), ϕ depends on two opposing forces, δ, which leads to strategic complementarity, and ψ, which generates strategic substitution.

As shown in its definition, Eq. (6), δ increases in δ_S and κ_b. The payment multiplier δ_S measures the strength of complementarity in the economic activities underlying agents' payments. It potentially depends on a great number of factors, for example, the input-output linkages in the production sector (see Carvalho and Tahbaz-Salehi, 2019).

Next, we focus on the payment velocity, κ_b, which has a sharp interpretation and is directly measurable in our sample: the ratio of total payments to total liquidity [see Eq. (3)]. Fig. 10 plots the 6-month rolling estimate of ϕ (spatial error model) together with the 6-month rolling average of payment

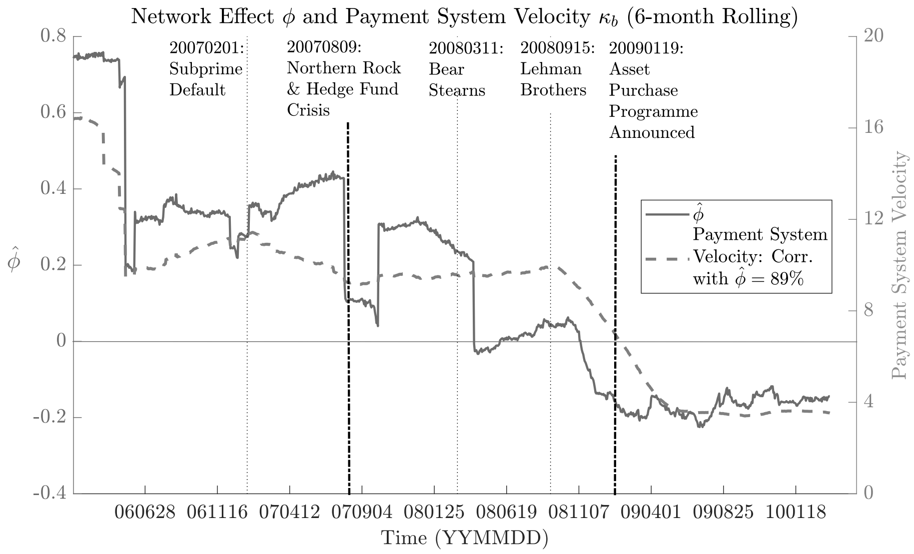

Fig. 10. Rolling estimate of ϕ (solid line, measured on left axis) using the specification in Eq. (22) and Eq. (23) and 6-month window, and payment system velocity (dashed line, measured on right axis).

system velocity (dashed line). The left Y-axis is for ϕ and the right Y-axis is for the velocity. A velocity that is equal to ten means that the liquidity in the payment system churns ten times as agents make payments to each other. The estimate of ϕ and the velocity have a correlation of 89.12%. Through δ, the payment system velocity drives the low-frequency movements of ϕ. As shown in our model, a high velocity leads to stronger strategic complementarity (i.e., a high δ, and thereby, high ϕ). Given a high velocity, a bank can support a large volume of depositors' payments by borrowing a small amount of liquidity from its neighboring banks. Through the complementarity among depositors, these payments in turn increase the overall demand for the bank's payment services, thus raising the marginal profits from holding its own liquidity to support payments.

In sum, our theoretical model not only guides our estimation of the *net* effects of strategic interactions, i.e., ϕ, among banks on the network. It also allows us to relate the estimate of ϕ to the underlying economic forces, and in particular, the velocity of the payment system, i.e., how fast the liquidity provided by banks circulates among depositors through payment activities. The strategic interactions among banks are not only functions of the characteristics of the banking system, but also critically depend on how banks' clients behave. As shown in Fig. 10, the unfolding of the financial crisis was accompanied by a decline of payment velocity, which explains the decline of ϕ – when the payment system could not churn liquidity as fast as before, the strategic complementarity in banks' decision to hold reserves weakened.

7. Conclusion

We develop a network model of banks' liquidity holding decisions and estimate the model to uncover the structural parameters that determine the type of equilibrium on the interbank network, i.e., strategic complementarity or substitution. Using the estimated parameters and the observed network topology, we construct measures of systemic risk. We find that the network topology is a main driver of the cross-sectional variation in banks' contribution to systemic risks. We propose empirical metrics to identify the banks that contribute the most to the systemic liquidity risk in the payment system.

We find that the network effects vary significantly through the sample period of 2006 to 2010. In the pre-crisis period, banks' liquidity holding decisions exhibited strategic complementarity, so shocks were amplified by the network. In contrast, during the crisis, the network multiplier declined significantly, suggesting that banks adjusted their liquidity management objectives in a way that reduced network domino effects. Finally, during the QE period, in response to the large liquidity injection, the equilibrium on the interbank network was characterized by strategic substitution, and accordingly, the network became a shock buffer.

To the best of our knowledge, we are the first to provide evidence on the substantial time variation in the nature of equilibrium on a financial network. Moreover, we show that, from a systemic risk perspective, the change in the type of equilibrium is the dominant force (rather than the change in network topology). This observation could rationalize the empirical puzzle of network topology changes having little impact on aggregate quantities in the calibration/simulation studies on interbank networks (e.g., Elsinger et al., 2006).

From a policy perspective, we are able to identify key risk contributors using our estimates of structural parameters and show that a subset of players are responsible for most of the systemic risk generated through network connections. Finally, we solve the choice of a benevolent planner and quantify the discrepancy between the planner's solution and the decentralized outcome in both the expected level and the volatility of aggregate liquidity. In particular, we find that during both the pre-crisis and the 2007–2009 crisis periods, the system was characterized by excessive risk, and during the crisis, too little liquidity buffer was held by individual banks relative to the social optimum.

References

Acemoglu, D., Carvalho, V.M., Ozdaglar, A., Tahbaz-Salehi, A., 2012. The network origins of aggregate fluctuations. Econometrica 80, 1977–2016.

Acharya, V.V., Merrouche, O., 2010. Precautionary hoarding of liquidity and inter-bank markets: Evidence from the sub-prime crisis. Working paper. New York University.

Afonso, G., Lagos, R., 2015. Trade dynamics in the market for federal funds. Econometrica 83, 263–313.

Afonso, G., Shin, H.S., 2011. Precautionary demand and liquidity in payment systems. Journal of Money, Credit and Banking 43, 589–619.

Allen, F., Carletti, E., Gale, D., 2008. Interbank market liquidity and central bank intervention. Working paper. New York University.

Allen, F., Gale, D., 2000. Financial contagion. Journal of Political Economy 108, 1–33.

Allen, F., Gale, D., 2017. How Should Bank Liquidity be Regulated. Working paper. Imperial College London.

Anselin, L., 1988. Spatial econometrics: methods and models. Studies in operational regional science, Kluwer Academic Publishers. URL: http://books.google.co.uk/books?id=3dPIXClv4YYC.

Armantier, O., Copeland, A., 2012. Assessing the quality of "Furfine-based" algorithms. Staff Reports 575. Federal Reserve Bank of New York. URL: http://EconPapers.repec.org/RePEc:fip:fednsr:575.

Ashcraft, A., McAndrews, J., Skeie, D., 2010. Precautionary reserves and the interbank market. Working paper. Federal Reserve Bank of New York.

Babus, A., Allen, F., 2009. Networks in finance, in: Kleindorfer, P., Wind, J. (Eds.), The Network Challenge: Strategy, Profit, and Risk in an Interlinked World. Pearson Education, Upper Saddle River, NJ, pp. 367–382.

Ballester, C., Calvo-Armengol, A., Zenou, Y., 2006. Who's who in networks. Wanted: The key player. Econometrica 74, 1403–1417.

Bech, M.L., Garratt, R., 2003. The intraday liquidity management game. Journal of Economic Theory 109, 198–219. URL: http://www.sciencedirect.com/science/article/pii/S0022053103000164, doi:https://doi.org/10.1016/S0022-0531(03)00016-4.

Benos, E., Garratt, R.J., Zimmerman, P., 2010. Bank behavior and risks in CHAPS following the collapse of Lehman Brothers. Working paper. UCSB.

Bernanke, B.S., Blinder, A.S., 1988. Credit, money, and aggregate demand. The American Economic Review 78, 435–439. URL: http://www.jstor.org/stable/1818164.

Bhattacharya, S., Gale, D., 1987. Preference shocks, liquidity, and central bank policy, in: Barnett, W., Singleton, K. (Eds.), New approaches to monetary economics. Cambridge University Press, Cambridge, U.K.

Bianchi, J., Bigio, S., 2014. Banks, Liquidity Management and Monetary Policy. Working paper 20490. National Bureau of Economic Research. URL: http://www.nber.org/papers/w20490, doi:10.3386/w20490.

Billio, M., Getmansky, M., Lo, A.W., Pelizzon, L., 2012. Econometric measures of connectedness and systemic risk in the finance and insurance sectors. Journal of Financial Economics 104, 535–559.

Bonacich, P., 1987. Power and centrality: A family of measures. American Journal of Sociology 92, 1170–1182.

Calvo-Armengol, A., Patacchini, E., Zenou, Y., 2009. Peer effects and social networks in education. Review of Economic Studies 76, 1239–1267.

Carvalho, V.M., Tahbaz-Salehi, A., 2019. Production networks: A primer. Annual Review of Economics 11, 635–663.

Castiglionesi, F., Feriozzi, F., Lorenzoni, G., 2017. Financial Integration and Liquidity Crises. Working paper 23359. National Bureau of Economic Research. URL: http://www.nber.org/papers/w23359, doi:10.3386/w23359.

Chang, B., Zhang, S., 2019. Endogenous Market making and Network Formation. Working paper. University of Wisconsin and LSE.

Chen, H., Wang, T., Yao, D.D., 2016. Financial network and systemic risk: A dynamic model. Working paper.

Cornett, M.M., McNutt, J.J., Strahan, P.E., Tehranian, H., 2011. Liquidity risk management and credit supply in the financial crisis. Journal of Financial Economics 101, 297–312. URL: http://www.sciencedirect.com/science/article/pii/S0304405X11000663, doi:https://doi.org/10.1016/j.jfineco.2011.03.001.

Debreu, G., Herstein, I., 1953. Nonnegative square matrices. Econometrica 21, 597–607.

Diamond, D.W., Dybvig, P.H., 1983. Bank runs, deposit insurance, and liquidity. Journal of Political Economy 91, 401–419. URL: http://www.jstor.org/stable/1837095.

Diamond, D.W., Kashyap, A.K., 2016. Liquidity Requirements, Liquidity Choice and Financial Stability. Working paper 22053. National Bureau of Economic Research. URL: http://www.nber.org/papers/w22053, doi:10.3386/w22053.

Diebold, F.X., Yılmaz, K., 2009. Measuring Financial Asset Return and Volatility Spillovers, with Application to Global Equity Markets. Economic Journal 119, 158–171. URL: https://ideas.repec.org/a/ecj/econjl/v119y2009i534p158-171.html.

Diebold, F.X., Yılmaz, K., 2014. On the network topology of variance decompositions: Measuring the connectedness of financial firms. Journal of Econometrics 182, 119–134. URL: https://ideas.repec.org/a/eee/econom/v182y2014i1p119-134.html.

Drechsler, I., Savov, A., Schnabl, P., 2014. A Model of Monetary Policy and Risk Premia. Working paper 20141. National Bureau of Economic Research. URL: http://www.nber.org/papers/w20141, doi:10.3386/w20141.

Drechsler, I., Savov, A., Schnabl, P., 2017. The Deposits Channel of Monetary Policy. The Quarterly Journal of Economics 132, 1819–1876. URL: https://doi.org/10.1093/qje/qjx019, doi:10.1093/qje/qjx019, arXiv:http://oup.prod.sis.lan/qje/article-pdf/132/4/1819/30637804/qjx019.pdf.

Duarte, F.M., Eisenbach, T.M., 2013. Fire-sale spillovers and systemic risk. Staff Reports 645. Federal Reserve Bank of New York. URL: https://ideas.repec.org/p/fip/fednsr/645.html.

Egan, M., Lewellen, S., Sunderam, A., 2017. The Cross Section of Bank Value. Working paper 23291. National Bureau of Economic Research. URL: http://www.nber.org/papers/w23291, doi:10.3386/w23291.

Eisenberg, L., Noe, T.H., 2001. Systemic risk in financial systems. Journal of Political Economy 47, 236–249.

Eisfeldt, A., Herskovic, B., Rajan, S., Siriwardane, E., 2020. OTC Intermediaries. Working paper. UCLA.

Elhorst, J.P., 2010a. Applied spatial econometrics: Raising the bar. Spatial Economic Analysis 5, 9–28.

Elhorst, J.P., 2010b. Spatial panel data models, in: Fischer, M.M., Getis, A. (Eds.), Handbook of Applied Spatial Analysis. Springer, Berlin, pp. 377–407.

Elsinger, H., Lehar, A., Summer, M., 2006. Risk assessment for banking systems. Management Science 52, 1301–1314.

Farboodi, M., 2019. Intermediation and Voluntary Exposure to Counterparty Risk. Working paper. Princeton University.

Fecht, F., Nyborg, K., Rocholl, J., 2010. The price of liquidity: Bank characteristics and market condition. Working paper. University of Zurich.

Frankel, M., 1962. The production function in allocation and growth: A synthesis. The American Economic Review 52, 996–1022. URL: http://www.jstor.org/stable/1812179.

Freixas, X., Martin, A., Skeie, D., 2011. Bank liquidity, interbank markets, and monetary policy. Review of Financial Studies 44, 2656–2692.

Freixas, X., Parigi, B., Rochet, J., 2000. Systemic risk, interbank relations and liquidity provision by the central bank. Journal of Money, Credit and Banking 32, 611–638.

Furfine, C., 2000. Interbank payments and the daily federal funds rate. Journal of Monetary Economics 46, 535–553.

Gofman, M., 2017. Efficiency and stability of a financial architecture with too-interconnected-to-fail institutions. Journal of Financial Economics 124, 113–146. URL: https://www.sciencedirect.com/science/article/pii/S0304405X16302471, doi:https://doi.org/10.1016/j.jfineco.2016.12.009.

Greenwood, R., Landier, A., Thesmar, D., 2015. Vulnerable banks. Journal of Financial Economics 115, 471–485.

Hart, O., Zingales, L., 2014. Banks Are Where The Liquidity Is. Working paper. Harvard University.

Herskovic, B., .

Herskovic, B., Kelly, B.T., Lustig, H.N., Nieuwerburgh, S.V., 2017. Firm Volatility in Granular Networks. Chicago Booth Research Paper 12-56. University of Chicago.

Hugonnier, J., Lester, B., Weill, P.O., 2014. Heterogeneity in decentralized asset markets. Working paper. National Bureau of Economic Research.

Jackson, M.O., 2003. Social and Economic Networks. Princeton University Press, N.J.

Jackson, M.O., Zenou, Y., 2012. Games on Networks. Technical Report 9127. C.E.P.R. Discussion Papers. URL: http://ideas.repec.org/p/cpr/ceprdp/9127.html.

Jovanovic, B., 1987. Micro shocks and aggregate risk. The Quarterly Journal of Economics 102, 395–409.

Kashyap, A.K., Stein, J.C., 2000. What do a million observations on banks say about the transmission of monetary policy? American Economic Review 90, 407–428. URL: http://www.aeaweb.org/articles?id=10.1257/aer.90.3.407, doi:10.1257/aer.90.3.407.

Katz, L., 1953. A new status index derived from sociometric analysis. Psychometrika 18, 39–43. URL: http://ideas.repec.org/a/spr/psycho/v18y1953i1p39-43.html.

Kelly, B.T., Lustig, H.N., Nieuwerburgh, S.V., 2013. Firm volatility in granular networks. Fama-Miller Working Paper; Chicago Booth Research Paper No. 12-56.

Kovner, A., Skeie, D., 2013. Evaluating the quality of fed funds lending estimates produced from Fedwire payments data. Staff Reports 629. Federal Reserve Bank of New York. URL: http://EconPapers.repec.org/RePEc:fip:fednsr:629.

LeSage, J., Pace, R., 2009. Introduction to Spatial Econometrics. Statistics, textbooks and monographs, CRC Press. URL: http://books.google.co.uk/books?id=EKiKXcgL-D4C.

Li, Y., 2017. Procyclical Finance: The Money View. Charles A. Dice Center for Research in Financial Economics Working Paper 2017-24. The Ohio State University Fisher College of Business.

Lucas, R.E., 1988. On the mechanics of economic development. Journal of Monetary Economics 22, 3–42. URL: http://www.sciencedirect.com/science/article/pii/0304393288901687, doi:https://doi.org/10.1016/0304-3932(88)90168-7.

Moore, J., 2012. Leverage stacks and the financial system. Working paper. Edinburgh University and London School of Economics.

Morris, S., Shin, H.S., 2002. Social value of public information. American Economic Review 92, 1521–1534. URL: https://www.aeaweb.org/articles?id=10.1257/000282802762024610, doi:10.1257/000282802762024610.

Newman, M.E.J., 2004. Analysis of weighted networks. Physical Review 70, 1–9.

Piazzesi, M., Schneider, M., 2017. Payments, Credit and Asset Prices. Working paper. Stanford University.

Primiceri, G.E., 2005. Time varying structural vector autoregressions and monetary policy. The Review of Economic Studies 72, 821–852. URL: http://www.jstor.org/stable/3700675.

Romer, P.M., 1986. Increasing returns and long-run growth. Journal of Political Economy 94, 1002–1037.

Shin, H.S., 2019. Distributed ledger technology and large value payments: a global game approach. Keynes Lecture. University of Cambridge.

Sims, C.A., Zha, T., 1999. Error bands for impulse responses. Econometrica 67, 1113–1155. URL: https://onlinelibrary.wiley.com/doi/abs/10.1111/1468-0262.00071, doi:10.1111/1468-0262.00071, arXiv:https://onlinelibrary.wiley.com/doi/pdf/10.1111/1468-0262.00071.

Stein, J.C., 2012. Monetary policy as financial-stability regulation. Quarterly Journal of Economics 127, 57–95.

Upper, C., 2011. Simulation methods to assess the danger of contagion in interbank markets. Journal of Financial Stability 7, 111–125.

Wang, Y., Whited, T.M., Wu, Y., Xiao, K., 2019. Bank Market Power and Monetary Policy Transmission: Evidence from a Structural Estimation. Working paper. University of Michigan.

Watts, D.J., Strogatz, S.H., 1998. Collective dynamics of 'small-world' networks. Nature 393, 440–442. doi:10.1038/30918.

Westwood, B., 2011. The money market liaison group sterling money market survey. Bank of England Quarterly Bulletin 51, 247–252.

Zawadowski, A., 2012. Entangled financial systems. Boston University working paper.

Zellner, A., 1962. An efficient method of estimating seemingly unrelated regressions and tests for aggregation bias. Journal of the American Statistical Association 57, 348–368.

Appendix A. Model Discussion and Additional Theoretical Results

Appendix A.1. Depositors' payment demand

In the payment system, each bank serves a unit mass of depositors in a region which, for example, can be defined geographically by a bank's branch locations. We model the depositors' demand for payment services. Let $d_{i,t}$ denote a representative depositor's demand for payment services, and $D_{i,t}$ denote the aggregate demand in region i. A representative depositor solves the following problem:

$$\max_{d_{i,t}} F\left(D_{i,t}d_{i,t}\right) - d_{i,t}P_{i,t}, \tag{A.1}$$

where $F(\cdot)$ is an increasing function. The complementarity between aggregate and individual payments, i.e., the product of $D_{i,t}$ and $d_{i,t}$ in $F(\cdot)$, captures a payment multiplier. Payments beget payments: when depositors make more payments, they trigger more economic activities and the new activities require more payments. This effect may work through the production input-output linkages (Carvalho and Tahbaz-Salehi, 2019). When downstream customers pay upstream suppliers for their products, upstream suppliers may in turn pay their own suppliers along the logistic chains. Another mechanism is that receiving payments relaxes agents' liquidity constraints and allows them to pay others (Shin, 2019). Such a feedback effect from aggregate activities to individual agents is also a key ingredient in models of economic growth (e.g., Frankel, 1962; Lucas, 1988; Romer, 1986).

The cost of payment services is P_i, which can be interpreted as a reduction in the deposit rate, for example, as depositors have to accept low interest rates on checking accounts for payment convenience. We do not model depositors' switching to different banks for cheaper payment services. In our empirical implementation, one period is one day, so the assumption is that depositors do not switch between banks intraday. Moreover, banks typically have deposit market power and a sticky customer base, which is well documented in the literature [e.g., (Drechsler et al., 2017; Wang et al., 2019)].

A representative depositor's first-order condition is

$$F'\left(D_{i,t}d_{i,t}\right)D_{i,t} = P_{i,t}. \tag{A.2}$$

Substituting the equilibrium condition, $D_{i,t} = d_{i,t}$, i.e., the aggregate demand for payment services from a unit mass of depositors is equal to the individual demand, we have the aggregate demand for payment services:

$$P_{i,t} = F'\left(D_{i,t}^2\right)D_{i,t} \equiv P\left(D_{i,t}\right). \tag{A.3}$$

Given the payment service market-clearing condition,

$$D_{i,t} = S_{i,t}, \tag{A.4}$$

bank i's revenues at t from supplying payment services are given by

$$V\left(S_{i,t}\right) \equiv P\left(D_{i,t}\right)D_{i,t} = P\left(S_{i,t}\right)S_{i,t} = F'\left(S_{i,t}^2\right)S_{i,t}^2, \tag{A.5}$$

where the payment service demand curve, $P\left(D_{i,t}\right) = F'\left(D_{i,t}^2\right)D_{i,t}$, is given by Eq. (A.3). In the main text, we linearize the marginal revenues, i.e., $F'\left(S_{i,t}^2\right) = \delta_S/2$. When $F\left(\cdot\right)$ is linear, the aggregate demand for payment services is upward-sloping (at least locally around the linearisation point), as shown by Eq. (A.3), which suggests that the positive feedback effect from the aggregate payment activities to individuals' payment activities is strong.

Appendix A.2. A more general model

In this section, we present a more general model. In our main model, when bank i exhausts its reserves through payment outflows, it can only borrow from bank j's reserves that are committed to the payment system, i.e., $z_{j,t}$. In the following, we allow bank j's total liquidity to be accessible via the network. As a reminder, the total liquidity is $l_{j,t} = q_{j,t} + z_{j,t}$, where $q_{j,t} = \alpha_j + \sum_{m=1}^{M}\beta_m x_{j,t}^m + \sum_{p=1}^{P}\beta_p x_t^p$ is bank j's liquidity held for its own intraday transactions. Let

$\rho \in [0,1]$ denote the fraction of $q_{j,t}$ that bank j is willing to lend out. When ρ is restricted to zero, the model is reduced to the main model.

Bank i's supply of payment services is given by

$$S_{i,t} = \kappa_b \left[z_{i,t} + \eta \sum_{j \neq i} \left(z_{j,t} + \rho q_{j,t} \right) \right]. \tag{A.6}$$

Given the same demand for payment services as before, we obtain bank i's revenues,

$$V\left(S_{i,t}\right) \equiv F'\left(S_{i,t}^2\right) S_{i,t}^2 . \tag{A.7}$$

As in Eq. (4) of the main model, the cost of liquidity is now parameterized as

$$\gamma \left[z_{i,t} + \eta \sum_{j \neq i} g_{ij,t} \left(z_{j,t} + \rho q_{j,t} \right) \right] + \frac{\psi}{2} \left[z_{i,t} + \eta \sum_{j \neq i} g_{ij,t} \left(z_{j,t} + \rho q_{j,t} \right) \right]^2 + \widetilde{\mu}_{i,t} \gamma' z_{i,t} + \frac{\psi'}{2} z_{i,t}^2, \tag{A.8}$$

where $z_{j,t}$ is now replaced by $z_{j,t} + \rho q_{j,t}$. As in the main model, we linearize the system by considering a constant $F'\left(S_{i,t}^2\right) \equiv \delta_S/2$, and define $\delta \equiv \delta_S \kappa_b$. The first-order condition for $z_{i,t}$ is given by

$$\delta \left[z_{i,t} + \eta \sum_{j \neq i} g_{ij,t} \left(z_{j,t} + \rho q_{j,t} \right) \right] = \gamma + \psi \left[z_{i,t} + \eta \sum_{j \neq i} g_{ij,t} \left(z_{j,t} + \rho q_{j,t} \right) \right] + \widetilde{\mu}_{i,t} \gamma' + \psi' z_{i,t}. \tag{A.9}$$

The same condition given by Eq. (7) applies for the uniqueness of the optimal solution.

Bank i's optimal choice of $z_{i,t}$ is given by

$$z_{i,t}^* = \phi \sum_{j \neq i} g_{ij,t} \left(z_{j,t} + \rho q_{j,t} \right) + \mu_{i,t}, \tag{A.10}$$

where, as in the main model, we define

$$\phi \equiv \left(\frac{\delta - \psi}{\psi' - (\delta - \psi)} \right) \eta \tag{A.11}$$

and

$$\mu_{i,t} \equiv \frac{(-\widetilde{\mu}_{i,t}\gamma' - \gamma)}{\psi' - (\delta - \psi)} = \bar{\mu}_i + \nu_{i,t}, \tag{A.12}$$

where $\nu_{i,t}$ has a normal distribution $\mathcal{N}\left(0, \sigma_i^2\right)$, independent over i and t. The equilibrium, $\left\{z_{i,t}^*\right\}_{i=1}^N$, solves the system of linear equations: $i = 1, ..., N$,

$$z_{i,t}^* = \phi \sum_{j \neq i} g_{ij,t}\left(z_{j,t}^* + \rho q_{j,t}\right) + \mu_{i,t}. \tag{A.13}$$

In Eq. (A.10), we can replace $z_{i,t}^*$ and $z_{j,t}^*$ by $l_{i,t} - q_{i,t}$ and $l_{j,t} - q_{j,t}$ respectively to obtain

$$l_{i,t} - q_{i,t} = \phi \sum_{j \neq i} g_{ij,t} l_{j,t} - \phi\left(1 - \rho\right) \sum_{j \neq i} g_{ij,t} q_{j,t} + \mu_{i,t}. \tag{A.14}$$

Rearranging the equation, we have

$$l_{i,t} = \phi \sum_{j \neq i} g_{ij,t} l_{j,t} + \breve{\mu}_t, \tag{A.15}$$

where we define

$$\begin{aligned}\breve{\mu}_t \equiv & q_{i,t} - \phi\left(1 - \rho\right) \sum_{j \neq i} g_{ij,t} q_{j,t} + \mu_{i,t} \qquad \text{(A.16)}\\ = & \alpha_i + \sum_{m=1}^{M} \beta_m x_{i,t}^m + \sum_{p=1}^{P} \beta_p x_t^p - \phi\left(1 - \rho\right) \sum_{j \neq i} g_{ij,t}\left(\alpha_j + \sum_{m=1}^{M} \beta_m x_{j,t}^m + \sum_{p=1}^{P} \beta_p x_t^p\right) + \mu_{i,t}.\end{aligned}$$

Note that α_i and $\bar{\mu}_i$ cannot be separately identified, so we drop the bank fixed effects:

$$\breve{\mu}_t = \sum_{m=1}^{M} \beta_m x_{i,t}^m + \sum_{p=1}^{P} \beta_p x_t^p - \phi\left(1 - \rho\right) \sum_{j \neq i} g_{ij,t}\left(\sum_{m=1}^{M} \beta_m x_{j,t}^m + \sum_{p=1}^{P} \beta_p x_t^p\right) + \mu_{i,t}. \tag{A.17}$$

Note that because $\sum_{j \neq i} g_{ij,t} = 1$, the expression of $\breve{\mu}_t$ can be simplified:

$$\breve{\mu}_t = \sum_{m=1}^{M} \beta_m x_{i,t}^m + \sum_{p=1}^{P} \chi_p x_t^p - \phi (1-\rho) \sum_{j \neq i} g_{ij,t} \sum_{m=1}^{M} \beta_m x_{j,t}^m + \mu_{i,t}, \tag{A.18}$$

where $\chi_p \equiv [1 - \phi(1-\rho)] \beta_p$. Then for $m = 1, ..., M + n$, we define $\theta_m \equiv -\phi (1-\rho) \beta_m$, and further simplify the expression of $\breve{\mu}_t$:

$$\breve{\mu}_t = \sum_{m=1}^{M} \beta_m x_{i,t}^m + \sum_{p=1}^{P} \chi_p x_t^p + \sum_{j \neq i} g_{ij,t} \sum_{m=1}^{M} \theta_m x_{j,t}^m + \mu_{i,t}. \tag{A.19}$$

Once we impose the restriction $\rho = 0$, we are back to the main model. Therefore, estimating this more general formulation serves as a specification test of the main model. The following result is immediate following the same steps as in the proof of Proposition 1 in the main text.

Proposition 3. *Suppose that $|\phi| < 1$. Then, there is a unique interior solution for the equilibrium outcome given by*

$$l_{i,t}^* (\phi, \mathbf{G}_t) = \{\mathbf{M}(\phi, \mathbf{G}_t)\}_{i.} \breve{\mu}_t, \tag{A.20}$$

where $\{\}_{i.}$ is the operator that returns the i-th row of its argument, $\breve{\mu}_t \equiv [\breve{\mu}_{1,t}, ..., \breve{\mu}_{N,t}]^\top$, and

$$\mathbf{M}(\phi, \mathbf{G}_t) \equiv I + \phi \mathbf{G}_t + \phi^2 \mathbf{G}_t^2 + \phi^3 \mathbf{G}_t^3 + ... = \sum_{k=0}^{\infty} \phi^k \mathbf{G}_t^k = (I - \phi \mathbf{G}_t)^{-1}, \tag{A.21}$$

where I is the $N \times N$ identity matrix.

The above result implies that, even in this more general model, the definitions of conditional volatility of liquidity, risk key player, and level key player, as well as their dependency on the network topology and equilibrium parameter ϕ, stay unchanged.[33]

[33] In this case, l^* should replace z^* in Eq. (A.23).

In our empirical implementation we can write the observed total reserve holdings, for $i = 1, ..., N$, $t = 1, ..., T$, as

$$l_{i,t} = \phi \sum_{j \neq i} g_{ij,t} l_{j,t} + \sum_{m=1}^{M} \beta_m x_{i,t}^m + \sum_{p=1}^{P} \chi_p x_t^p + \sum_{j \neq i} g_{ij,t} \sum_{m=1}^{M} \theta_m x_{j,t}^m + \bar{\mu}_t + \nu_{i,t}. \tag{A.22}$$

This empirical counterpart of the more general model is a spatial Durbin model, i.e., Eq. (36) in the main text. The network effect on banks' liquidity holding decisions is no longer confined in the residual term, $z_{i,t}$, but rather on the total level of liquidity.

Appendix A.3. Level key player

Similar to the risk key player, we can identify the "systemic level key player", whose removal from the system causes the largest aggregate liquidity reduction in expectation.[34]

Definition 3 (Level key player). *The level key player τ_t^* is the player that, when removed, causes the maximum expected reduction in the overall level of total liquidity. We use $\mathbf{G}_{\setminus\tau,t}$ to denote the new adjacency matrix obtained by setting to zero all of $\mathbf{G}_t$'s τ-th row and column coefficients. The resulting network is $g_{\setminus\tau,t}$. The level key player τ_t^* is found by solving*

$$\tau_t^* = \underset{\tau=1,\ldots,N}{\arg\max} \ \mathbb{E}\left[\sum_i z_i^*(\phi, g_t) - \sum_{i \neq \tau} z^*(\phi, g_{\setminus\tau,t}) \middle| g_t, \tau \right], \tag{A.23}$$

where $\mathbb{E}$ is the expectation operator.

We define the level key player under the assumption that the removal of banks does not trigger immediately the formation of new links. Hence, we

[34] This definition is in the same spirit as the concept of key player in the crime network literature, e.g., Ballester et al. (2006), where targeting key players is important for crime reduction. Here, it is useful to consider the ripple effect on the aggregate liquidity when a bank fails and exits from the system. Injecting liquidity to the key level players might be necessary to avoid major disruptions to the whole system.

capture the short-run effects of a bank's sudden failure. Since we do not observe bank failure in our sample, we cannot provide a precise time frame for link formation after removal. However, our definition can be operational from a policy perspective, especially during a crisis when banks shun each other and link formation becomes less likely. Using Proposition 1, we have the following corollary.

Corollary 1. *A player τ_t^* is the level key player that solves Eq. (A.23) if and only if*

$$\tau_t^* = \underset{\tau=1,\ldots,N}{\arg\max} \quad \underbrace{\{\mathbf{M}(\phi, \mathbf{G}_t)\}_{\tau.}\bar{\mu}}_{\text{Indegree effect}} + \underbrace{\mathbf{1}^\top \{\mathbf{M}(\phi, \mathbf{G}_t)\}_{.\tau}\bar{\mu}_\tau}_{\text{Outdegree effect}} - \underbrace{m_{\tau\tau}(\phi, \mathbf{G}_t)\bar{\mu}_\tau}_{\text{Double count correction}} \quad , \tag{A.24}$$

where $m_{\tau\tau}(\phi, \mathbf{G}_t)$ is the τ-th element of the diagonal of $\mathbf{M}(\phi, \mathbf{G}_t)$.

When bank τ is removed, its liquidity disappears from the system. This is the first component, the indegree effect, which depends on neighbors' $\bar{\mu}$ through $\{\mathbf{M}(\phi, \mathbf{G}_t)\}_{\tau.}$, the routes from neighbors to τ. The second component reflects bank τ's impact on other banks, so its own $\bar{\mu}_\tau$ is multiplied by the sum of the routes from τ to neighbors, i.e., $\mathbf{1}^\top\{\mathbf{M}(\phi, \mathbf{G}_t)\}_{\tau.}$. This outdegree effect captures the network externality. The level key player metric is particularly relevant for a central planner who decides on which bank to help to sustain the aggregate liquidity buffer. Such a decision depends on a bank's own contribution to aggregate liquidity and the spillover effects through the network linkages. As in the risk key player metric, focusing on the network alone is not enough. Both the attenuation factor ϕ and bank-specific characteristics, now captured by $\bar{\mu}$, are important inputs in computing key players.

Network Risk and Key Players: A Structural Analysis of Interbank Liquidity – Online Appendices

Edward Denbee[a], Christian Julliard[b], Ye Li[c], Kathy Yuan[b]

[a] *Bank of England*
[b] *London School of Economics, SRC, and CEPR*
[c] *The Ohio State University, Fisher College of Business*

Abstract

The online appendices provide the institutional background of our empirical setting, details of our empirical methodology, and additional figures and tables. In Appendix O.1, we review the institutional setting of banks' liquidity (reserve) management, such as U.K. monetary policy framework, the U.K. payment and settlement systems, and the sterling overnight interbank market. Appendix O.2 provides details on the quasi-maximum likelihood formulation and identification for both the baseline spatial error model and the more general spatial Durbin model, the calculation of confidence bands for the network impulse response functions, and details on variables construction. In Appendix O.3, we provide time-series plots of several key variables and tables of detailed estimation results for both the baseline spatial error model (and its robustness checks) and the more general spatial Durbin model.

O. Appendices

O.1. Reserves schemes, payment systems, and interbank liquidity

Banks in the UK choose the amount of central bank reserves that they hold to support a range of short-term liquidity needs. Reserves are the ultimate set-

Email addresses: edward.denbee@bankofengland.co.uk (Edward Denbee), c.julliard@lse.ac.uk (Christian Julliard), li.8935@osu.edu (Ye Li), K.Yuan@lse.ac.uk (Kathy Yuan)

tlement asset for interbank payments. Whenever payments are made between the accounts of customers at different commercial banks, they are ultimately settled by transferring central bank money (reserves) between the reserves accounts of those banks. Reserve balances are used to buffer against intraday payment imbalances (i.e., cumulative outflows larger than inflows). Additionally, central bank reserves are the most liquid asset that banks can draw upon in the presence of unexpected outflows of funds. Since 2006, the starting year of our sample, banks choose their reserve holdings on a discretionary basis, i.e., reserve holdings are not mandatory. However, their reserve holding decisions depend on the policy framework in which they operate.

O.1.1. Monetary policy framework

Since the 1998 Banking Act, the Bank of England (BoE) has had independent responsibility for setting interest rates to ensure that inflation, as measured by the Consumer Price Index (CPI), meets the inflation target of 2%. Each month, the Monetary Policy Committee (MPC) meets to decide the appropriate level of the Bank rate (the policy interest rate) to meet the inflation target in the medium term. The Sterling Monetary Framework changed over time. During our sample period, the Bank of England had three distinct monetary frameworks: prior to May 18, 2006, the Bank of England operated an unremunerated reserve scheme; this was then replaced by a reserves average scheme; since March 2009 and the initiation of quantitative easing, the reserves average scheme has been suspended.

Pre-2006 Reform: Prior to the 2006 reforms, the Sterling Monetary Framework (SMF) was based upon voluntary unremunerated reserves. There were no reserve requirements and no reserve averaging over a maintenance period. The only requirement was that banks were obliged to maintain a minimum zero balance at the end of each day. In practice, due to uncertainties from end of day cash positions, banks opted for small positive reserve balances.

Reserve Averaging: In May 2006, the Bank of England undertook a major reform of the Sterling Monetary Framework. The new scheme was voluntary remunerated reserves with a period-average maintenance requirement. Each maintenance period – the period between two meetings of the Monetary Policy Committee – banks were required to decide upon a reserves target. This voluntary choice of reserves target is a feature unique to the UK system. Over the course of each maintenance period, the banks would manage their reserves so that, on average, their reserves hit the target. Where banks were unable to hit the target, standing borrowing and deposit facilities were available. Within a range of ±1% of the target, reserves are remunerated at the Bank Rate.[1] Holding an average level of reserves outside the target range attracts a penalty charge.[2] However, a bank can ensure it hits its target by making use of the Bank's Operational Standing Facilities (OSFs). These bilateral facilities allow banks to borrow overnight from the Bank (against high-quality collateral) at a rate above Bank Rate or to deposit reserves overnight with the Bank at a rate below Bank Rate. The possibility of arbitrage between interbank market rates and reserves remunerated at Bank Rate is the main mechanism through which market rates are kept in line with Bank Rate. In both schemes before quantitative easing (QE), the BoE would ensure sufficient reserves supply for banks to meet their reserves target. Banks then use the interbank market to reallocate reserves from banks in surplus to banks in deficit.

Post-Quantitative Easing: Quantitative easing in UK started in March 2009 when the MPC decided that in order to meet the inflation target in the medium term, it would need to supplement the use of interest rate (which had hit the practical lower bound of 0.5%) with the purchase of assets using central bank reserves. This consisted of the BoE's boosting the money supply by creating central bank reserves and using them to purchase assets, predominantly UK gilts. Furthermore, the BoE suspended the average reserve targeting regime, and now remunerates all reserves at the Bank rate.

[1] At various points during the crisis, this ±1% range was increased to give banks more flexibility.

[2] Settlement banks also pay a penalty if their reserves account is overdrawn at the end of any day.

The effect of reserve targeting: Before the QE period, the average reserve targeting regime imposes restrictions on banks' liquidity choice, because missing the target in a maintenance period can be costly. However, as previously explained, a bank can ensure it hits its target by making use of the Bank's Operational Standing Facilities (OSFs). Our model in the main text does not feature restrictions associated with the reserve schemes, because data on banks' reserve targets is unavailable. However, we may still test the impact of such restrictions on our results by adding the lagged liquidity holdings into our baseline specification. A direct implication of a rigid targeting regime is that banks' liquidity holdings exhibits mean-revertion – positive deviations tend to be followed by negative ones so that, on average, banks can hit the targets. Specifically, this suggests a negative coefficient on the lagged liquidity. Table O.5 in Section O.3 reports the results. $\hat{\phi}$ does not change much in comparison with the baseline estimate. Moreover, the coefficients on the lagged liquidity holdings are positive, against the hypothesis of a rigid regime reserve targeting regime.

O.1.2. Payment and settlement systems

Banks use central bank reserves to, inter alia, meet their demand for intraday liquidity in the payment and settlement systems. Reserves act as a buffer to cover regular timing mismatches between incoming and outgoing payments, for example, due to exceptionally large payments, operational difficulties, or stresses that impact upon a counterparty's ability, or willingness to send payments. There are two major payment systems in the UK: CHAPS and CREST.[3] These two systems play a vital role in the UK financial system. On average, in 2011, £700 billion in transactions was settled every day within the two systems. This amount equates to the UK 2011 nominal GDP being settled every two days.

CHAPS is the UK's large-value payment system. It is used for real time settlement of payments between its member banks. These banks settle payments on behalf of hundreds of other banks through correspondent relationships. Typi-

[3]There are also four retail payment systems (Bacs, the Faster Payments Service (FPS), Cheque and Credit Clearing (CCC) and LINK) that are operated through the BoE.

cal payments are business-to-business payments, home purchases, and interbank transfers. Payments relating to unsecured interbank money markets are settled in CHAPS. CHAPS opens for settlement at 8 am and closes at 4:20 pm. Payments made on behalf of customers cannot be made after 4 pm. The system has throughput guidelines which require members to submit 50% of their payments by noon and 75% by 14:30. This helps ensure that payments are settled throughout the day and do not cluster towards the end of the day.

In 2011, CHAPS settled an average of 135,550 payments each day valuing £254bn. CHAPS is a real-time gross settlement (RTGS) system. This means that payments are settled finally and irrevocably in real time. To fund these payments, banks have to access liquidity intraday. If a bank has, at any point during the day, cumulatively sent more payments than it has received, then it needs liquidity to cover this difference. This comes either from central bank reserves or intraday borrowing from the BoE. Furthermore, when a bank sends funds to another bank in the system, it exposes itself to liquidity risk, that is, the risk that the bank may not get those fund inflows back during the day and thus will run down their own liquidity holdings or borrow from the BoE. Therefore, it is important to choose an appropriate level of liquidity buffer. In addition to maintaining a liquidity buffer, banks manage liquidity by borrowing from and lending to each other in the unsecured overnight markets. According to Bank of England estimates, payments relating to overnight market activity (advances and repayments) account for approximately 20% of CHAPS values (Wetherilt et al., 2010).

CREST is a securities settlement system. Its Delivery-vs-Payment (DVP) mechanism ensures simultaneous transfer of funds and securities. When a liquidity need is identified, the CREST system's intraday liquidity mechanism with the BoE works automatically through "Self-Collateralising Repos" (SCRs): if a CREST settlement bank would otherwise have insufficient funds to settle a transaction, a secured intraday loan is generated using as eligible collateral either the purchased security (if eligible) or other securities.

O.1.3. The sterling unsecured overnight interbank market

Interbank markets are the markets where banks and other financial institutions borrow and lend assets, typically with maturities of less than one year. At the shortest maturity, overnight, banks borrow and lend central bank reserves. Monetary policy aims at influencing the rate at which these markets transact in order to control inflation in the wider economy. There is limited information available about the size and the structure of the sterling money markets. The Bank of England estimates suggest that the overnight unsecured market is approximately £20–30 billion per day during our sample period. Wetherilt et al. (2010) describe the network of the sterling unsecured overnight money market. They find that the network has a small core of highly connected participants, surrounded by a wider periphery of banks loosely connected with each other, but with connections to the core. It is believed that prior to the recent financial crisis, the unsecured market was much larger than the secured market. We identify interbank borrowing and lending transactions in CHAPS settlement data.

O.2. Details of the empirical methodology

O.2.1. Quasi-maximum likelihood formulation and identification

The main model.. Writing the variables and coefficients of the spatial error model in Eq. (22) and Eq. (23) in matrix form as[4]

$$B := [\alpha_1^{time}, ..., \alpha_t^{time}, ..., \alpha_T^{time}, \alpha_1^{bank}, ..., \alpha_i^{bank}, ..., \alpha_N^{bank}, \\ \beta_1^{bank}, .., \beta_m^{bank}, ..., \beta_M^{bank}, \beta_1^{macro}, ..., \beta_p^{macro}, ..., \beta_P^{macro}]^\top,$$

$$L := [l_{1,1}, ..., l_{N,1}, ..., l_{i,t}, ..., l_{1,T}, ..., l_{N,T}]^\top, \ \ \mathbf{z} := [z_{1,1}, ..., z_{N,1}, ..., z_{i,t}, ..., z_{1,T}, ..., z_{N,T}]^\top$$

$$\nu := [\nu_{1,1}, ..., \nu_{N,1}, ..., \nu_{i,t}, ..., \nu_{1,T}, ..., \nu_{N,T}], \ \ \underline{\mu} := \mathbf{1}_T \otimes \bar{\mu} = \mathbf{1}_T \otimes [\bar{\mu}_1, ..., \bar{\mu}_N]^\top,$$

[4]This is similar to the spatial formulation in Lee and Yu (2010).

$$\mathbf{G} := diag\left(\mathbf{G}_t\right)_{t=1}^{T} = \begin{bmatrix} \mathbf{G}_1 & \mathbf{0} & ... & \mathbf{0} \\ \mathbf{0} & \mathbf{G}_2 & ... & ... \\ ... & ... & ... & \mathbf{0} \\ \mathbf{0} & ... & \mathbf{0} & \mathbf{G}_T \end{bmatrix}, \ \mathbf{X} := \left[\mathbf{D}, \mathbf{F}, \mathbf{X}^{bank}, \mathbf{X}^{macro}\right],$$

where $\mathbf{D} := I_T \otimes \mathbf{1}_N$, $\mathbf{F} := \mathbf{1}_T \otimes I_N$, and

$$\mathbf{X}^{macro} = \begin{bmatrix} x_1^1 & ... & x_1^p & ... & x_1^P \\ ... & ... & ... & ... & ... \\ x_t^1 & ... & x_t^p & ... & x_t^P \\ ... & ... & ... & ... & ... \\ x_T^1 & ... & x_T^p & ... & x_T^P \end{bmatrix} \otimes \mathbf{1}_N, \ \ \mathbf{X}^{bank} = \begin{bmatrix} x_{1,1}^1 & ... & x_{1,1}^m & ... & x_{1,1}^M \\ ... & ... & ... & ... & ... \\ x_{N,1}^1 & ... & x_{N,1}^m & ... & x_{N,1}^M \\ ... & ... & ... & ... & ... \\ x_{N,T}^1 & ... & x_{N,T}^m & ... & x_{N,T}^M \end{bmatrix},$$

we can then rewrite the empirical model as

$$L = \mathbf{X}B + \mathbf{z}, \ \ \mathbf{z} = \underline{\mu} + \phi \mathbf{G}\mathbf{z} + \nu, \ \ \nu_{i,t} \sim iid\left(0, \sigma_i^2\right). \tag{O.1}$$

This, in turn, implies that

$$\nu\left(B, \underline{\mu}, \phi\right) = \left(I_{N\times T} - \phi\mathbf{G}\right)\left(L - \mathbf{X}B\right) - \underline{\mu}. \tag{O.2}$$

Finally, using the Gaussian distribution to model the exogenous error terms ν yields the log likelihood

$$\ln \mathcal{L}\left(B, \phi, \underline{\mu}, \left\{\sigma_i^2\right\}_{i=1}^{N}\right) \equiv -\frac{TN}{2}\ln\left(2\pi\right) - \frac{T}{2}\sum_{i=1}^{N}\ln\sigma_i^2 - \sum_{i=1}^{N}\frac{1}{2\sigma_i^2}\sum_{t=1}^{T}\nu_{i,t}\left(B, \underline{\mu}, \phi\right)^2, \tag{O.3}$$

and the above can be estimated using standard optimization methods.

The separate identification of the bank fixed effects, $\alpha^{bank} := \left[\alpha_1^{bank}, ..., \alpha_N^{bank}\right]^\top$, and the network-bank fixed effects, $\bar{\mu} := \left[\bar{\mu}_1, ..., \bar{\mu}_N\right]'$, deserve some further remarks. Isolating the role of these fixed effects, Eq. (O.2) can be rewritten as

$$\begin{aligned}\nu\left(B,\underline{\mu},\phi\right) &= \left(I_{N\times T}-\phi\mathbf{G}\right)\left(L-\tilde{\mathbf{X}}\tilde{B}-\mathbf{F}\alpha^{bank}\right)-\underline{\mu} \\ &= \left(I_{N\times T}-\phi\mathbf{G}\right)\left(L-\tilde{\mathbf{X}}\tilde{B}\right)-\mathbf{1}_T\otimes\left(\bar{\mu}+\alpha^{bank}\right)+\phi\mathbf{G}\mathbf{F}\alpha^{bank}\end{aligned} \tag{O.4}$$

where $\tilde{\mathbf{X}} := \left[\mathbf{D},\mathbf{X}^{bank},\mathbf{X}^{macro}\right]$ and $\tilde{B}$ is simply the vector B without the α^{bank} elements.

Several observations are in order. First, the above implies that if $\phi = 0$, then $\bar{\mu}$ and α^{bank} cannot be separately identified (nevertheless the parameters $\tilde{B}$ are still identified). Second, if $\mathbf{G}_t$ is a right stochastic matrix (i.e., with row sums equal to one or $\mathbf{G}_t\mathbf{1}_N = \mathbf{1}_N$) for every t, separate identification of $\bar{\mu}$ and α^{bank} can be achieved only up to a parameter normalization. To understand the lack of separate identification, note that Eq. (O.1) can be rewritten as

$$L = \mathbf{X}B + \mathbf{1}_T\otimes I_N\alpha^{bank} + \left(I_{N\times T}-\phi\mathbf{G}\right)^{-1}\underline{\mu}+\epsilon. \tag{O.5}$$

where the last error term, $\epsilon := \left(I_{N\times T}-\phi\mathbf{G}\right)^{-1}\nu$, is orthogonal to $\mathbf{X}$, and

$$Var\left[\epsilon\right] = \left(I_{N\times T}-\phi\mathbf{G}\right)^{-1}\left(I_T\otimes\Sigma_v\right)\left(I_{N\times T}-\phi\mathbf{G}^T\right)^{-1}.$$

Therefore, separately identifying α^{bank} and $\underline{\mu}$ requires that $\mathbf{1}_T\otimes I_N$ and $\left(I_{N\times T}-\phi\mathbf{G}\right)^{-1}$ are linear independent (see Eq. (O.5)). However, if $\mathbf{G}_t$ is right stochastic, i.e., $\mathbf{G}_t\mathbf{1}_N = \mathbf{1}_N$ for any t, we have

$$\left(I_{N\times T}-\phi\mathbf{G}\right)^{-1}\mathbf{1}_{N\times T} = \sum_{k=0}^{\infty}\phi^k\mathbf{G}^k\mathbf{1}_{N\times T} = \left(\frac{1}{1-\phi}\right)\mathbf{1}_{N\times T} = \left(\frac{1}{1-\phi}\right)\sum_{i=1}^{N}\left\{\mathbf{1}_T\otimes I_N\right\}_i,$$

which is exactly the sum, i.e., a linear combination, of columns in $\mathbf{1}_T\otimes I_N$. As a result, α^{bank} and $\underline{\mu}$ cannot be separately identified in general, unless we normalize some of the parameters, for example, by setting one of the $\bar{\mu}_i = 0$.

Nevertheless, in our subsample estimation, such normalization is not needed, as noted in the main text. This is due to a special feature of our data. Note that the lack of separate identification for $\bar{\mu}$ and α^{bank} arises because $\mathbf{G}_t$ is always a right stochastic matrix, i.e., $\mathbf{G}\mathbf{1}_{N\times T} = \mathbf{1}_{N\times T}$ for any t. However, in our sample, bank 7 did not have connections with other banks in 14 days, and bank 11 did not have connections with other banks in 145 days. These 159 days do not overlap. They cover 13.5% of the time and spread across our three subsamples. In such days, one row of $\mathbf{G}_t$ has every element equal to zero, and thus, $\mathbf{G}\mathbf{1}_{N\times T} = \mathbf{1}_{N\times T}$ does not hold (either the sum of row 7 or 11 is zero). As a result, we can separately identify $\bar{\mu}$ and α^{bank}. In contrast, in our rolling estimation (Fig. 9), because the rolling windows are smaller than our subsamples and some do not contain any of the 159 days, we set $\bar{\mu}_{11}$ to zero. The estimate of ϕ is robust to setting other $\bar{\mu}_i$ to zero since ϕ is recovered from the covariance matrix of the residuals in Eq. (O.5), and a consistent estimate of this covariance does not require separate identification of α^{bank} and $\underline{\mu}$.

Below, we explain the numeric method of likelihood maximization. First, we estimate B using ordinary least squares (OLS), and use the first-order condition for σ_i^2, i.e.,

$$\hat{\sigma_i^2} = \frac{1}{T}\sum_{t=1}^{T} \nu_{i,t}\left(B, \underline{\mu}, \phi\right)^2,$$

to substitute out σ_i^2 in the log likelihood function, forming a concentrated likelihood that only depends on ϕ. By maximizing the concentrated likelihood, we obtain $\hat{\phi}$, and then, using the aforementioned first-order conditions for σ_i^2, we obtain $\hat{\sigma}_i^2$. We then re-estimate B as in feasible generalized least squares (FGLS), using $\hat{\phi}$ and $\hat{\sigma}_i^2$ to form the heteroskedastic covariance matrix in the observational equation of L. Next, $\hat{B}$ is used to form a new concentrated likelihood, which is used to update the estimate of ϕ. We iterate this process until convergence.

A more general model.. As discussed in Section 4.4, our main model is nested by the spatial Durbin model. Define

$$\gamma^{bank} := [\gamma_1^{bank}, .., \gamma_m^{bank}, ..., \gamma_M^{bank}]^\top, \text{ and } \gamma^{macro} = [\gamma_1^{macro}, ..., \gamma_p^{macro}, ..., \gamma_P^{macro}]^\top.$$

As in the main text, we simplify the notation by merging bank fixed effects into bank characteristics and time fixed effects into macro control variables. Following the previous matrix notation, this model can be written in matrix form as

$$L = X^{macro}\gamma^{macro} + X^{bank}\gamma^{bank} + \rho\mathbf{G}L + \mathbf{G}X^{bank}\theta + \underline{\mu} + \nu, \quad \nu_{i,t} \sim iid\left(0, \sigma_i^2\right), \tag{O.6}$$

which implies that

$$\nu = \left(I_{N\times T} - \phi\mathbf{G}\right)\left(L - X^{macro}\gamma^{macro} - X^{bank}\gamma^{bank} - \mathbf{G}X^{bank}\theta\right) - \underline{\mu}. \tag{O.7}$$

Note that as long as $\mathbf{G}$ and $I_{N\times T}$ are not linear dependent, which is true by the construction of $\mathbf{G}$, we can separately identify γ^{bank} and θ. As in the estimation of SEM, we can form a log likelihood function and follow an iterating procedure to estimate the parameters.

O.2.2. Confidence bands for the network impulse response functions

The ϕ estimator outlined in the previous section has an asymptotic Gaussian distribution with variance s_ϕ^2 (that can be readily estimated from the QMLE covariance matrix based, as usual, on the Hessian and gradient of the log likelihood in Eq. (O.3)). That is, $\sqrt{T}\left(\hat{\phi} - \phi_0\right) \xrightarrow{d} N\left(0, s_\phi^2\right)$, where ϕ_0 denotes the true value of ϕ. Writing

$$a_1(\phi) := \frac{\partial \mathbf{1}^\top \left\{\left(\mathbf{I} - \phi\mathbf{G}\right)^{-1}\right\}_{.i}}{\partial\phi}, \quad a_2(\phi) = \frac{\partial \mathbf{1}^\top \left\{\left(\mathbf{I} - \phi\mathbf{G}\right)^{-1}\phi\mathbf{G}\right\}_{.i}}{\partial\phi}$$

we have from Lemma 2.5 of Hayashi (2000) that

$$\sqrt{T}\left[NIRF_i\left(\hat{\phi}, 1\right) - NIRF_i\left(\phi_0, 1\right)\right] \xrightarrow{d} N\left(0, a_1\left(\phi_0\right)^2 s_\phi^2\right),$$
$$\sqrt{T}\left[NIRF_i^e\left(\hat{\phi}, 1\right) - NIRF_i^e\left(\phi_0, 1\right)\right] \xrightarrow{d} N\left(0, a_2\left(\phi_0\right)^2 s_\phi^2\right).$$

Therefore, since $a_j\left(\hat{\phi}\right) \xrightarrow{p} a_j\left(\phi_0\right)$, $j = 1, 2$, by the continuous mapping theorem, and by Slutsky's theorem, $a_j\left(\hat{\phi}\right)\hat{s}_\phi^2 \xrightarrow{p} a_j\left(\phi_0\right)^2 s_\phi^2$, where $\hat{s}_\phi^2$ is a consistent variance estimator, we can construct confidence bands for the network impulse response functions using the sample estimates of ϕ and s_ϕ^2.

O.2.3. Details on variables construction

Bank-level variables

- Liquidity holdings ($l_{i,t}$, i.e., the dependent variable): the logarithm of reserve balances plus collateral posted to the BoE at the beginning at the day.

- Intraday liquidity available (LA) is the amount of liquidity to meet payment requirements and is measured as the sum of reserves ($SDAB$, Start of Day Account Balance) plus the value of intraday repo available with the BoE (PC, Posting of Collateral). As time passes, the liquidity available in CHAPS is calculated by subtracting the money moved to CREST from the liquidity available in the previous time interval. In this way, we can trace for bank i the liquidity available at any time t in day s:

$$LA(t, i, s) = SDAB_{i,s} + PC_{i,s} - \sum\nolimits_{\tau=1}^{t} CREST_{i,s,\tau}.$$

  This variable is used for the constructions of $\ln VolPay_{i,t-1}$.

- $\ln VolPay_{i,t-1}$: log intraday variance of liquidity available, lagged by one day.

- $\ln LU_{i,t-1}$: liquidity used is defined as follows,

$$LU(i, s) = \max\{\max_T [CNP(T; i, s)], 0\}.$$

  The first (inside) maximum operator picks the highest level of cumulative net debit position (CNP) within a day. Regarding the second (outside) maximum operator, if the highest level is negative, the bank i is always a liquidity contributor on day s, so LU is equal to zero. When used in estimation, it is lagged by one day and in logarithms.

- $\ln LevPay_{i,t-1}$: total intraday payment level (lagged by one day, in logarithms).
- $rK^{in}_{i,t-1}$: right kurtosis of incoming payment time, lagged by one day.
- $rK^{out}_{i,t-1}$: right kurtosis of outgoing payment time, lagged by one day.
- *Interbank Rate*: interbank borrowing rate, lagged by one day.
- *Total Lending and Borrowing (log)*: total lending and borrowing in the interbank market (lagged by one day, in logarithms).
- *Total Assets (log)*: total asset (lagged, monthly, in logarithms).
- $\frac{Repo\ Liability}{Assets}$: repo liability to total asset ratio (lagged, monthly).
- $\frac{Deposits}{Assets}$: the log cumulative change in retail deposit to asset ratio (lagged, monthly).
- *CDS Spread*: an index (log cumulative change) of 5-year senior unsecured CDS spread.
- *Stock Return*: gross stock return including dividends (lagged by one day).

Macro variables

- $\ln VolPay_{t-1}$: intraday variance of aggregate liquidity available (lagged by one day, in logarithms). "Liquidity available" is defined above at the bank level.
- TOR_{t-1}: lagged turnover rate in the payment system. To define the turnover rate, we need first to define the Cumulative Net (Debit) Position (CNP):

$$CNP(T, i, s) = \sum_{t=1}^{T} (P^{OUT}_{i,s,t} - P^{IN}_{i,s,t}),$$

where $P^{OUT}_{i,s,t}$ is bank i's total payment outflow at time t in day s. $P^{IN}_{i,s,t}$ is the payment inflow. The turnover rate (in day s) is defined as

$$TOR_s = \frac{\sum_{i=1}^{N}\sum_{t=1}^{88} P^{OUT}_{i,s,t}}{\sum_{i=1}^{N}\max\{\max_T[CNP(T;i,s)],0\}} \tag{O.8}$$

The numerator is the total payment made in the system at day s. The denominator sums the maximum cumulative net debt position of each bank at day s. Note that in the denominator, if the cumulative net position of a certain bank is always below zero (that is, this bank's cumulative inflow always exceeds its cumulative outflow), this bank actually absorbs liquidity from the system. If there are banks absorbing liquidity from the system, there must be banks injecting liquidity into the system. When we calculate the turnover rate (the ratio between the total amount circulating and the base), we should only consider one of the two. That is why we take the first (outside) maximum operator. The reason for the inside operator goes as follows: any increase in the cumulative net debit position (wherever positive) incurs an injection of liquidity into the system, so the maximum of the cumulative net position is the total injection from the outside to the payment system. Additionally, the sum over different banks gives the total injection through all the membership banks. A higher turnover rate means a more frequent reuse of liquidity injected from outside into the payment system.

- rK_{t-1}: lagged right kurtosis of the intraday time of aggregate payment outflow:

$$rK_t = \frac{\sum_{\tau>m_t}(\frac{\tau-m_t}{\sigma_t})^4}{\sum_{\tau=1}^{88}(\frac{\tau-m_t}{\sigma_t})^4}$$

where

$$m_t = \frac{1}{88}\sum_{\tau=1}^{88}\tau\left(\frac{P^{OUT}_{t,\tau}}{\sum_{\tau=1}^{88}P^{OUT}_{t,\tau}}\right),\ \ \sigma_t^2 = \frac{1}{88-1}\sum_{\tau=1}^{88}(\tau-m_t)^2\left(\frac{P^{OUT}_{t,\tau}}{\sum_{\tau=1}^{88}P^{OUT}_{t,\tau}}\right)$$

and $P^{OUT}_{t,\tau}$ is the aggregate payment outflow at time interval τ. Note that transactions are recorded for 88 10-minute time intervals within each day (from 5:00 to 19:30). The variable m_t is the average of payment time weighted by the payment outflow.

- *LIBOR*: daily LIBOR rate, lagged by one day.
- *Interbank Rate Premium:* average interbank rate minus LIBOR, lagged by one day.

O.3. Additional figures and tables

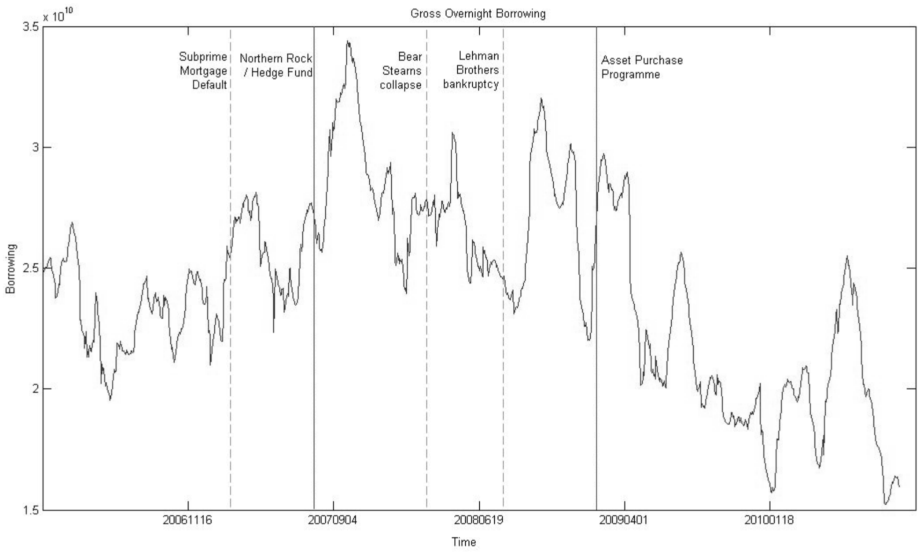

Fig. O.1. Daily gross interbank borrowing (rolling monthly average; unit: £1).

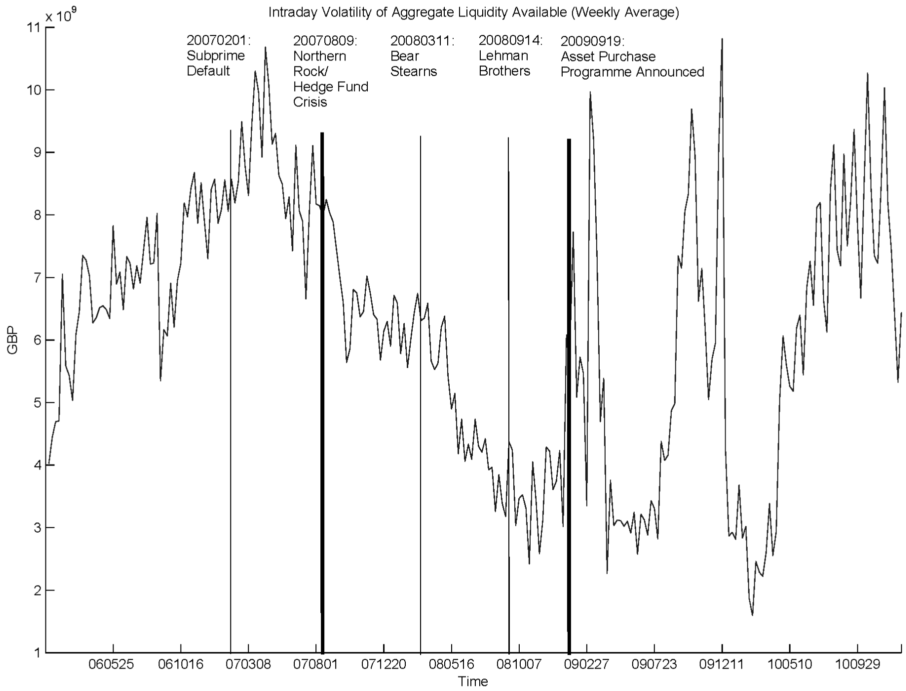

Fig. O.2. Intraday variance of aggregate outflows (Unit: £1).

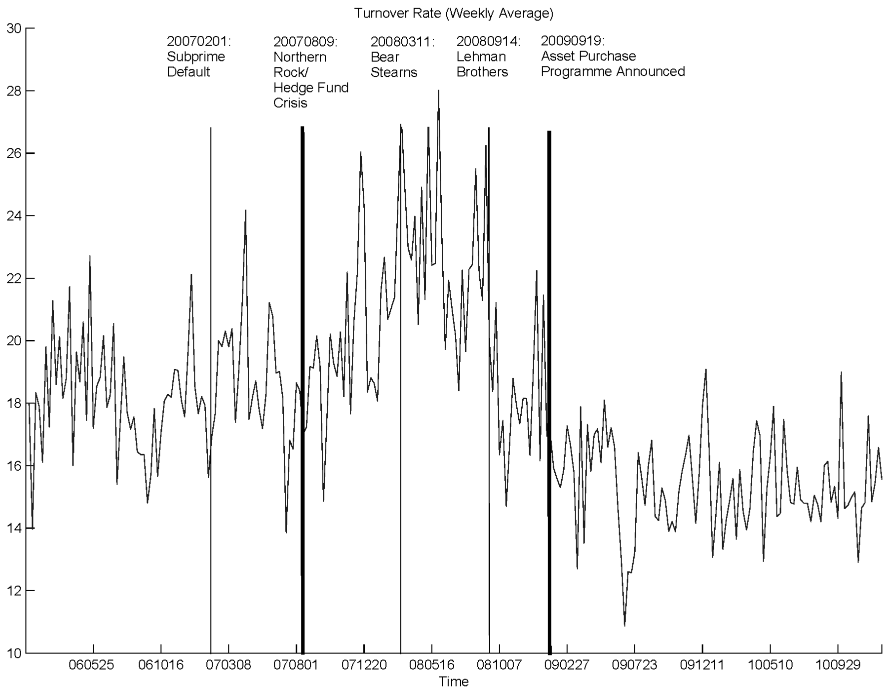

Fig. O.3. Turnover rate in the payment system as defined in Eq. (O.8).

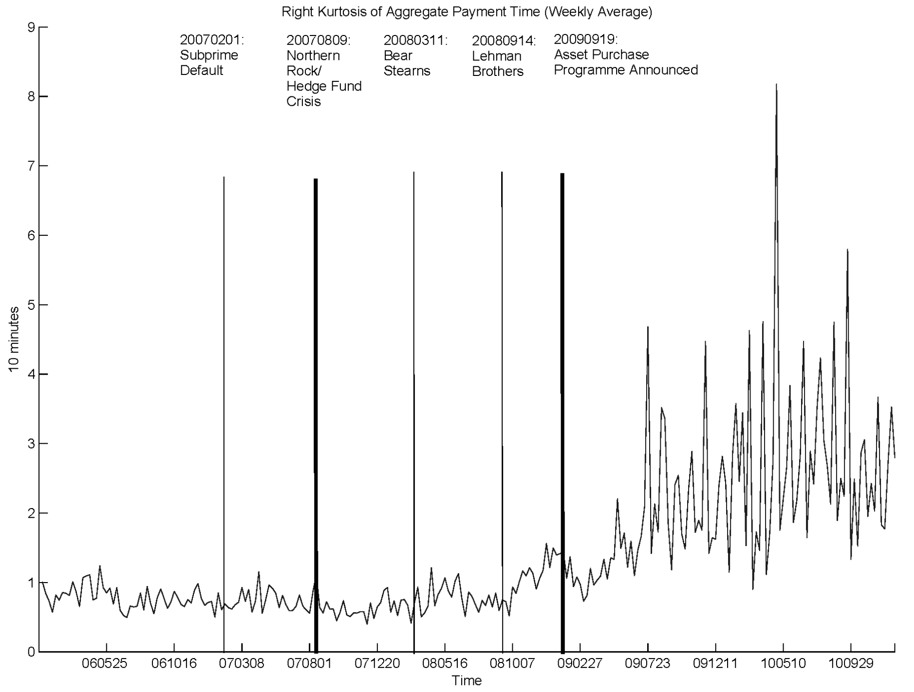

Fig. O.4. Right kurtosis of aggregate payment times, defined as the kurtosis generated by payment times above the average payment time of the day.

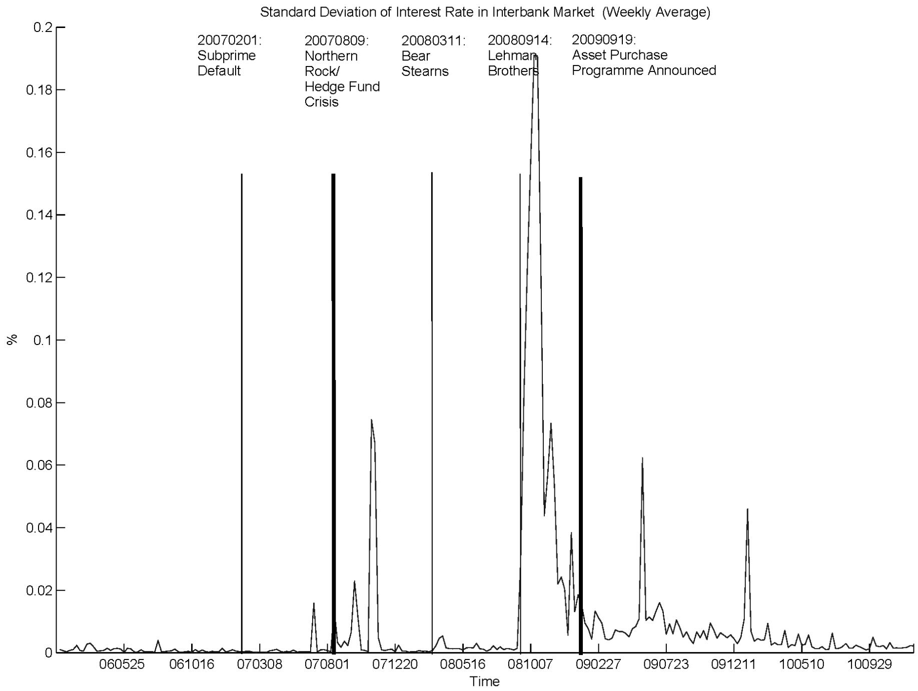

Fig. O.5. Cross-sectional standard deviation of interbank interest rate rates (weekly average).

Table O.1
Spatial Error Model Estimation Results. Estimation results for Eq. (22) and Eq. (23). Periods 1, 2 and 3 correspond, respectively, to before the Northern Rock/BNP Paribas Fund Crisis, after it but before the first BoE announcement of Asset Purchase Programme, and the QE period. The t-statistics are reported in parentheses under the estimated coefficients, and * denotes statistically significant estimates at a 10% or higher confidence level. Standard errors are QMLE-robust ones, and for the average network multiplier, $1/(1-\hat{\phi})$, the delta method is employed.

	Period 1	*Period 2*	*Period 3*
$\hat{\phi}$	0.8137^*	0.3031^*	-0.1794^*
	(21.47)	(1.90)	(−4.96)
$1/\left(1-\hat{\phi}\right)$	5.3677^*	1.4349^*	0.8479^*
	(4.92)	(4.37)	(32.61)
Macro Control Variables			
rK_{t-1}	0.1845	0.0084	-0.0032^*
	(1.30)	(0.55)	(−3.88)
$\ln VolPay_{t-1}$	−0.4451	0.0308	0.0291
	(−1.00)	(1.17)	(1.72)
TOR_{t-1}	0.0166	0.0007	0.0018
	(1.80)	(0.69)	(1.75)
LIBOR	0.2378	0.0928	0.5800^*
	(0.27)	(1.28)	(2.52)
Interbank Rate Premium	3.8845	−0.0405	0.6973^*
	(1.61)	(−0.33)	(3.00)
Bank Characteristics/Micro Control Variables			
Interbank Rate	−0.2081	−0.0473	−0.0880
	(−0.98)	(−1.03)	(−1.92)
$\ln LevPay_{i,t-1}$	−0.0235	0.0802^*	0.0808^*
	(−0.62)	(3.29)	(5.09)
$rK^{in}_{i,t-1}$	0.0010	−0.0086	0.0045
	(0.14)	(−0.63)	(1.03)
$rK^{out}_{i,t-1}$	0.0090	0.0320^*	−0.0061
	(0.92)	(3.62)	(−1.32)
$\ln VolPay_{i,t-1}$	0.0129^*	0.0039	0.0196^*
	(4.59)	(1.92)	(5.96)
$\ln LU_{i,t-1}$	-0.0038^*	-0.0039^*	-0.0027^*
	(−2.86)	(−3.41)	(−3.79)
Total Assets (log)	1.2590^*	0.6328^*	1.0170^*
	(5.39)	(10.31)	(18.92)
$\frac{\text{Repo Liability}}{\text{Assets}}$	-5.5625^*	0.0282	−0.3057
	(−3.61)	(0.43)	(−1.45)
$\frac{\text{Deposits}}{\text{Assets}}$	−0.0014	0.0149^*	0.0481^*
	(−0.20)	(5.15)	(11.76)
Total Lending and Borrowing (log)	-0.1882^*	0.0612^*	−0.0025
	(−5.57)	(2.95)	(−1.27)
CDS Spread	0.0051	-0.1212^*	-0.0383^*
	(0.13)	(−6.61)	(−4.00)
Stock Return	−0.5667	0.1927	0.2574
	(−0.88)	(1.49)	(1.88)
R^2	66.01%	92.09%	91.53%

Table O.2

Ratio of network to idiosyncratic volatility. The table reports $\sqrt{\frac{Var(\hat{z}_{i,t})}{Var(\hat{v}_{i,t})}}$ for each bank and each period considered. Periods 1, 2 and 3 correspond, respectively, to: before the Northern Rock/BNP Paribas Fund Crisis, after it but before the first BoE announcement of Asset Purchase Programme, and the QE period.

	Period 1	*Period 2*	*Period 3*
Bank 1	2.54	1.05	0.98
Bank 2	2.10	1.04	1.02
Bank 3	1.83	1.06	0.87
Bank 4	2.62	1.06	1.08
Bank 5	2.41	1.10	1.02
Bank 6	1.65	1.09	1.03
Bank 7	1.47	0.97	1.13
Bank 8	1.69	1.09	1.03
Bank 9	2.12	1.09	1.03
Bank 10	1.62	0.99	1.09
Bank 11	2.04	1.14	1.31
Mean	2.01	1.06	1.05

Table O.3
Spatial Error Model with Counterparty-Adjusted G. Estimation results for Eq. (22) and Eq. (23). Periods 1, 2 and 3, correspond, respectively, to before the Northern Rock/BNP Paribas Fund Crisis, after it but before the first BoE announcement of Asset Purchase Programme, and the QE period. The t-statistics are reported in parentheses under the estimated coefficients, and * denotes statistically significant estimates at a 10% or higher confidence level. Standard errors are QMLE-robust ones, and for the average network multiplier, $1/(1-\hat{\phi})$, the delta method is employed.

	Period 1	*Period 2*	*Period 3*
$\hat{\phi}$	0.8159^* (21.68)	0.3090^* (1.92)	-0.1948^* (-5.05)
$1/\left(1-\hat{\phi}\right)$	5.4318^* (4.89)	1.4472^* (4.30)	0.8370^* (30.95)
Macro Control Variables			
rK_{t-1}	0.1746 (1.26)	0.0085 (0.55)	-0.0032^* (-3.87)
$\ln VolPay_{t-1}$	-0.4325 (-0.98)	0.0304 (1.16)	0.0303 (1.78)
TOR_{t-1}	0.0164 (1.82)	0.0007 (0.69)	0.0017 (1.70)
LIBOR	0.2404 (0.28)	0.0932 (1.30)	0.5843^* (2.55)
Interbank Rate Premium	3.7057 (1.59)	-0.0377 (-0.31)	0.7264^* (3.13)
Bank Characteristics/Micro Control Variables			
Interbank Rate	-0.2145 (-1.01)	-0.0472 (-1.03)	-0.0949 (-2.05)
$\ln LevPay_{i,t-1}$	-0.0240 (-0.63)	0.0821^* (3.37)	0.0817^* (5.07)
$rK^{in}_{i,t-1}$	0.0012 (0.17)	-0.0081 (-0.59)	0.0039 (0.88)
$rK^{out}_{i,t-1}$	0.0099 (1.01)	0.0310^* (3.53)	-0.0056 (-1.21)
$\ln VolPay_{i,t-1}$	0.0128^* (4.57)	0.0041 (2.03)	0.0198^* (6.00)
$\ln LU_{i,t-1}$	-0.0039^* (-2.96)	-0.0039^* (-3.47)	-0.0027^* (-3.77)
Total Assets (log)	1.2143^* (5.22)	0.6207^* (9.98)	1.0000^* (18.04)
$\frac{\text{Repo Liability}}{\text{Assets}}$	-5.6703^* (-3.66)	0.0224 (0.34)	-0.2643 (-1.20)
$\frac{\text{Deposits}}{\text{Assets}}$	-0.0030 (-0.44)	0.0145^* (4.98)	0.0492^* (11.76)
Total Lending and Borrowing (log)	-0.1940^* (-5.70)	0.0645^* (3.07)	-0.0015 (-0.76)
CDS Spread	0.0076 (0.19)	-0.1203^* (-6.59)	-0.0382^* (-3.93)
Stock Return	-0.5734 (-0.88)	0.1890 (1.47)	0.2462 (1.82)
R^2	67.42%	92.08%	91.61%

Table O.4

Planner's Solution vs. Decentralized Equilibrium. This table reports the percentage difference between the volatility of aggregate liquidity of the planner's solution and that of the decentralized equilibrium, conditional on the network structure. Periods 1, 2 and 3 correspond, respectively, to before the Northern Rock/BNP Paribas Fund Crisis, after it but before the first BoE announcement of Asset Purchase Programme, and the QE period.

Panel A: $\eta = 9$	γ	*Period 1*	*Period 2*	*Period 3*
$\frac{\sqrt{Var\left(Z_t^p \mid \mathbf{G}_t=\bar{\mathbf{G}}\right)}-\sqrt{Var\left(Z_t^* \mid \mathbf{G}_t=\bar{\mathbf{G}}\right)}}{\sqrt{Var\left(Z_t^* \mid \mathbf{G}_t=\bar{\mathbf{G}}\right)}}$		-90.3%	-36.5%	-12.3%
$\mathbb{E}\left[Z_t^p - Z_t^* \mid \mathbf{G}_t = \bar{\mathbf{G}}\right]$ (unit: £billion)	-0.59	-89.1	4.1	-100.0
	-0.53	-82.5	15.5	-200.0
	-0.50	-78.6	22.2	-300.0

Panel A: $\eta = 11$	γ	*Period 1*	*Period 2*	*Period 3*
$\frac{\sqrt{Var\left(Z_t^p \mid \mathbf{G}_t=\bar{\mathbf{G}}\right)}-\sqrt{Var\left(Z_t^* \mid \mathbf{G}_t=\bar{\mathbf{G}}\right)}}{\sqrt{Var\left(Z_t^* \mid \mathbf{G}_t=\bar{\mathbf{G}}\right)}}$		-88.5%	-34.7%	-12.4%
$\mathbb{E}\left[Z_t^p - Z_t^* \mid \mathbf{G}_t = \bar{\mathbf{G}}\right]$ (unit: £billion)	-0.17	-37.5	88.3	-100.0
	-0.12	-31.3	98.8	-200.0
	-0.09	-27.7	104.9	-300.0

Table O.5

Spatial Error Model Estimation with Lagged Liquidity. Estimation results for Eq. (22) and Eq. (23) with the lagged liquidity holdings as one of the bank characteristics. Periods 1 and 2 correspond, respectively, to before the Northern Rock/BNP Paribas Fund Crisis, and after it but before the first BoE announcement of Asset Purchase Programme. The t-statistics are reported in parentheses under the estimated coefficients, and * denotes statistically significant estimates at a 10% or higher confidence level. Standard errors are QMLE-robust ones, and for the average network multiplier, $1/(1-\hat{\phi})$, the delta method is employed.

	Period 1	*Period 2*
$\hat{\phi}$	0.8230* (24.30)	0.4663* (5.24)
$1/\left(1-\hat{\phi}\right)$	5.6497* (5.23)	1.8737* (6.00)
Lagged Liquidity Holdings		
$l_{i,t-1}$ (Lagged Dependent Variable)	0.2183* (4.12)	0.5510* (17.80)
Macro Control Variables		
rK_{t-1}	0.2099 (1.27)	0.0282 (1.52)
$\ln VolPay_{t-1}$	−0.6076 (−1.08)	0.0599 (1.90)
TOR_{t-1}	0.0127 (1.20)	0.0042* (3.32)
LIBOR	0.8841 (0.97)	0.0974 (1.66)
Interbank Rate Premium	2.4106 (1.09)	0.0856 (0.77)
Bank Characteristics/Micro Control Variables		
Interbank Rate	−0.1148 (−0.60)	0.0136 (0.34)
$\ln LevPay_{i,t-1}$	−0.0136 (−0.38)	0.0413* (2.19)
$rK^{in}_{i,t-1}$	0.0040 (0.57)	0.0197 (1.80)
$rK^{out}_{i,t-1}$	0.0058 (0.58)	−0.0005 (−0.07)
$\ln VolPay_{i,t-1}$	0.0108* (3.79)	0.0036 (1.91)
$\ln LU_{i,t-1}$	−0.0052* (−3.66)	−0.0072* (−6.82)
Total Assets (log)	1.0059* (4.48)	0.2849* (4.78)
$\frac{\text{Repo Liability}}{\text{Assets}}$	−4.2080* (−3.11)	−0.0278 (−0.59)
$\frac{\text{Deposit}}{\text{Assets}}$	−0.0022 (−0.36)	0.0046 (1.72)
Total Lending and Borrowing (log)	−0.1586* (−4.84)	0.0081 (0.47)
CDS (log)	0.0098 (0.26)	−0.0624* (−4.31)
Stock Return (Inc. Dividend)	−0.5334 (−0.84)	0.0404 (0.36)
R^2	67.70%	94.48%

References

Hayashi, F., 2000. Econometrics. Princeton University Press: Princeton.

Lee, L.f., Yu, J., 2010. A spatial dynamic panel data model with both time and individual fixed effects. Econometric Theory 26, 564–597. URL: http://ideas.repec.org/a/cup/etheor/v26y2010i02p564-597_10.html.

Wetherilt, A., Zimmerman, P., Soramaki, K., 2010. The sterling unsecured loan market during 2006-08: insights from network theory. Bank of England working papers 398. Bank of England. URL: http://ideas.repec.org/p/boe/boeewp/0398.html.